



SCIENCE OF TSUNAMI HAZARDS

Journal of Tsunami Society International

Volume 40

Number 1

2021

EVALUATION OF SEISMIC AND TSUNAMI RESISTANCE OF POTENTIAL SHELTERS FOR VERTICAL EVACUATION IN CASE OF A TSUNAMI IMPACT IN BAHIA DE CARÁQUEZ, CENTRAL COAST OF ECUADOR 1

Pablo Ezequiel Suárez-Acosta¹, Cristian David Cañamar-Tipan¹, Darlin Alexis Ñato- Criollo¹, Juan Daniel Vera-Zambrano¹, Kevinn Luis Galarza-Vega¹, Paola Michelle Guevara-Álvarez¹, Cintya Natali Fajardo-Cartuche¹, Kimberlyn Karen Herrera- Garcés¹, Carlos Vicente Ochoa-Campoverde¹, Jhandry Santiago Torres-Orellana¹, Wellington Rentería², Kervin Chunga³, Oswaldo Padilla¹, Izar Sinda-González¹, Débora Simón-Baile¹ and Theofilos Toulkeridis^{1,4*}

¹Universidad de las Fuerzas Armadas ESPE, Sangolquí, ECUADOR

²University of Southern California, Los Angeles, USA

³Universidad Técnica de Manabí, Portoviejo, ECUADOR

⁴Universidad de Especialidades Turísticas, Quito, ECUADOR

DEVELOPMENT OF RESEARCH ROADMAP OF THE EXCELLENCE 38

Madlazim*, Fida Rachmadiarti, Masriyah, Sifak Indana, Elok Sudibyo, and Binar Kurnia Prahani

¹Faculty of Mathematic and Natural Science, Universitas Negeri Surabaya, Surabaya 60231, INDONESIA.

SIMULATION OF TSUNAMI ALONG NORTH SUMATRA AND PENINSULAR MALAYSIA ALLIED WITH THE INDONESIAN TSUNAMI OF 2004 USING A SHALLOW WATER MODEL 48

Md. Fazlul Karim

Department of Mathematical and Physical Sciences, East West University, Dhaka-1212, BANGLADESH

THE GREAT LISBON EARTHQUAKE AND TSUNAMI OF 1 NOVEMBER 1755
Evaluation of the Compression Convergence Mechanism 62

George Pararas-Carayannis

Tsunami Society International

Copyright © 2021 - TSUNAMI SOCIETY INTERNATIONAL

WWW.TSUNAMISOCIETY.ORG

TSUNAMI SOCIETY INTERNATIONAL, 1741 Ala Moana Blvd. #70, Honolulu, HI 96815, USA.

SCIENCE OF TSUNAMI HAZARDS is a CERTIFIED OPEN ACCESS Journal included in the prestigious international academic journal database DOAJ, maintained by the University of Lund in Sweden with the support of the European Union. SCIENCE OF TSUNAMI HAZARDS is also preserved, archived and disseminated by the National Library, The Hague, NETHERLANDS, the Library of Congress, Washington D.C., USA, the Electronic Library of Los Alamos, National Laboratory, New Mexico, USA, the EBSCO Publishing databases and ELSEVIER Publishing in Amsterdam. The vast dissemination gives the journal additional global exposure and readership in 90% of the academic institutions worldwide, including nation-wide access to databases in more than 70 countries.

OBJECTIVE: Tsunami Society International publishes this interdisciplinary journal to increase and disseminate knowledge about tsunamis and their hazards.

DISCLAIMER: Although the articles in SCIENCE OF TSUNAMI HAZARDS have been technically reviewed by peers, Tsunami Society International is not responsible for the veracity of any statement, opinion or consequences.

EDITORIAL STAFF

Dr. George Pararas-Carayannis, Editor
<mailto:drgeorgepc@yahoo.com>

EDITORIAL BOARD

Dr. Hermann FRITZ, Georgia Institute of Technology, USA
Prof. George CURTIS, University of Hawaii -Hilo, USA
Dr. Zygmunt KOWALIK, University of Alaska, USA
Dr. Galen GISLER, NORWAY
Prof. Kam Tim CHAU, Hong Kong Polytechnic University, HONG KONG
Dr. Jochen BUNDSCHUH, (ICE) COSTA RICA, Royal Institute of Technology, SWEDEN
Acad. Dr. Yurii SHOKIN, Novosibirsk, RUSSIAN FEDERATION
Dr. Radiana Triatmadja - Tsunami Research Group, Universitas Gadjah Mada, Yogyakarta, INDONESIA

TSUNAMI SOCIETY INTERNATIONAL, OFFICERS

Dr. George Pararas-Carayannis, President
Dr. Carolyn Forbes, Secretary

Submit manuscripts of research papers, notes or letters to the Editor. If a research paper is accepted for publication the author(s) must submit a scan-ready manuscript, a Doc, TeX or a PDF file in the journal format. Issues of the journal are published electronically in PDF format. There is a minimal publication fee for authors who are members of Tsunami Society International for three years and slightly higher for non-members. Tsunami Society International members are notified by e-mail when a new issue is available. Permission to use figures, tables and brief excerpts from this journal in scientific and educational works is granted provided that the source is acknowledged.

Recent and all past journal issues are available at: <http://www.TsunamiSociety.org> CD-ROMs of past volumes may be purchased by contacting Tsunami Society International at postmaster@tsunamisociety.org Issues of the journal from 1982 thru 2005 are also available in PDF format at the U.S. Los Alamos National Laboratory Library <http://epubs.lanl.gov/tsunami/>

WWW.TSUNAMISOCIETY.ORG



SCIENCE OF TSUNAMI HAZARDS

Journal of Tsunami Society International

Volume 40

Number 1

2021

EVALUATION OF SEISMIC AND TSUNAMI RESISTANCE OF POTENTIAL SHELTERS FOR VERTICAL EVACUATION IN CASE OF A TSUNAMI IMPACT IN BAHIA DE CARÁQUEZ, CENTRAL COAST OF ECUADOR

Pablo Ezequiel Suárez-Acosta¹, Cristian David Cañamar-Tipan¹, Darlin Alexis Ñato-Criollo¹, Juan Daniel Vera-Zambrano¹, Kevinn Luis Galarza-Vega¹, Paola Michelle Guevara-Álvarez¹, Cintya Natali Fajardo-Cartuche¹, Kimberlyn Karen Herrera-Garcés¹, Carlos Vicente Ochoa-Campoverde¹, Jhandry Santiago Torres-Orellana¹, Willington Rentería², Kervin Chunga³, Oswaldo Padilla¹, Izar Sinde-González¹, Débora Simón-Baile¹ and Theofilos Toulkeridis^{1,4*}

¹Universidad de las Fuerzas Armadas ESPE, Sangolquí, Ecuador

²University of Southern California, Los Angeles, USA

³Universidad Técnica de Manabí, Portoviejo, Ecuador

⁴Universidad de Especialidades Turísticas, Quito, Ecuador

*Corresponding author: ttoulkeridis@espe.edu.ec

ABSTRACT

Ecuador has been the target of many tsunamis in its past documented history. Therefore, we performed a detailed assessment of the seismic and tsunami resistance of existing buildings, which may serve as temporary potential shelters in Bahía de Caráquez, in the coast of Ecuador. Prior to this evaluation we used the extensively validated tsunami modelling tool, which allowed to yield tsunami run up and tsunami amplitude based on a modeled 8Mw event, near the studied area. Furthermore, we calculated and elaborated evacuation times and routes based on the assumption of a potential tsunami impact, with a variety of GIS tools. Based on the short time of reaction for the vulnerable population within the potential flooded area, we opted to suggest a nearby solution with a vertical evacuation in buildings along the coastal line. In order to evaluate the potential of such 26 buildings, we used the Modified Italian Methodology in order to calculate the seismic vulnerability index (SVI) and later also determine the tsunami vulnerability index (TVI).

The results indicate that only one of the 26 assessed buildings fall within acceptable values below 30 for both, SVI and TVI. As all buildings are of private property, both entrance and stairs remains limited for the general public, hence, new regulations should improve access during a tsunami emergency within an evacuation plan as well as an installed early alert system.

Keywords: *Vertical evacuation, physical structural vulnerability, tsunami resistance, early alert system, Ecuador*

1. INTRODUCTION

Tsunamis are a destructive force of nature, especially where human settlements have been constructed in their course of flow (Pararas-Carayannis, 1977; Pararas-Carayannis, 2002; Pararas-Carayannis, 2003; Pararas-Carayannis, 2006; Pheng et al., 2006; Pararas-Carayannis, 2010; Mikami et al., 2012; Rodriguez et al., 2016; Toulkeridis et al., 2017a; Rodriguez et al., 2017). Such phenomenon occurs relatively frequently and worldwide but predominantly in coastal areas, of which the major appearance is related to the Pacific Ring of Fire, which includes the coasts of Ecuador in northwestern South America (Pararas-Carayannis, 2012; Chunga and Toulkeridis, 2014; Pararas-Carayannis, 2017; Toulkeridis et al., 2017b). Like many other countries, which are situated in this geodynamic setting, Ecuador has suffered the impact of a variety of tsunamis within the recorded history and beyond as indicated by historic documents, eye witness reports and paleo-tsunami deposits (Chunga and Toulkeridis, 2014; Ioualalen et al., 2014; Chunga et al., 2017; 2018; Toulkeridis et al., 2018; Toulkeridis et al., 2019). Hereby, the past and recent destructive events demonstrated the high vulnerability of the infrastructure and population as well as the low degree of preparation of the corresponding authorities and the public (Celorio-Saltos et al., 2018; Matheus-Medina et al., 2018; Edler et al., 2020; Martinez and Toulkeridis, 2020). Due to the developments of the societies, it has been inevitably to construct human settlements and their associated needs in areas of a high degree of vulnerability towards the impact zones of tsunamis, without considering recurrent natural processes which may turn to become disasters (Alcántara-Ayala, 2002; Papatoma & Dominey-Howes, 2003; Frankenberg et al., 2013;). Massive residences, factories and other industrial or strategic constructions, as well as commercial and touristic activities are among the most inopportune situated places within these zones of high vulnerability in Ecuador and elsewhere (Papatoma et al., 2003; Calgaro & Lloyd, 2008; Calgaro et al., 2014; Barros et al., 2015; Matheus-Medina et al., 2018;).

Therefore, living with the risk has been the common policy of Ecuador, when applying risk assessment measures towards natural hazards of hydro-meteorological or geologic origin, such as floods, droughts, hydric deficit, climate change, mass movements and landslides, volcanic activities, earthquakes and especially tsunamis (Toulkeridis et al. 2007,

Padrón et al., 2008; Ridolfi et al., 2008; Padrón et al., 2012; Toulkeridis et al., 2015a; b; Toulkeridis et al. 2016; Vaca et al., 2016; Rodriguez et al., 2017; Toulkeridis and Zach, 2017; Mato and Toulkeridis, 2017; Jaramillo Castelo et al., 2018; Zafrir Vallejo et al., 2018; Aguilera et al., 2018; Palacios Orejuela, and Toulkeridis, 2020; Toulkeridis et al., 2020a; b; Poma et al., 2020). Nonetheless, due to the last catastrophic events, such as the earthquake of 2016 and the volcanic crisis of 2015, Ecuador's policy started to change from a passive way of reacting to disasters after their occurrence towards a more proactive risk assessment, improved and more controlled land use management, signage of evacuation routes, drilling of the population and preventive education as well as even mitigation structures where affordable prior potential impacts (Toulkeridis, 2016; Toulkeridis et al., 2020c; Yépez et al., 2020; Herrera-Enríquez et al., 2020). In case of the coastal part of Ecuador, a high amount of tsunami evacuation signs have been installed, although many more are needed, while several are inadequately placed, indicating a longer than needed path towards safety among other issues (Celorio-Saltos et al., 2018; Matheus-Medina et al., 2018).

Furthermore, evacuation routes may be often too long in order to arrive safe in case of a short-time warning of a tsunami (Matheus Medina et al., 2016; Rodriguez et al., 2016; Toulkeridis et al., 2017a). For this specific situation, buildings with a sufficient amount of floors may be used for a vertical evacuation as a temporary shelter (Yeh et al., 2005; Park et al., 2012; Matheus Medina et al., 2016; Mostafizi et al., 2019). Such buildings however, need to be resistant themselves towards telluric movements of high intensity or magnitude as well as for the impact of the incoming waves of tsunamis (Lukkunaprasit & Ruangrassamee, 2008; Meyyappan et al., 2013; Navas et al., 2018; Belash & Yakovlev, 2018; Aviles-Campoverde et al., 2021).

Based on the aforementioned aspects, the current study has been applied within a high frequented touristic village in Ecuador, where an evaluation of the resistance of seismic movements and tsunami impacts of temporal shelters shall indicate, which of these buildings are conformably assigned to stand as a safe area for the evacuating public. Such evacuation has been based on a formal analysis of escape times and routes as well as potential tsunami impact scenarios and modeled wave heights. This pioneering investigation based on international criteria may serve as an example of contemporary risk assessment and management which allows a better relationship and compatibility between existing hazard zones and a corresponding land use policy in the coastal area of Ecuador.

2. GEODYNAMIC SETTING AND STUDY AREA

Tsunamis with some devastating results, originated from the local, regional and far geodynamic environments prone to hit the Ecuadorian coastal areas and its relatively unprepared population as well as their settlements, which are situated within an active continental margin (Pararas-Carayannis, 1980; Herd et al., 1981; Kanamori & McNally,

1982; Mendoza & Dewey, 1984; Pararas-Carayannis, 2012; Ioualalen et al., 2011; 2014; Chunga & Toulkeridis, 2014; Heidarzadeh et al., 2017). The coastal continental platform of Ecuador is situated along the Pacific Rim and therefore within an area which is impacted regularly by tsunamis due to a severe earthquake activity (Gusiakov, 2005; Pararas-Carayannis, 2012; Rodriguez et al., 2016). The geodynamic constellation results from the subduction of the oceanic Nazca Plate (together with its above situated Carnegie Ridge) below the continental South American and Caribbean Plates, which are both separated by the Guayaquil-Caracas Mega Shear (Fig. 1; Kellogg et al., 1995; Gutscher et al., 1999; Egbue and Kellog, 2010). This active continental margin give rise to a variety of tsunamis of tectonic as well submarine landslide origin (Moberly et al., 1982; Pontoise and Monfret, 2004; Ratzov et al, 2007; 2010; Ioualalen et al., 2011; Pararas-Carayannis, 2012). Furthermore, tsunamis or even iminamis may be generated by massive sector collapses of volcanoes in the Galapagos archipelago (Kates, 1976; Cannon, 1994; Keating & McGuire, 2000; Pararas-Carayannis, 2002; Whelan & Kelletat, 2003; McGuire, 2006; Glass et al., 2007; Pinter & Ishman, 2008; Toulkeridis, 2011).

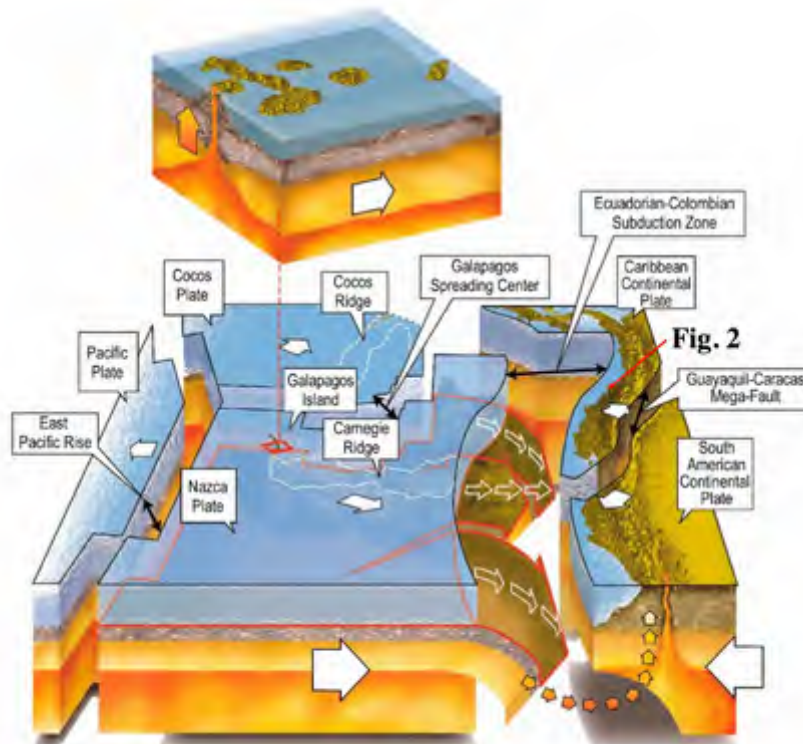


Fig. 1. Geodynamic setting of Ecuador with associated oceanic and continental plates and a variety of plate boundaries, such as the divergent plate boundaries named East Pacific Rise and Galapagos Spreading Center, the convergent plate boundary represented by the Ecuadorian-Colombian Subduction zone, as well as the transcurrent plate boundary represented by the Guayaquil-Caracas Mega-Fault. Also shown the Galapagos Islands and the Carnegie Ridge. Adapted from Toulkeridis, 2013, modified of Toulkeridis et al., 2017a.

Due to the aforementioned geodynamic setting, Ecuador has been impacted by several seismic and tsunami hazards, based on the occurrence of local earthquakes, such as on January 31, 1906 (8.8 Mw), October 2, 1933 (6.9 Mw), May 14, 1942 (7.8 Mw), December 12, 1953 (7.3 Mw), January 16, 1956 (7.0), January 19, 1958 (7.6 Mw), December 12, 1979 (8.2 Mw), August 4, 1998 (7.2 Mw) and April 16, 2016 (7.8 Mw), besides other less intense occurrences (Berninghausen, 1962; Kanamori and McNally, 1982; Pararas-Carayannis, 2012; Chunga and Toulkeridis, 2014; Toulkeridis et al., 2017a; 2017b; 2018). Besides the short time impacts of local tsunamis, Ecuador has been also the target of distant origin tsunamis, like the one generated in Japan on March 11, 2011 (8.9 Mw), which resulted to a considerable run-up in the Galápagos islands and the Ecuadorian mainland (Simons et al., 2011; Norio et al., 2011; Rentería et al., 2012; Lynett et al., 2013).

The study area comprises the city of Bahía de Caráquez, which is situated on the northern coastal area of the Province of Manabí, and is considered one of the most beautiful and picturesque sites of the entire country due to its interesting landscape and its contact with the ocean. The characteristic of this city is that of having a sinuous morphology, with hills of medium to high heights and also flat areas, being almost at sea level, which correspond to terraces of the Chone River and to deposits of sand accumulation of fluvio-marine origin (Fig. 2).



Fig. 2. Geographic setting of the study area with the city of Bahía de Caráquez, next to the village of San Vicente, separated by the Chone River. Width of image is about 17 km.

Low, practically flat areas could be severely damaged with the occurrence of a tsunami, as the waves would practically pass from one side to the other on the shoreline. Such flat area is currently occupied by a modern and important physical infrastructure, since this sector is the one with the highest added value, where also the tourist potential of the city is



Fig. 3. The city of Bahía de Caráquez with some important elements such as road network, hotels, educational institutions and other strategic buildings

concentrated. The hilly sector has been occupied by poor settlements, therefore the infrastructure is of low quality (mixed constructions), with almost no basic services, with the exception of electricity. In addition, the flanks of the hills are very unstable, especially in the rainy season and within seismic stresses. The accesses to the hilly sector lack to be easy due to the strong inclination of the land, its unstable slopes, its occupation and the vegetation cover. There are few roads to enter the sector, which are built for community purposes (access to drinking water storage tanks, radio and telephone transmission antennas, etc.), and extensive and intricate bleachers for the use of the inhabitants of this elevated sector area (Fig. 3; Barrio La Cruz, next to Mirador La Cruz).

The flat part of the city of Bahía de Caráquez is built on clastic sediments (clay and sandstone) of Miocene to the Pliocene ages, which belong to the Onzole and Borbón Formations (Stainforth, 1948). However, a large part of the extreme seaward side is built on top of fillings which stretched the city to the Lighthouse (El Faro) of the past (Fig. 3, 4). The city recently suffered great damage with the earthquake of August 4, 1998 (7.2 Mw), which epicenter was barely 3 km from the center of the city, with the far-distant tsunami of March 11, 2011 of Japan with slight damages, and lately with the earthquake of April 16, 2016 (Mw 7.8) with the epicenter about 105 km to the north (Pararas-Carayannis, 2011; Toulkeridis et al., 2017b; Morales et al., 2018; Chunga et al., 2019a; b). The city counts with some 57,159 permanent citizens, with a population density of 143.55 persons per km². An important strategic element of the city is represented by the largest bridge of the country, called “Los Caras” (Fig. 3, 5). This bridge which connects Bahía de Caráquez with San Vicente was constructed in 2010 and counts with seismic isolators (Aroca et al., 2018).



Fig. 4. Note in the image of 1960 the distance of the old Lighthouse and the main city of Bahía de Caráquez, which was later filled and the city extended.

In the peninsula of Bahía de Caráquez the tropical Savanna climate predominates, to the north the climate changes to tropical monsoon. The Savanna-type climate presents a marked dry trend between June and November, as well as a trend of rain or winters between January and April. In winter, there is greater wear on the ground cover and a greater flow of debris descending the slope, where some houses may collapse.



Fig. 5. Aerial panoramic view of Bahía de Caráquez, from north to south. Left side is the estuary of the Chone River, as well as part of the San Vicente – Bahía bridge and towards the right side is the Pacific Ocean.

The collapsed buildings in Bahía are directly related to the types of soils, which are colluvial that covered paleo-fluvial channels, where the amplifications of the seismic waves lasted longer. Other types of mainly sandy soils may also occur in the coastal plain zone. Geological field reconnaissance (Fig. 6) has allowed to corroborate the geomechanical behavior and instability of the slope, in fact, rotational and translational landslide escarpments have movement trends along the axis of the river tributaries. The easy disintegration of the rocky substrate by the runoff waters increases the openings of the traction cracks and forms subsequent collapses of silt strata. It should be noted that these strata have joints or cracks, which are filled and placed by plaster or gypsum. In several homes in the upper part of the La Cruz de Mirador site, multiple traction cracks are able to be seen with openings that reach between 15 and 30 cm, while their opening dimensions decrease when approaching the street, where there are cracks between the 10 to 15 cms. The distances between cracks are in the order of 0.8m, 1m, 1.4m and 1.6 meters apart.

Evidence of potentially active quiescent landslide escarpments are located in the frontal part near the Cruz del Mirador. From a structural geological analysis point of view, they tend structurally in the same direction $N100^{\circ}$ to $N110^{\circ}$, being the same tendency to the inclination of the slope, which makes it a site with a high level of instability. The soil layer and colluvial slope material are vertically displaced by a recent rotational-type sliding escarpment in a quiescent manner, where the vertical displacement is 40 cm high, with a trend of $N100^{\circ}$ running parallel to the direction of the inclination of the slope. This structural guideline has a bearing trend of $N12^{\circ}$.

Unstable geological features of cracks and landslide escarpments were already evident at the Cruz del Mirador site, when in 1999 the first houses began to be built in this upper part of the city of Bahía de Caráquez. In 2013, the houses already reported damage to their walls and floors, and the back part already showed signs of detachment due to being in an area of unstable natural slope. During the earthquake of 1998, in the La Cruz del Mirador sector, 56 homes that already had a record of minor damage that were left uninhabitable, collapsed during the strong earthquake of April 16, 2016 (Mw 7.8).

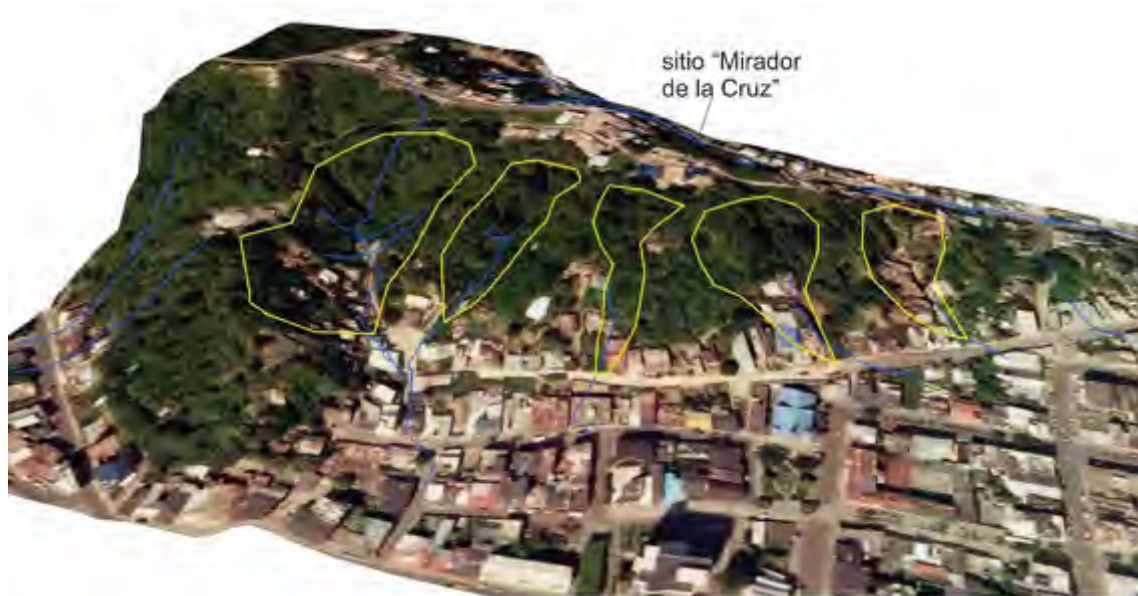


Fig. 6. Delineation of river sub-basins (yellow lines) characterized by intermittent streams, active only in winter seasons and “El Niño” phenomenon, and formation of deep furrows by incision of runoff waters on the slope, around the lower part of the “Mirador” de la Cruz site.

3. METHODOLOGY

a) Evaluation of wave heights and potential impact scenario

In this research, we use the extensively validated tsunami modelling tool, the ComMIT/MOST model (Community Model Interface for Tsunami), which is an internet-enabled interface to the community tsunami model developed by the NOAA Center for Tsunami Research (NCTR). This interface let one run the MOST model (Method of splitting tsunami), a non-linear shallow water model, which has been extensively validated from field observations and laboratory experiments (Fig. 7; Titov et al., 2011; Titov et al., 2016).

We have created a numerical domain for the coordinates $[-0.7510, -0.3868]$ $[-80.7862, -80.2887]$, a grid size of $[598 \times 438]$, with a raw resolution of 3 arcsec (~ 92.8 meters). This

is a very constraint resolution, since it limits one to differentiate the change between sea and land, and also affects the performance of the flooding algorithm of the model. The lack of high-resolution information of this area, should be considered as a constraint. This particular behavior in global bathymetry datasets, has been extensively discussed in Griffin et al., 2015.

Considering the geodynamic settings and the hazard evaluation regards to potential earthquakes in this area, we simulated a 8 Mw earthquake , which is greater than the

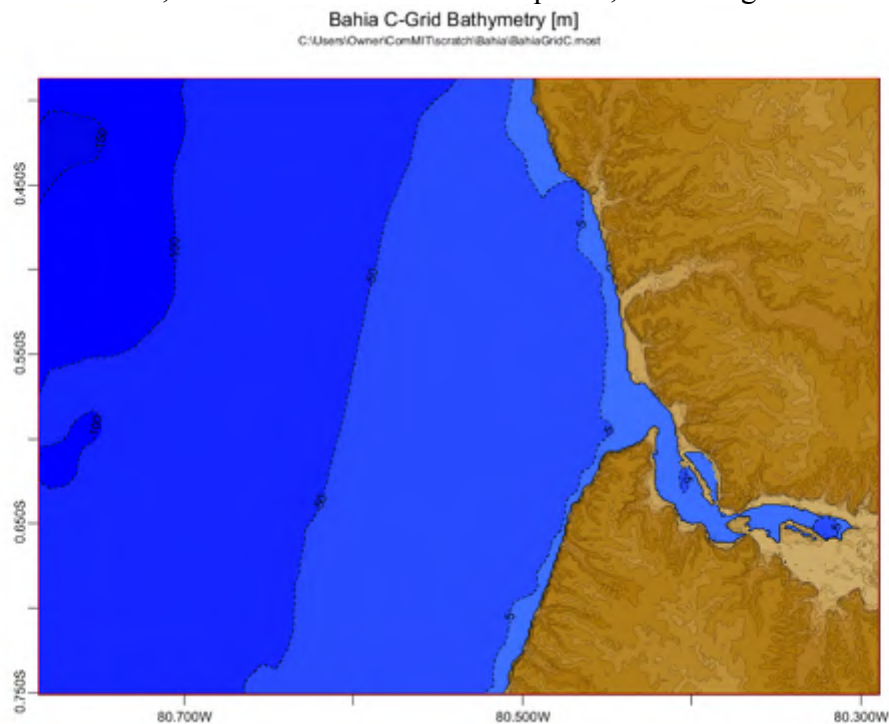


Fig. 7. Grid bathymetry for the area of interest, taken from global dataset, based on Commit/Most app.

historic events, but let us cover the lack of reliable information in the for the national catalogue about earthquakes. Based on this model, we are able to evaluate the potential model with the corresponding wave amplitude, and not the run up (Intergovernmental Oceanographic Commission, 2019). It is important do not confuse the wave amplitude with the run up, the latter is the maximum height of the water running into the land, but as we mentioned before, the data resolution constraint of ours results, in this case limiting to have a good information in horizontal flooding (Fig. 8).

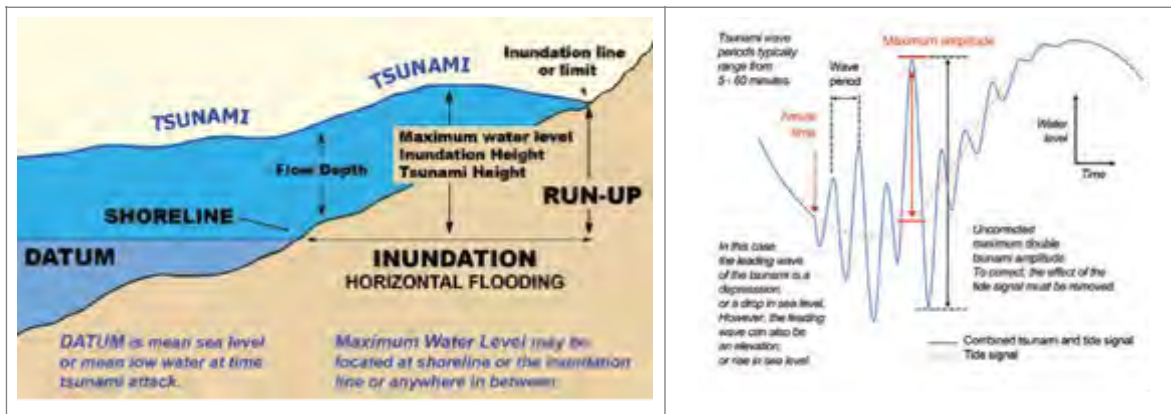


Fig. 8. Definition of Tsunami Run up and Tsunamis amplitude (Intergovernmental Oceanographic Commission, 2019)

b) Analysis of evacuation times and routes

Almost independent of the arrival times of tsunami waves, the population involved in this area needs to be evacuated when the phenomenon occurs. With this criterion, a safety distance was taken for the inhabitants of about 50m in the periphery of the potential tsunami waves, which means in a necessary margin in which the population needs to mobilize outside such sector. In other words, the flood areas were taken unifying them in a single polygon with a buffer of 50m around it, calling it the Safety Zone (SZ). The 50 meters has been decided taking as an element that offers a margin of safety that would allow anyone to escape from this area. This was decided based on safety criteria adopted from previous experiences (Saji, 2014; Wood et al., 2014; Mostafizi et al., 2019).

Hereby, for the analysis it is essential to define three elements for calculating evacuation times: safety points, evacuation points and road axes (Fig. 9). Taking the road network, the road axes were intersected with the SZ. Each of the points that are at the end of the road axes and on the edge of the SZ are the Security Points (SP). To define the Evacuation Points (EP), points were taken along the road axes located every 20 meters, which corresponds to an approximate distance between the portals of each of the houses. Subsequently, the model will be run with more precise data with points located in each portal of the homes in the study area.

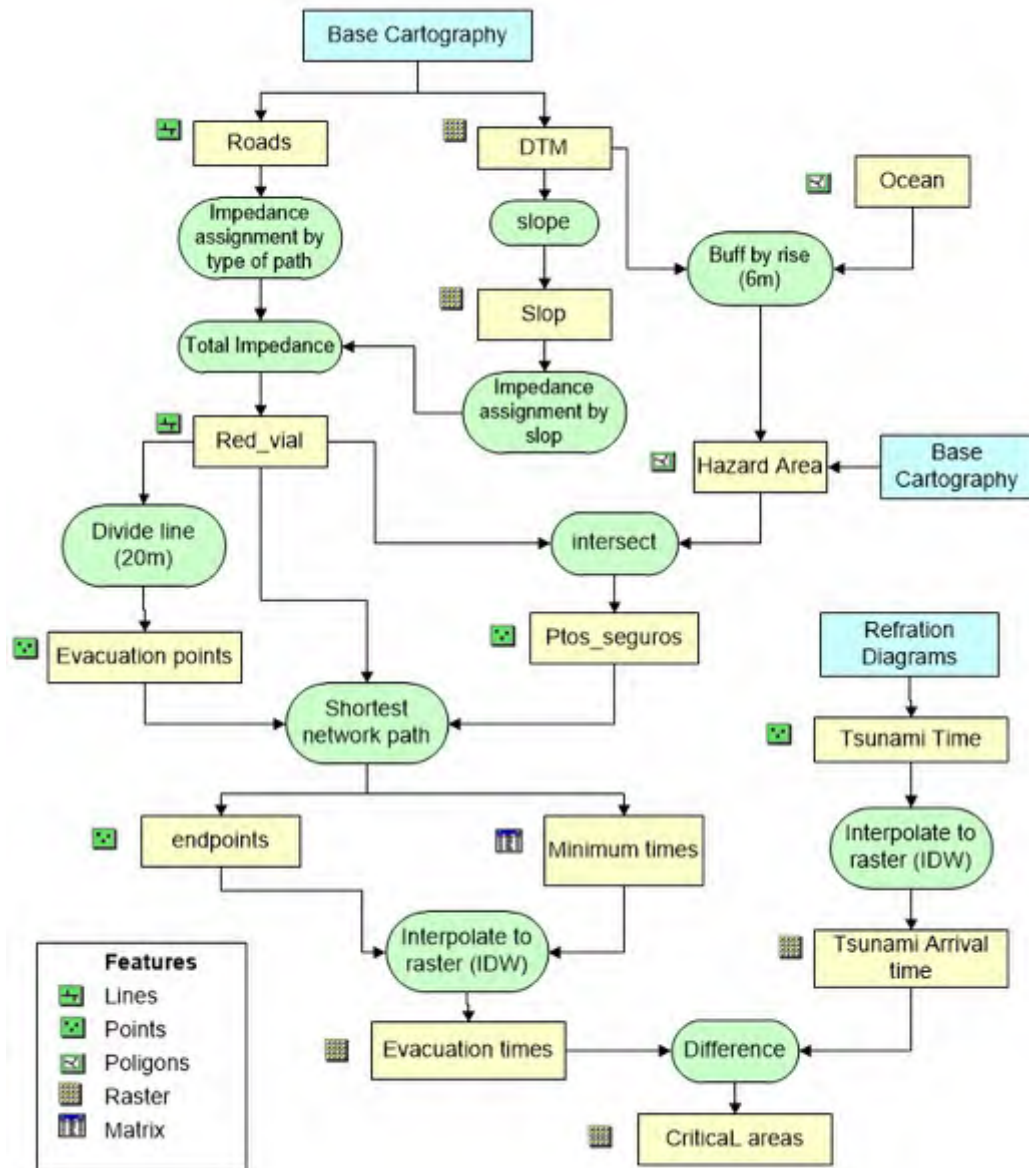


Figure 9. Methodology used in the evaluation and generation of evacuation times and routes

With these three elements SP, EP and Road Axes, the distances between each of the points of origin (EP) to each point of arrival (SP) were calculated (Fig. 10). This problem may have some possible solutions, the simplest taking into account the distances of each of the arcs between the two points. In the current study, the value multiplied by the distance of each of these segments was considered as impedance. The impedance values in each one of the roads were assigned fundamentally with the times of vehicular circulation in peak hours. The possibilities may vary only depending on the type of problem you are planning to solve. The solution could be expressed in the following equation:

$$Dc = \text{DistMin } ij (\Sigma \text{dijk} * Iijk)$$

Where:

| | |
|------------|--|
| Dc | Solution or shortest path |
| DistMin ij | Selection function of the minimum value between points i and j |
| dijk | distance of each of the arcs of the network k |
| Iijk | impedance value of each arc in the network |

The solution possibilities of this expression, depends on the initial conditions of the network and the specific problem to be solved. The total number of data can be very large, so the Shortest Network Path subroutine was used as a calculation aid, which was loaded in the ArcView 3.2 platform™, taking the total databases and selecting the lowest times in each of the routes. This database was linked to the EP elements, obtaining a map of points with the smallest values of evacuation time and the point towards which they should escape to (SP).

As mentioned, the ideal is that each portal becomes an evacuation point with information on use and number of people who live, for this it is necessary to perform the calculations with bases of the most current data and with a Workstation with good processing characteristics (Fig. 11). This point database was used to generate the Evacuation Time Map, which was calculated using the inverse distance interpolation model (IDW), which in this case gives better results because the variable that needs to be calculated must have a spatial continuity or in this case temporal, obtaining the Map of evacuation times.

The map of first wave times (Fig. 14), corresponds to the tsunami arrival times obtained in minutes, over the different zones of the work area. It contains information of a polygonal type with times in integer values, corresponding to a variable of a discrete type. For the subsequent comparison between evacuation times and times of the first wave, it is necessary that these variables be continuous, in addition, this will allow a better

cartographic representation. The previously digitized time map was taken, transforming the polygons into lines and selecting the cut segments between each unit time range, assigning it the same value in the database, for later by interpolation (ArcGis™ IDW) in order to obtain the map of arrival times of the first wave of the potential tsunami.

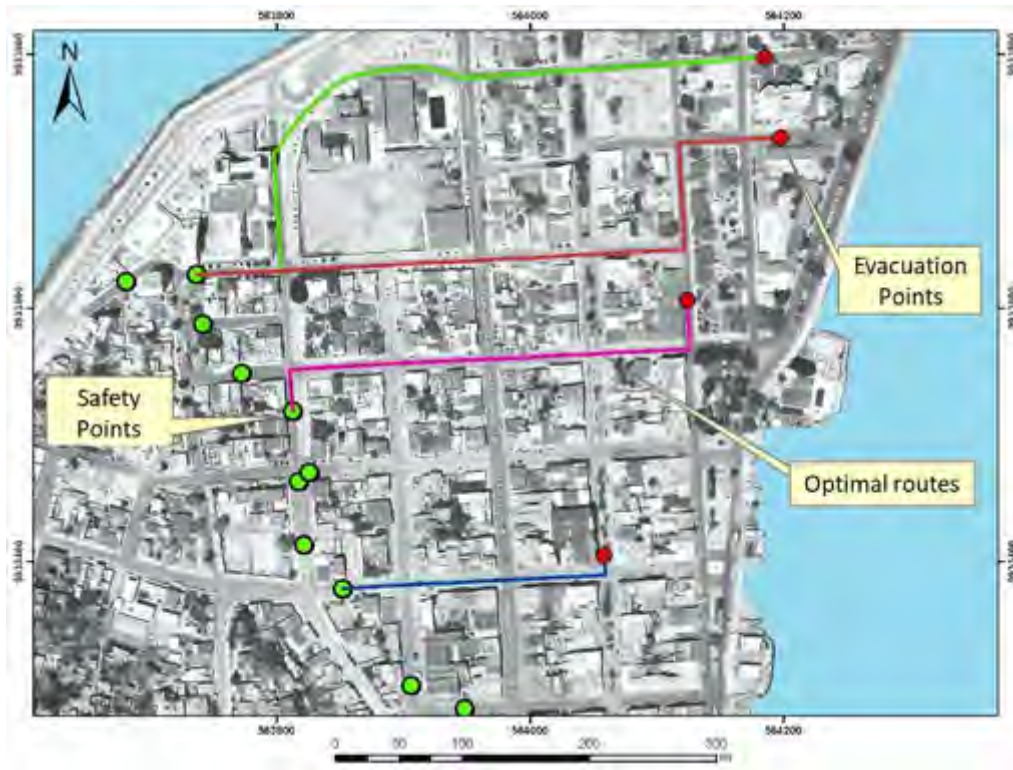


Figure 10. Evacuation and safety points along the potential most optimal routes



Figure 11. Main part of the flooded area and the analysis of given evacuation points.

With the evacuation times and first wave arrival times maps (Fig. 14), a map of time differences between the two was obtained. All positive values indicate areas in which evacuation times are greater than the arrival times of the first wave (the warning time of the first wave is not yet taken into account, based on a still uninstalled early warning system). In the map of Fig. 15 the time differences are illustrated, in which only the areas in which the values are positive (areas in conflict) are indicated, although a greater margin should be taken considering the areas where the values are close to 0 (zero).

$T_e - T_{po} \geq 0$ Conflict area

$T_e - T_{po} \approx 0$ Areas with approximately equal times

$T_e - T_{po} \leq 0$ Areas with shorter evacuation times

Where:

T_e corresponds to evacuation time

T_{po} corresponds to arrival time of the first wave

However, an additional objective has been to encounter some ways to represent these variables with a simple and intuitive cartographic language that can be understood by all those involved in the phenomenon, that is, from a technical specialist to any member of the affected population in the area, therefore the representation was chosen to be by three-dimensional variables. In order to represent different variables in the same vector space, it is necessary that they lie on the same plane (thematic variables) or the same units (heights). In this case, the aim was to represent basically two different types of variables in a three-dimensional space: time and heights. It is clear that both are on different scales and units. A simple representation solution resulted in normalizing the variables (Carver, 1991). This allowed the variables of time (minutes) and elevation (masl) to be represented in the same view.

In evacuations realized in buildings, it is estimated that an adult without physical impediments has a horizontal displacement speed of one meter per second, which would be equal to 60 meters in 1 minute (Thompson & Marchant, 1995; Zhong et al., 2008; Tsai et al., 2011). However, to calculate the evacuation times in the present work, a displacement speed of 50 meters per minute was assigned, considering that the population to evacuate includes children and the elderly. In order to calculate the evacuation times, the minimum roads calculation routine was used, using as initial data the population displacement speed of 50 meters per minute, using the following equation, for each segment of the road network (Cheng et al., 2011; Zhang et al., 2016; Sun et al., 2017).

$$Time = \frac{Impedance * Length}{Velocity}$$

In turn, with the evacuation times obtained, the critical area was calculated, that is an area in which people will not have enough time to evacuate. In such area the evacuation times are greater than the arrival times of the incoming tsunami (Fig. 15).

c) Criteria used for seismic and tsunami resistance evaluation of potential provisional shelters

A total of 26 buildings along the coastline of Bahía de Caráquez were evaluated for their seismic as well as tsunami resistance (Fig. 12) in order to assess their feasibility as provisional shelters for vertical evacuation in case of an impact by a tsunami (Fig. 9). The pre-selection of buildings was performed according to their height, considering those with more than four floors, based on the own calculation and modeling of an incoming tsunami to have a height of at least six meters. The evaluation of each building was performed by couples with civil engineering expertise in order to minimize the subjectivity.

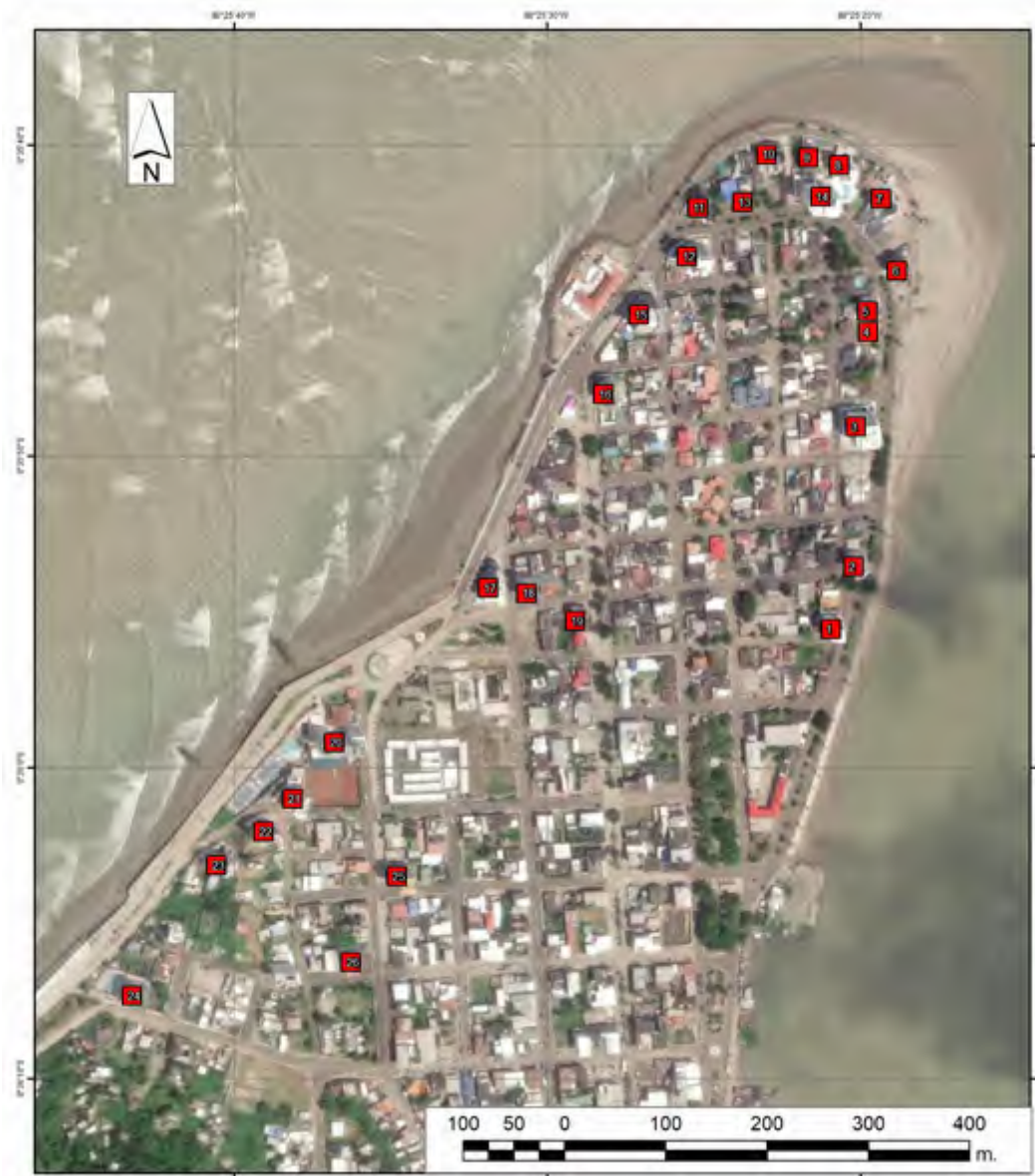


Fig 12. Map with the location of the 26 evaluated buildings

First, general data were collected such as name of the building, geographical location, address, total number of floors, number of floors below and above surface, average altitude of each floor, area and year of construction, current use as well as capacity. After this initial part, an evaluation was performed in order to reveal the seismic resistance of each building, by using twelve criteria based on the Modified Italian Methodology in order to calculate the seismic vulnerability index (SVI) (Table 1; Calvi et al., 2006; Amellal et al., 2012; Kassem et al., 2019).

Table 1: Modified Italian Methodology to calculate the SVI (Aguiar&Rivas, 2018)

| Criteria | Classes / Ki | | | Weighting W_i |
|---|--------------|----|----|-----------------|
| | A | B | C | |
| 1. Organization of the resistant system | 0 | 6 | 12 | 1,00 |
| 2. Quality of the resistant system | 0 | 6 | 12 | 0,50 |
| 3. Conventional Resistance | 0 | 11 | 22 | 1,00 |
| 4. Position of the building and foundations | 0 | 2 | 4 | 0,50 |
| 5. (Floor)Slab | 0 | 3 | 6 | 1,00 |
| 6. Floor configuration | 0 | 6 | 12 | 1,00 |
| 7. Configuration in Elevation | 0 | 11 | 22 | 1,00 |
| 8. Connection in critical elements | 0 | 3 | 6 | 0,75 |
| 9. Low ductility elements | 0 | 6 | 12 | 1,00 |
| 10. Non-structural elements | 0 | 4 | 10 | 0,25 |
| 11. State of Conservation | 0 | 10 | 20 | 1,00 |
| 12. Structure reinforced after earthquake | 0 | 11 | 22 | 1,00 |

Furthermore, we added an additional evaluation, for the corresponding tsunami resistance of each building (Table 2). Hereby, the tsunami evaluation contained ten criteria which were defined by following the Guidelines for Design of Structures for Vertical Evacuation from Tsunamis of the Federal Emergency Management Agency of the United States of America (FEMA, 2019).

Table 2. Methodology to calculate the tsunami vulnerability index

| Criteria | Classes / Ki | | | Weighting Wi |
|---|--------------|----|----|-----------------|
| | A | B | C | |
| 1. Building orientation | 0 | 6 | 12 | 1,2 |
| 2. Access. Entrance | 0 | 6 | 12 | 1,2 |
| 3. Access. Stairs | 0 | 6 | 12 | 1,2 |
| 4. Building location. Potential hazards | 0 | 6 | 12 | 0,5 |
| 5. Building location. Parking, traffic, streets | 0 | 6 | 12 | 0,5 |
| 6. Structural system | 0 | 6 | 12 | 1,00 |
| 7. Foundation system | 0 | 6 | 12 | 0,5 |
| 8. Year of construction | 0 | 6 | 12 | 1,00 |
| 9. Building Height | 0 | 11 | 22 | 1,50 |
| 10. Floor system | 0 | 6 | 12 | 1,00 |

In both the seismic and the tsunami evaluation of vulnerability, each criteria was classified in three vulnerability classes, being “A”, “B” and “C”. In this case “A” shall represent the most resistant building, while “C” shall reflect the most vulnerable structure, where each class corresponds to a value (Ki). Furthermore, each criteria was assigned to a fixed weighting coefficient (Wi) according to the importance of the criteria. The total seismic and tsunami vulnerability index for each building was calculated according to the equation:

$$I_v = \sum_{i=1}^{12(S) \text{ or } 10(T)} K_i W_i$$

According to table 1, the maximum value for the seismic vulnerability index is 143 while the maximum value for the tsunami vulnerability index is 130.2 (Table 2). Considering the aforementioned, the following general categorization for vulnerability is proposed:

- Resistant structure
if $I_v \leq 30$
- Highly vulnerable structure
If $I_v \geq 80$

Further evaluation is needed:

If $30 < I_v < 80$

This occurs especially with the calculation of the ratio between the building height and the vibration period of the structure (Duque Eslava et al., 2017; Aguiar and Zambrano 2018; Rodriguez, 2019).

4. RESULTS AND DISCUSSION

a) Wave height of tsunami

Based on the used Community Model Interface for Tsunami, our results suggest a tsunami wave height from 2 to 3 meters along the coast, which has been computed without the influence of the tide, taking the reference level to the mean sea level. According to the Tide table of INOCAR, we have a tide range of 3 meters, which means that we need plus 1.5 meters due the high tide, then easily the wave amplitude at the coastline should reach the 4.5 meters (Fig. 12). Considering the bathymetry constraint as it has been showed by Griffin et al., 2015, the models results along the coastline, showing the maximum wave amplitude.

b) Evacuation times and routes

Unfortunately, in the entire country of Ecuador and similar to equivalent developing countries, land use with respect to hazards zoning has not been a priority in the state's policy as evidenced in several cases (Suango Sánchez et al., 2019; Echegaray-Aveiga et al., 2019; Herrera-Enríquez et al., 2020; Robayo et al., 2020; Zapata et al., 2020; Barreto-Álvarez et al., 2020). Bahía de Caráquez is not an exception, where, in order to extend the city's land, landfilling has been applied in order to expand the area of construction towards the previously islet of the Lighthouse (El Faro) by incorporating it. This extension, is nowadays an enlargement of the city's vulnerability towards potential tsunamis and represents additionally an instability in respect to future earthquake shaking. Therefore, logically, in the city of Bahía de Caráquez, the areas furthest from the beaches of Pacific Ocean and the estuary of the Chone River, which correspond to the foothills and the hills themselves, are considered to be relatively safe. Therefore, the inhabitants of the central neighborhoods, located at the foot of the hills, need shorter evacuation times (between 0 to 8 minutes) to reach these sectors (Fig. 12).

The population located in the vicinity of the boardwalk, both in the beach sector and along the river bank, is far from the indicated safety zone, which is approximately 1 kilometer away, so it needs longer evacuation times. This evacuation time is between 16 to 24 minutes, as can be seen in figure 11.

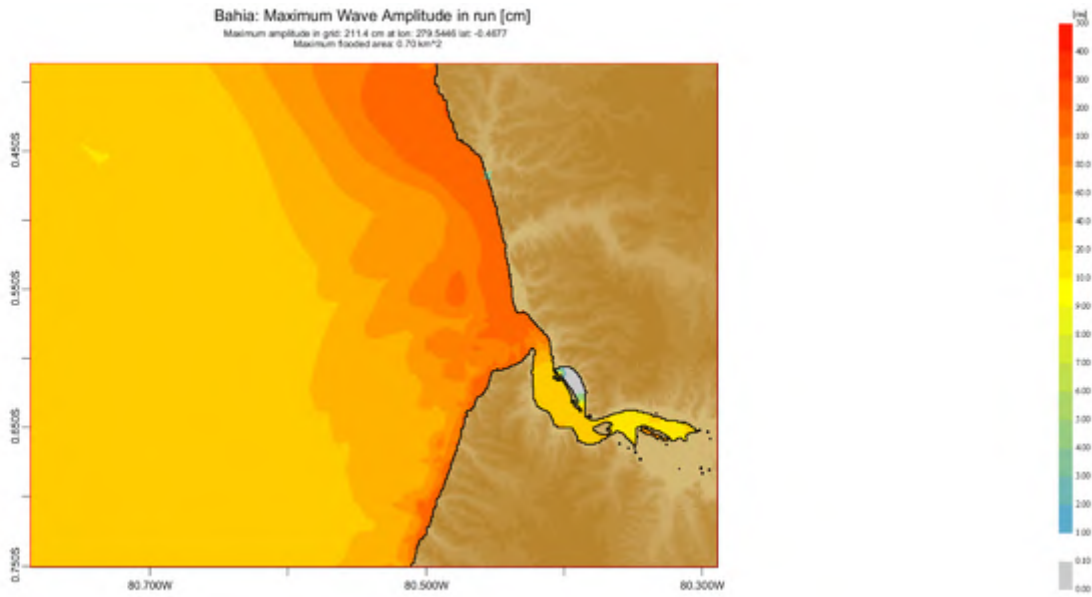


Fig. 12: Maximum Wave Amplitude, MWA, along the coastline cover the Bahia de Caraquez area. Note the MWA is in the range 2-3 meters.



Figure 13. Map with the evacuation times



Figure 14. Map with tsunami arrival times

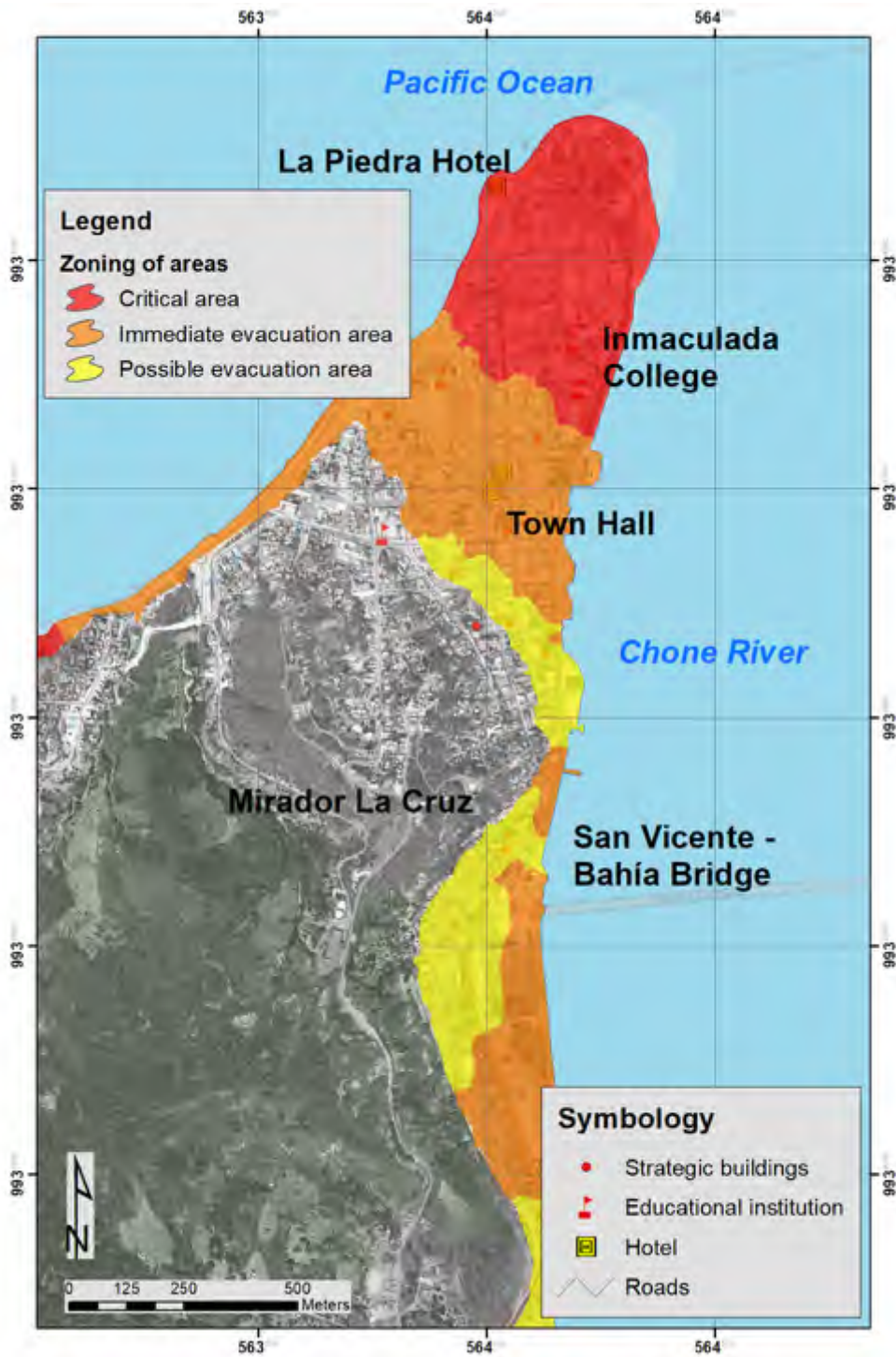


Figure 15. Zoning of areas in respect of the calculated evacuation times of the public and the modeled and calculated arrival times of the potential tsunami.

The times calculated for the arrival of the first wave are in the order of 4 to 12 minutes (Fig. 13). For this reason, the sector next to the Pacific Ocean constitutes a critical area, highly vulnerable, as shown in figure 12. The side of the city that faces the Chone River will also be impacted by the tsunami wave, but a little later than the seaside. The southern part of the city towards the San Vicente - Bahía Bridge will be impacted as the latest part of the incoming tsunami.

Taking into consideration the results of Fig. 13 of the time of the horizontal evacuation together with the results of Fig. 14 of the tsunami arrival times, we elaborated a zoning of the different degrees of vulnerability in form of distinctive areas, being critical areas, areas of immediate evacuation and areas possible evacuation (Fig. 15). Therefore, the only alternative for survival for the population located in critical areas is vertical evacuation in buildings considered earthquake-resistant and also tsunami-resistant, that is, in those in which it is certain that they will not suffer structural damage from effect of the generating earthquake or by the hydraulic effect of the waves, or having vehicles for mass transport of people, which can evacuate towards the upper parts or towards the interior, that is, south of the city, and away from the Chone River, as appropriate.

Furthermore, due to its characteristics, also the “Dos Caras” bridge, which connects San Vicente with the city of Bahía de Caráquez may be considered a safe area or site for the incoming tsunami. This bridge, as aforementioned, counts with seismic isolators and has withstood without any damage the most recent 7.8Mw earthquake of 2016, while a variety of buildings collapsed on both ends of the bridge (Toulkeridis et al., 2017b; Aroca et al., 2018).

c) Seismic and tsunami vulnerability assessment of existing buildings

The property status, as well the use, of all the buildings evaluated is private. A high percentage (96.15%) of the 26 buildings are of residential use, and only one of the damaged buildings (# 25) was previously used as a hotel (Fig. 16, 17). As for the year of construction, seventeen (65.38%) of the buildings were constructed prior to the earthquake of 1998 with 1990, 1993 and 1994 as the most frequent years of construction. Another seven were built after the earthquake of 1998, and two more buildings are less than five years old, therefore, those two were built after the Ecuador earthquake (Mw 7.8) of the 16 April 2016. The total area of construction of the 26 buildings sum up to more than 9000 m², while the average area of construction is 367,4 m². The largest area of construction corresponds to the building Dos Hemisferios (#20) with 1720 m² followed by the Centinela (#24) with 1200 m² and Ocean Bay Tower (#15) with 710 m², a higher area of construction would be related to a higher capacity in case of evacuation. Regarding the total number of floors, most of the buildings, a total of twenty, present eight, nine or ten floors whereas four buildings have less than seven floors. Two buildings reach eleven floors. Only two out of the 26 buildings have one and two floors respectively below the surface.

Concerning the average altitude of each floor, the minimum is 2.4 meters while the maximum is 3.5 meters. Seven buildings show an average altitude of ≤ 2.6 meters per floor

whereas four buildings reach more than 3 meters per floor. The most frequent average altitude per floor are 3 and 2.8 meters with nine and five buildings respectively. 22 out of the 26 buildings are located right in the beachfront (Fig.12) and within the critical and immediate evacuation area (Fig.15) Among the 26 buildings evaluated, 4 of them exhibit clear damage and were uninhabited and abandoned, while 3 of them are in their last stage of construction as January 2021.



Figure 16. A: Akuaba (#1); B: Nautilus (#2); C: Albatros (#4); D: Spondylus (#5); E: Capitán (#8); F: Ocean Bay Tower (#15); G: Torre Mariana (#26); H: Dos hemisferios(#20).



Figure 17. A: Agua Marina (#16); B: No name, damaged (#19); C: Sucre (#21); D: Horizonte (#22); E: Las Brisas (#23); F: Hotel Patricio's (#25).

The building stock exhibits an intermediate overall seismic vulnerability, as the nine resistant structures with vulnerability index (I_v) ≤ 30 account for about 34.61 % in terms of number of buildings, while highly vulnerable buildings with $I_v \geq 80$ sum up five of them. Almost half of the evaluated structures (12, 46.15%) exhibit a seismic vulnerability index between 30 and 80, therefore, further evaluation is needed. The minimum seismic I_v is 9 and is achieved by two buildings, being Akuaba (#1) and by the building El Faro (#12). The highest vulnerability index values are performed, as expected, by the four buildings that are already abandoned due to their damage during previous earthquakes (Table 3). Since they could possibly collapse in future earthquakes posing a threat to adjacent buildings and inhabitants, these four buildings should be subject to a controlled demolition.

The distribution of the nine seismic resistant structures is heterogenous across the evaluated area, although a slight higher concentration of four safe buildings could be encountered towards the northeastern tip of the peninsula of Bahía de Caráquez (Fig. 18). Three of those buildings, being Albatros (#4), Torre Mar (#6) and Cariló (#14) are recent constructions from 2019, 2018 and 2015 respectively, whereas Mykonos is an exception for being an older construction from 1993.

Table 3: Summary of seismic and tsunami vulnerability index (Iv)

| Building | Seismic Index | Tsunami Index |
|---------------------|----------------------|----------------------|
| 1-Akuaba | 9.00 | 43.8 |
| 2-Nautilus | 42.00 | 39.6 |
| 3-Torre Molinos | 38.25 | 52.2 |
| 4-Albatros | 28.25 | 34.2 |
| 5-Spondylus | 43.50 | 52.8 |
| 6-Torre Mar | 14.00 | 40.8 |
| 7-Mykonos | 26.00 | 32.4 |
| 8-Capitán | 43.25 | 58.5 |
| 9-Vista Mar | 48.50 | 49.8 |
| 10-Neptuno | 54.75 | 48.6 |
| 11-Punta Norte | 105.25 | 72.0 |
| 12-El faro | 9.00 | 37.8 |
| 13-Las Gaviotas | 56.75 | 69.8 |
| 14-Cariló | 18.00 | 20.4 |
| 15-Ocean Bay Tower | 34.00 | 36.6 |
| 16-Agua Marina | 34.00 | 36.6 |
| 17-El Pirata | 12.00 | 58.2 |
| 18-Torre Sol | 93.25 | 64.2 |
| 19-No Name, damaged | 95.25 | 68.0 |
| 20-Dos Hemisferios | 45.50 | 48.6 |

| | | |
|---------------------|--------|------|
| 21-Sucre | 49.00 | 30.6 |
| 22-Horizonte | 19.00 | 46.8 |
| 23-Las Brisas | 126.50 | 73.0 |
| 24-Centinela | 26.00 | 40.8 |
| 25-Hotel Patricio's | 116.50 | 75.6 |
| 26-Torre Mariana | 54.00 | 36.6 |

All of the buildings evaluated, except one, exhibit a tsunami vulnerability index (I_v) between 30 and 80, hence, require further evaluation for tsunami resistance. None of the structures reach $I_v \geq 80$. Only one out of 26 buildings is categorized as a tsunami resistant structure with $I_v \leq 30$, being the building Cariló (#14) with a TVI of 20.4. However, another seven buildings indicate tsunami vulnerability indexes below 38 being moderately close to the tsunami resistant category (Table 3).

Therefore, when assessing together the seismic and tsunami vulnerability indexes, only one building is categorized as resistant to both hazards and could be considered for vertical evacuation in case of tsunami impact. Building Cariló (#14) is the only structure with I_v lower than 30 for both the seismic and tsunami assessments, which seems to be related to a combination of attributes including that it was built in 2015 following the stricter building standards established in the Ecuadorian Code of Construction (NEC), hence, it did not suffer structural damage at all when it was hit by the earthquake of 2016 (NEC, 2015). The structural attributes that allows to be Cariló a resistant seismic and tsunami building include a strong and well organized system with reserve capacity to resist extreme forces as well as an adequate connection in critical elements.

Furthermore, the long direction of Cariló is oriented parallel to the most potential direction of the incoming tsunami wave from the Pacific coast, hence, it will experience smaller hydrodynamic forces. It is one of the few buildings evaluated which is not in the beachfront but in a second beach line, and features a large entrance from a wider street than the street right by the estuary where buildings #6 to #12 are located. Overall, Cariló is located in the critical tsunami area (Fig. 15 and 18) and could serve to evacuate around 200 people thanks to its ten floors of height, and the amplitude of its construction area (600 m²).

Moreover, we propose physical adaptations to improve the vertical circulation to the appropriate shelter level of the structure such as installation of supplemental entrances, ramps, and stairs. In order to facilitate the construction, and provide unobstructed access with high visibility, the auxiliary ingress could be placed in the exterior of the structure (FEMA, 2019). As a further option, the city of Bahía de Caráquez should consider the design and construction of a public and accessible multipurpose tsunami resistant building in the central area of the critical zone (Fig. 15) equidistant to the hilly sector and the Cariló

building, which could serve to evacuate the people who could reach neither the hills nor the Cariló. All of the proposed activities in case of a potential disaster by an incoming tsunami are pending of the implementation of an early alert system as previously proposed (Toulkeridis et al., 2018; 2019).



Fig.18. Maps representing the three categories assigned to seismic and tsunami vulnerability of the evaluated buildings. Green: Resistant structure with $I_v \leq 30$; Orange: Further evaluation is needed with $30 < I_v < 80$, and Red: Highly vulnerable structure with $I_v \geq 80$.

5. CONCLUSIONS

The population and the tourists of the city of Bahía de Caráquez have only a limited time to reach an elevated, safe area in case of an incoming tsunami. Such area would be the hilly, southern part of the city.

Based on the vulnerability evaluation of seismic and tsunami resistance of the 26 existing buildings along the Chone river and the beachside towards the Pacific Ocean, we may ascertain that many of the buildings could withstand a seismic event and most potentially an impact by a tsunami.

The 26 evaluated buildings have a limited if any capacity of obtaining the escaping public in case of an incoming tsunami, as being almost all in private property, lack to allow

other than residents to enter the buildings and perform a vertical evacuation. Although currently only one building is considered suitable as potential tsunami shelter, other buildings could improve their tsunami performance if access is improved, ideally through external adaptations.

It is necessary to implement an early alert system for tsunamis and have an agreement between municipality and owners of the buildings which will allow the escaping public and tourists to enter the buildings and stay safe in elevated floors during a tsunami crisis.

6. REFERENCES

- Aguiar, R. & Rivas, A. (2018). Microzonificación sísmica de Ambato. Gobierno Autónomo Descentralizado de Ambato, Ambato, Ecuador.
- Aguiar, R. & Zambrano, V. (2018). Relation h/t in structures of Bahía de Caraquez and the 2016 Earthquake. *Revista Internacional de Ingeniería de Estructuras*, 23, 2, 227-241
- Aguilera, C., Viteri, M., Seqqat, R., Ayala, L., Toulkeridis, T., Ruano, A., & Torres, M. (2018). Biological impact of exposure to extremely fine-grained volcanic ash. *Journal of Nanotechnology*, Article number 7543859
- Alcántara-Ayala, I. (2002). Geomorphology, natural hazards, vulnerability and prevention of natural disasters in developing countries. *Geomorphology*, 47(2-4), 107-124.
- Amellal, O., Bensaibi, M., & Grine, K. (2012). Seismic vulnerability index method for steel structures. In *Proceedings of the 15th World Conference on Earthquake Engineering (WCEE)*.
- Aroca, J., Gómez, M., Morales, E., & Romo, M. (2018). Study of the performance of seismic isolators of Pier no. 12 of the Bridge "Los Caras", during the earthquake of April 16. *Revista Internacional de Vol*, 23(3), 305-339.
- Aviles-Campoverde, D., Chunga, K., Ortiz-Hernández, E., Vivas-Espinoza, E., Toulkeridis, T., Morales-Delgado, A., & Delgado-Toala, D. (2021). Seismically induced soil liquefaction and geological conditions in the city of Jama due to the Mw7.8 Pedernales earthquake in 2016, NW Ecuador. *Geosciences*, 11, 20
- Barreto-Álvarez, D.E., Heredia-Rengifo, M.G., Padilla-Almeida, O. & Toulkeridis, T. (2020). Multitemporal evaluation of the recent land use change in Santa Cruz Island, Galapagos, Ecuador. In *Conference on Information and Communication Technologies of Ecuador* (pp. 519-534). Springer, Cham.
- Barros, J. L., Tavares, A. O., Santos, A., & Fonte, A. (2015). Territorial vulnerability assessment supporting risk managing coastal areas due to tsunami impact. *Water*, 7(9), 4971-4998.
- Belash, T. A. & Yakovlev, A. D. (2018). Seismic stability of a tsunami-resistant residential buildings. *Magazine of Civil Engineering*, 80(4).

- Berninghausen, W.H. (1962). Tsunamis reported from the west coast of South America 1562-1960. *Bull. of the Seismological Soc. of America*, 52 (4): 915-921.
- Calgaro, E. and Lloyd, K. (2008). Sun, sea, sand and tsunami: examining disaster vulnerability in the tourism community of Khao Lak, Thailand. *Singapore Journal of Tropical Geography*, 29(3), 288-306.
- Calgaro, E., Dominey-Howes, D., & Lloyd, K. (2014). Application of the Destination Sustainability Framework to explore the drivers of vulnerability and resilience in Thailand following the 2004 Indian Ocean Tsunami. *Journal of Sustainable Tourism*, 22(3), 361-383.
- Calvi, G. M., Pinho, R., Magenes, G., Bommer, J. J., Restrepo-Vélez, L. F., & Crowley, H. (2006). Development of seismic vulnerability assessment methodologies over the past 30 years. *ISET journal of Earthquake Technology*, 43(3), 75-104.
- Cannon, T. (1994). Vulnerability analysis and the explanation of 'natural' disasters. *Disasters, development and environment*, 1, 13-30.
- Carver, S. J. (1991). Integrating multi-criteria evaluation with geographical information systems. *International Journal of Geographical Information System*, 5(3), 321-339.
- Celorio-Saltos, J.C., García-Arias, J.M., Guerra-Luque, A.B., Barragan-Aroca, G., & Toulkeridis, T. (2018). Vulnerability analysis based on tsunami hazards in Crucita, central coastal of Ecuador. *Science of Tsunami Hazards*, 38(3): 225-263.
- Cheng, C., Qian, X., Zhang, Y., Wang, Q., & Sheng, J. (2011). Estimation of the evacuation clearance time based on dam-break simulation of the Huaxi dam in Southwestern China. *Natural Hazards*, 57(2), 227-243.
- Chunga, K. & Toulkeridis, T. (2014). First evidence of paleo-tsunami deposits of a major historic event in Ecuador. *Science of tsunami hazards*, 33: 55-69.
- Chunga, K., Mulas, M., Alvarez, A., Galarza, J., & Toulkeridis, T. (2019a): Characterization of seismogenetic crustal faults in the Gulf of Guayaquil, Ecuador. *Andean Geology*, 46(1): 66-81.
- Chunga, K., Livio, F.A., Martillo, C., Lara-Saavedra, H., Ferrario, M.F., Zevallos, I., & Michetti, A.M. (2019b). Landslides Triggered by the 2016 Mw 7.8 Pedernales, Ecuador Earthquake: Correlations with ESI-07 Intensity, Lithology, Slope and PGA-h. *Geosciences*, 9, 371.
- Chunga K., Livio F., Mulas M., Ochoa-Cornejo, Besenzon D., Ferrario M., & Michetti AM. (2018). Earthquake ground effects and intensity of the 16 April 2016, Mw 7.8 Pedernales Earthquake (Ecuador): implications for the source characterization of large subduction earthquakes. *Bulletin of the Seismological Society of America* 108 (6): 3384-3397.
- Chunga, K., Toulkeridis, T., Vera-Grunauer, X., Gutierrez, M., Cahuana, N., & Alvarez, A. (2017). A review of earthquakes and tsunami records and characterization of capable faults on the northwestern coast of Ecuador. *Science of tsunami hazards*, 36: 100-127.

- Duque Eslava, A.C., Rojas Mendoza, F. A., Rodríguez Gómez, H., & Vielma Pérez, J.C. (2017). Analysis of outer RC beam-column joint strengthened with CFRP. *Revista Internacional de Ingeniería de Estructuras*, 22, 2, 113-134.
- Echegaray-Aveiga, R.C., Rodríguez, F., Toulkeridis, T., & Echegaray-Aveiga, R.D. (2019). Effects of potential lahars of the Cotopaxi volcano on housing market prices. *J. of Applied Volcanology*, 9, 1-11.
- Edler, D., Otto, K.H., & Toulkeridis, T. (2020). Tsunami hazards in Ecuador – Regional differences in the knowledge of Ecuadorian high-school students. *Science of Tsunami Hazards*, 39(2), 86-112.
- Egbue, O., & Kellogg, J. (2010). Pleistocene to present North Andean “escape”. *Tectonophysics*, 489(1-4), 248-257.
- FEMA (2019). Guidelines for design of structures for vertical evacuation from tsunamis. FEMA P646. Washington, DC: FEMA. 202pp
- Frankenberg, E., Sikoki, B., Sumantri, C., Suriastini, W., & Thomas, D. (2013). Education, vulnerability, and resilience after a natural disaster. *Ecology and society: a journal of integrative science for resilience and sustainability*, 18(2), 16.
- Glass, J. B., Fornari, D. J., Hall, H. F., Cougan, A. A., Berkenbosch, H. A., Holmes, M. L.,... & De La Torre, G. (2007). Submarine volcanic morphology of the western Galápagos based on EM300 bathymetry and MR1 side-scan sonar. *Geochemistry, Geophysics, Geosystems*, 8(3).
- Griffin, J., Latief, H., Kongko, W., Harig, S., Horspool, N., Hanung, R., ... & Cummins, P. (2015). An evaluation of onshore digital elevation models for modeling tsunami inundation zones. *Frontiers in Earth Science*, 3, 32.
- Gusiakov, V. K. (2005). Tsunami generation potential of different tsunamigenic regions in the Pacific. *Marine Geology*, 215(1-2), 3-9.
- Gutscher, M.A., Malavieille, J.S.L., & Collot, J.-Y. (1999). Tectonic segmentation of the North Andean margin: impact of the Carnegie Ridge collision. *Earth and Planetary Science Letters* 168, 255–270.
- Heidarzadeh, M., Murotani, S., Satake, K., Takagawa, T., & Saito, T. (2017). Fault size and depth extent of the Ecuador earthquake (Mw 7.8) of 16 April 2016 from teleseismic and tsunami data. *Geophysical Research Letters*, 44(5), 2211-2219.
- Herd, D. G., Youd, T. L., Meyer, H., Arango, J. L., Person, W. J., & Mendoza, C. (1981). The great tumaco, colombia earthquake of 12 december 1979. *Science*, 211(4481), 441-445.
- Herrera-Enríquez, G., Toulkeridis, T., Rodríguez-Rodríguez, G., & Albuja-Salazar (2020). Critical Factors of Business Adaptability during Resilience in Baños de Agua Santa, Ecuador, due to Volcanic Hazards . CIT, in press
- Intergovernmental Oceanographic Commission. Fourth Edition. *Tsunami Glossary* (2019). Paris, UNESCO, IOC Technical Series, 85. (English, French, Spanish, Arabic, Chinese) (IOC/2008/TS/85 rev.4).

- Ioualalen, M., Monfret, T., Béthoux, N., Chlieh, M., Adams, G. P., Collot, J. Y., ... & Gordillo, G. S. (2014). Tsunami mapping in the Gulf of Guayaquil, Ecuador, due to local seismicity. *Marine Geophysical Research*, 35(4), 361-378.
- Ioualalen, M., Ratzov, G., Collot, J. Y., & Sanclemente, E. (2011). The tsunami signature on a submerged promontory: the case study of the Atacames Promontory, Ecuador. *Geophysical Journal International*, 184(2), 680-688.
- Jaramillo Castelo, C.A., Padilla Almeida, O., Cruz D'Howitt, M., & Toulkeridis, T. (2018). Comparative determination of the probability of landslide occurrences and susceptibility in central Quito, Ecuador. 2018 5th International Conference on eDemocracy and eGovernment, ICEDEG 2018 8372318: 136-143.
- Kanamori, H. & McNally, K.C. (1982). Variable rupture mode of the subduction zone along the Ecuador-Colombia coast. *Bulletin of the Seismological Society of America*, 72(4): 1241-1253.
- Kassem, M. M., Nazri, F. M., & Farsangi, E. N. (2019). Development of seismic vulnerability index methodology for reinforced concrete buildings based on nonlinear parametric analyses. *MethodsX*, 6, 199-211.
- Kates, R. W. (1976). Experiencing the environment as hazard. In *Experiencing the environment* (pp. 133-156). Springer, Boston, MA.
- Keating, B. H., & McGuire, W. J. (2000). Island edifice failures and associated tsunami hazards. *Pure and Applied Geophysics*, 157(6-8), 899-955.
- Kellogg, J. N., Vega, V., Stallings, T. C., & Aiken, C. L. (1995). Tectonic development of Panama, Costa Rica, and the Colombian Andes: constraints from global positioning system geodetic studies and gravity. *Special Papers-Geological Society of America*, 75-75.
- Lukkunaprasit, P., & Ruangrassamee, A. (2008). Building damage in Thailand in the 2004 Indian Ocean tsunami and clues for tsunami-resistant design. *The IES Journal Part A: Civil & Structural Engineering*, 1(1), 17-30.
- Lynett, P., Weiss, R., Renteria, W., Morales, G. D. L. T., Son, S., Arcos, M. E. M., & MacInnes, B. T. (2013). Coastal impacts of the March 11th Tohoku, Japan tsunami in the Galapagos Islands. *Pure and Applied Geophysics*, 170(6-8), 1189-1206.
- Martinez, N. & Toulkeridis, T. (2020). Tsunamis in Panama – History, preparation and future consequences. *Science of Tsunami Hazards*, 39(2), 53-68.
- Matheus Medina, A.S., Cruz D'Howitt, M., Padilla Almeida, O., Toulkeridis, T., & Haro, A.G. (2016). Enhanced vertical evacuation applications with geomatic tools for tsunamis in Salinas, Ecuador. *Science of Tsunami Hazards*, 35, (3): 189-213
- Matheus-Medina, A.S., Toulkeridis, T., Padilla-Almeida, O., Cruz-D' Howitt, M., & Chunga, K. (2018). Evaluation of the tsunami vulnerability in the coastal Ecuadorian tourist centers of the peninsulas of Bahia de Caráquez and Salinas. *Science of Tsunami Hazards*, 38(3): 175-209.

- Mato, F. & Toulkeridis, T. (2017). The missing Link in El Niño's phenomenon generation. *Science of tsunami hazards*, 36: 128-144.
- McGuire, W. J. (2006). Lateral collapse and tsunamigenic potential of marine volcanoes. *Geological Society, London, Special Publications*, 269(1), 121-140.
- Mendoza, C., & Dewey, J. W. (1984). Seismicity associated with the great Colombia-Ecuador earthquakes of 1942, 1958, and 1979: Implications for barrier models of earthquake rupture. *Bulletin of the seismological society of America*, 74(2), 577-593.
- Meyyappan, P., Sekar, T., & Sivapragasam, C. (2013). Investigation on Behaviour Aspects of Tsunami Resistant Structures-An Experimental Study. *Disaster advances*, 6(2), 39-47.
- Mikami, T., Shibayama, T., Esteban, M., & Matsumaru, R. (2012). Field survey of the 2011 Tohoku earthquake and tsunami in Miyagi and Fukushima prefectures. *Coastal Engineering Journal*, 54(1), 1250011-1.
- Moberly, R., Shepherd, G. L., & Coulbourn, W. T. (1982). Forearc and other basins, continental margin of northern and southern Peru and adjacent Ecuador and Chile. *Geological Society, London, Special Publications*, 10(1), 171-189.
- Morales, E., Filiatrault, A., & Aref, A. (2018). Seismic floor isolation using recycled tires for essential buildings in developing countries. *Bulletin of Earthquake Engineering*, 16(12), 6299-6333.
- Mostafizi, A., Wang, H., Cox, D., & Dong, S. (2019). An agent-based vertical evacuation model for a near-field tsunami: Choice behavior, logical shelter locations, and life safety. *International journal of disaster risk reduction*, 34, 467-479.
- Navas, L., Caiza, P., & Toulkeridis, T. (2018). An evaluated comparison between the molecule and steel framing construction systems – Implications for the seismic vulnerable Ecuador. *Malaysian Construct. Res. J.* 26 (3), 87–109.
- NEC (Norma Ecuatoriana de la Construcción) (2015). *Estructura de Acero, Cargas No Sísmicas*.
- Norio, O., Ye, T., Kajitani, Y., Shi, P., & Tatano, H. (2011). The 2011 eastern Japan great earthquake disaster: Overview and comments. *International Journal of Disaster Risk Science*, 2(1), 34-42.
- Padrón, E., Hernández, P.A., Marrero, R., Melián, G, Toulkeridis, T., Pérez., N.M., Virgili, G., & Notsu, K. (2008). Diffuse CO₂ emission rate from the lake-filled Cuicocha and Pululagua calderas, Ecuador. *Journal of Volcanology and Geothermal Research (Special Volume on Continental Ecuador volcanoes)*, 176: 163-169.
- Padrón, E., Hernández, P.A., Pérez, N.M., Toulkeridis, T., Melián, G., Barrancos, J., Virgili, G., Sumino H., & Notsu, K. (2012). Fumarole/plume and diffuse CO₂ emission from Sierra Negra volcano, Galapagos archipelago. *Bull. Of Volcanol.*, 74: 1509-1519.

- Palacios Orejuela, I. & Toulkeridis, T. (2020). Evaluation of the susceptibility to landslides through diffuse logic and analytical hierarchy process (AHP) between Macas and Riobamba in Central Ecuador. 2020 7th International Conference on eDemocracy and eGovernment, ICEDEG 2020, 200-206
- Papathoma, M., & Dominey-Howes, D. (2003). Tsunami vulnerability assessment and its implications for coastal hazard analysis and disaster management planning, Gulf of Corinth, Greece. *Natural Hazards and Earth System Sciences*, 3(6), 733-747.
- Papathoma, M., Dominey-Howes, D., Zong, Y., & Smith, D. (2003). Assessing tsunami vulnerability, an example from Herakleio, Crete. *Natural Hazards and Earth System Sciences*, 3(5), 377-389.
- Pararas-Carayannis, G. (1977). Catalog of tsunamis in Hawaii (Vol. 4). World Data Center A for Solid Earth Geophysics.
- Pararas-Carayannis, G. (1980). Earthquake and tsunami of 12 December 1979 in Colombia. *Tsunami Newsletter*, 13(1), 1-9.
- Pararas-Carayannis, G. (2002). Evaluation of the threat of mega tsunami generation from postulated massive slope failures of island stratovolcanoes on La Palma, Canary Islands, and on the island of Hawaii. *Science of Tsunami Hazards*, 20(5), 251-277.
- Pararas-Carayannis, G. (2003). Near and far-field effects of tsunamis generated by the paroxysmal eruptions, explosions, caldera collapses and massive slope failures of the Krakatau volcano in Indonesia on august 26-27, 1883. *Science of Tsunami Hazards*.
- Pararas-Carayannis, G. (2006). The potential of tsunami generation along the Makran Subduction Zone in the northern Arabian Sea: Case study: The earthquake and tsunami of November 28, 1945. *Science of Tsunami Hazards*, 24(5), 358-384.
- Pararas-Carayannis, G. (2010). The earthquake and tsunami of 27 February 2010 in Chile– Evaluation of source mechanism and of near and far-field tsunami effects. *Science of Tsunami Hazards*, 29, 2: 96-126.
- Pararas-Carayannis, G. (2011). Tsunamigenic source mechanism and efficiency of the march 11, 2011 Sanriku earthquake in Japan. *Science of Tsunami Hazards*, 30(2): 126-152
- Pararas-Carayannis, G. (2012). Potential of tsunami generation along the Colombia/ Ecuador subduction margin and the Dolores-Guayaquil Mega-Thrust. *Science of Tsunami Hazards*, 31, 3: 209-230.
- Pararas-Carayannis, G., & Zoll, P. (2017). Incipient evaluation of temporal El Nino and other climatic anomalies in triggering earthquakes and tsunamis - Case Study: The Earthquake and Tsunami of 16 April 2016 in Ecuador. *Science of Tsunami Hazards*, 36(4), 262-291.
- Park, S., Van de Lindt, J. W., Gupta, R., & Cox, D. (2012). Method to determine the locations of tsunami vertical evacuation shelters. *Natural hazards*, 63(2), 891-908.
- Pheng, L. S., Raphael, B., & Kit, W. K. (2006). Tsunamis: some pre-emptive disaster planning and management issues for consideration by the construction industry. *Structural survey*, 24(5), 378-396.

- Pinter, N., & Ishman, S. E. (2008). Impacts, mega-tsunami, and other extraordinary claims. *GSA today*, 18(1), 37-38.
- Poma, P., Usca, M., Fdz-Polanco, M., Garcia-Villacres, A., & Toulkeridis, T. (2020). Landslide and environmental risk from oil spill due to the rupture of SOTE and OCP pipelines, San Rafael Falls, Amazon Basin, Ecuador. CIT, in press
- Pontoise, B., & Monfret, T. (2004). Shallow seismogenic zone detected from an offshore-onshore temporary seismic network in the Esmeraldas area (northern Ecuador). *Geochemistry, Geophysics, Geosystems*, 5(2).
- Ratzov, G., Collot, J. Y., Sosson, M., & Migeon, S. (2010). Mass-transport deposits in the northern Ecuador subduction trench: Result of frontal erosion over multiple seismic cycles. *Earth and Planetary Science Letters*, 296(1-2), 89-102.
- Ratzov, G., Sosson, M., Collot, J. Y., Migeon, S., Michaud, F., Lopez, E., & Le Gonidec, Y. (2007). Submarine landslides along the North Ecuador–South Colombia convergent margin: possible tectonic control. In *Submarine mass movements and their consequences* (pp. 47-55). Springer, Dordrecht.
- Rentería, W., Lynett, P., Weiss, R. & De La Torre, G. (2012). Informe de la investigación de campo de los efectos del tsunami de Japón Marzo 2011, en las islas Galápagos. *Acta Oceanográfica del Pacífico*. Vol. 17(1): 177 - 203.
- Ridolfi, F., Puerini, M., Renzulli, A., Menna, M., & Toulkeridis, T. (2008). The magmatic feeding system of El Reventador volcano (Sub-Andean zone, Ecuador) constrained by mineralogy, textures and geothermobarometry of the 2002 erupted products. *Journal of Volcanology and Geothermal Research (Special Volume on Continental Ecuador volcanoes)*, 176: 94-106.
- Robayo N, A., Llorca, J., & Toulkeridis, T. (2020). Population, territorial and economic analysis of a potential volcanic disaster in the city of Latacunga, Central Ecuador based on GIS techniques – Implications and potential solutions. In *Conference on Information and Communication Technologies of Ecuador* (pp. 549-563). Springer, Cham.
- Rodríguez Espinosa, F., Toulkeridis, T., Salazar Martínez, R., Cueva Girón, J., Taipei Quispe, A., Bernaza Quiñonez, L., Padilla Almeida, O., Mato, F., Cruz D'Howitt, M., Parra, H., Sandoval, W., & Rentería, W. (2017). Economic evaluation of recovering a natural protection with concurrent relocation of the threatened public of tsunami hazards in central coastal Ecuador. *Science of tsunami hazards*, 36: 293-306.
- Rodríguez, F., Cruz D'Howitt, M., Toulkeridis, T., Salazar, R., Ramos Romero, G.E., Recalde Moya, V.A., & Padilla, O. (2016). The economic evaluation and significance of an early relocation versus complete destruction by a potential tsunami of a coastal city in Ecuador. *Science of tsunami hazards*, 35, 1: 18-35.
- Rodríguez, F., Toulkeridis, T., Padilla, O., & Mato, F. (2017). Economic risk assessment of Cotopaxi volcano Ecuador in case of a future lahar emplacement. *Natural Hazards*, 85, (1): 605-618.

- Rodríguez, M.E. (2019). Interpretación de los daños y colapsos en edificaciones observados en la ciudad de México en el terremoto del 19 de septiembre 2017. *Revista de Ingeniería Sísmica*, 101, 1-18
- Saji, G. (2014). Safety goals for seismic and tsunami risks: Lessons learned from the Fukushima Daiichi disaster. *Nuclear Engineering and Design*, 280, 449-463.
- Simons, M., Minson, S.E., Sladen, A., Ortega, F., Jiang, J., Owen, S.E., Meng, L., Ampuero, J.P., Wei, S., Chu, R., & Helmberger, D.V. (2011). The 2011 magnitude 9.0 Tohoku-Oki earthquake: Mosaicking the megathrust from seconds to centuries. *science*, 332(6036), pp.1421-1425.
- Stainforth, R. M. (1948). Applied micropaleontology in Coastal Ecuador, *Jour. Paleontology*, 22: 142- 146.
- Suango Sánchez, V. d. R., Acosta Tafur, J.R., Rodríguez De la Vera, K., Andrade Sánchez, M.S., López Alulema, A.C., Avilés Ponce, L.R., Proaño Morales, J.L., Zambrano Benavides, M.J., Reyes Pozo, M.D., Yépez Campoverde, J.A., & Toulkeridis, T. (2019). Use of geotechnologies and multicriteria evaluation in land use policy – the case of the urban area expansion of the city of Babahoyo, Ecuador. 2019 6th International Conference on eDemocracy and eGovernment, ICEDEG 2019, 194-202.
- Sun, C., Xu, J., Jia, L., Qin, Y., Zhan, K., & Zhang, J. (2017, October). Passenger Flow Assignment of Evacuation Path in the Station Based on Time Reliability. In *International Conference on Electrical and Information Technologies for Rail Transportation* (pp. 301-310). Springer, Singapore.
- Thompson, P. A., & Marchant, E. W. (1995). A computer model for the evacuation of large building populations. *Fire safety journal*, 24(2), 131-148.
- Titov, V. V., Moore, C. W., Greenslade, D. J. M., Pattiaratchi, C., Badal, R., Synolakis, C. E., & Kânoğlu, U. T. (2011). A new tool for inundation modeling: Community Modeling Interface for Tsunamis (ComMIT). *Pure and Applied Geophysics*, 168(11), 2121-2131.
- Titov, V., Kânoğlu, U. and Synolakis, C. (2016). “Development of MOST for Real-Time Tsunami Forecasting.” *Journal of Waterway, Port, Coastal, and Ocean Engineering* 142, no. 6: 03116004.
- Toulkeridis, T. & Zach, I. (2017). Wind directions of volcanic ash-charged clouds in Ecuador – Implications for the public and flight safety. *Geomatics, Natural Hazards and Risks*, 8(2): 242-256.
- Toulkeridis, T. (2011). *Volcanic Galápagos Volcánico*. Ediecuatorial, Quito, Ecuador: 364 pp
- Toulkeridis, T. (2013). *Volcanes activos Ecuador*. Santa Rita, Quito, Ecuador: 152pp
- Toulkeridis, T. (2016). Unexpected results of a seismic hazard evaluation applied to a modern hydroelectric plant in central Ecuador. *Journal of Structural Engineering*, 43, (4): 373-380.

- Toulkeridis, T., Arroyo, C.R., Cruz D'Howitt, M., Debut, A., Vaca, A.V., Cumbal, L., Mato, F., & Aguilera, E. (2015a). Evaluation of the initial stage of the reactivated Cotopaxi volcano - Analysis of the first ejected fine-grained material. *Natural Hazards and Earth System Sciences*, 3, (11): 6947-6976.
- Toulkeridis, T., Buchwaldt, R., & Addison, A. (2007). When Volcanoes Threaten, Scientists Warn. *Geotimes*, 52: 36-39.
- Toulkeridis, T., Chunga, K., Rentería, W., Rodríguez, F., Mato, F., Nikolaou, S., Cruz D'Howitt, M., Besenon, D., Ruiz, H., Parra, H., & Vera-Grunauer, X. (2017b). The 7.8 M_w Earthquake and Tsunami of the 16th April 2016 in Ecuador - Seismic evaluation, geological field survey and economic implications. *Science of tsunami hazards*, 36: 197-242.
- Toulkeridis, T., Mato, F., Toulkeridis-Estrella, K., Perez Salinas, J.C., Tapia, S., & Fuertes, W. (2018). Real-Time Radioactive Precursor of the April 16, 2016 Mw 7.8 Earthquake and Tsunami in Ecuador. *Science of tsunami hazards*, 37: 34-48.
- Toulkeridis, T., Parra, H., Mato, F., Cruz D'Howitt, M., Sandoval, W., Padilla Almeida, O., Rentería, W., Rodríguez Espinosa, F., Salazar martinez, R., Cueva Girón, J., Taipei Quispe, A., & Bernaza Quiñonez, L. (2017a). Contrasting results of potential tsunami hazards in Muisne, central coast of Ecuador. *Science of tsunami hazards*, 36: 13-40
- Toulkeridis, T., Porras, L., Tierra, A., Toulkeridis-Estrella, K., Cisneros, D., Luna, M., Carrión, J.L., Herrera, M., Murillo, A., Perez-Salinas, J.C., Tapia, S., Fuertes, W., & Salazar, R. (2019). Two independent real-time precursors of the 7.8 Mw earthquake in Ecuador based on radioactive and geodetic processes - Powerful tools for an early warning system. *Journal of Geodynamics*, 126: 12-22
- Toulkeridis, T., Rodríguez, F., Arias Jiménez, N., Simón Baile, D., Salazar Martínez, R., Addison, A., Freyre Carryon, D., Mato, F., & Díaz Perez, C. (2016). Causes and consequences of the sinkhole at El Trébol of Quito, Ecuador - Implications for economic damage and risk assessment. *Natural Hazards and Earth Science System*, 16: 2031-2041
- Toulkeridis, T., Rojas-Agramonte, Y., & Noboa, G. P. (2020c). Ocean Policy of the UNCLOS in Ecuador Based on New Geodynamic and Geochronological Evidences. *Smart Innovation, Systems and Technologies.*, 181: 485-495
- Toulkeridis, T., Seqqat, R., Torres, M., Ortiz-Prado, E., & Debut, A. (2020b). COVID-19 Pandemic in Ecuador: a health disparities perspective. *Revista de Salud Publica de Colombia*, 22 (3), 1-5.
- Toulkeridis, T., Simón Baile, D., Rodríguez, F., Salazar Martínez, R., Arias Jiménez, N., & Carreon Freyre, D. (2015b). Subsidence at the "trébol" of Quito, Ecuador: An indicator for future disasters?. *Proceedings of the International Association of Hydrological Sciences*, Volume 372, 12 November 2015: 151-155

- Toulkeridis, T., Tamayo, E., Simón-Baile, D., Merizalde-Mora, M.J., Reyes –Yunga, D.F., Viera-Torres, M., & Heredia, M. (2020a). Climate change according to Ecuadorian academics–Perceptions versus facts. *La Granja*, 31(1), 21-49
- Tsai, J., Fridman, N., Bowring, E., Brown, M., Epstein, S., Kaminka, G. A., ... & Tambe, M. (2011, May). ESCAPES: evacuation simulation with children, authorities, parents, emotions, and social comparison. In *AAMAS* (Vol. 11, pp. 457-464).
- Vaca, A.V., Arroyo, C.R., Debut, A., Toulkeridis, T., Cumbal. L., Mato, F., Cruz D’Howitt, M., & Aguilera, E. (2016). Characterization of fine-grained material ejected by the cotopaxi volcano employing X-ray diffraction and electron diffraction scattering. *Biology and Medicine*, 8: 3
- Whelan, F., & Kelletat, D. (2003). Submarine slides on volcanic islands-a source for megatsunamis in the Quaternary. *Progress in Physical Geography*, 27(2), 198-216.
- Wood, N., Jones, J., Schelling, J., & Schmidlein, M. (2014). Tsunami vertical-evacuation planning in the US Pacific Northwest as a geospatial, multi-criteria decision problem. *International journal of disaster risk reduction*, 9, 68-83.
- Yeh, H. H. J., Robertson, I., & Preuss, J. (2005). Development of design guidelines for structures that serve as tsunami vertical evacuation sites (Vol. 4). Washington: Washington State Department of Natural Resources, Division of Geology and Earth Resources.
- Yépez V., Toledo, J., & Toulkeridis, T. (2020). The Armed Forces as a State institution in immediate response and its participation as an articulator in the risk management in Ecuador. *Smart Innovation, Systems and Technologies* 181, 545-554.
- Zafir Vallejo, R., Padilla-Almeida, O., Cruz D’Howitt, M., Toulkeridis, T., Rodriguez Espinosa, F., Mato, F., & Morales Muñoz, B. (2018). Numerical probability modeling of past, present and future landslide occurrences in northern Quito, Ecuador – Economic implications and risk assessments. 2018 5th International Conference on eDemocracy and eGovernment, ICEDEG 2018 8372318: 117-125.
- Zapata, A., Sandoval, J., Zapata, J., Ordoñez, E., Suango, V., Moreno, J., Mullo, C., Tipán, E., Rodríguez, K.E., & Toulkeridis, T. (2020). Application of quality tools for evaluation of the use of geo-information in various municipalities of Ecuador. In *Conference on Information and Communication Technologies of Ecuador* (pp. 420-433). Springer, Cham.
- Zhang, L., Liu, M., Wu, X., & AbouRizk, S. M. (2016). Simulation-based route planning for pedestrian evacuation in metro stations: A case study. *Automation in Construction*, 71, 430-442.
- Zhong, M., Shi, C., Tu, X., Fu, T., & He, L. (2008). Study of the human evacuation simulation of metro fire safety analysis in China. *Journal of Loss Prevention in the Process Industries*, 21(3), 287-298.



SCIENCE OF TSUNAMI HAZARDS

Journal of Tsunami Society International

Volume 40

Number 1

2021

DEVELOPMENT OF RESEARCH ROADMAP OF THE EXCELLENCE FIELD OF SCIENCE UNESA: TSUNAMI SCIENCE

**Madlazim^{*}, Fida Rachmadiarti, Masriyah, Sifak Indana, Elok Sudibyو,
and Binar Kurnia Prahani**

¹*Faculty of Mathematic and Natural Science, Universitas Negeri Surabaya, Surabaya 60231, INDONESIA. E-mail: madlazim@unesa.ac.id*

ABSTRACT

This research aims to produce a Research Roadmap of the Excellent Field of Science Unesa: Tsunami Science. The design of this research was Educational Design Research (EDR). The research site was chosen at the Surabaya State University (Unesa). This research was conducted using the modified ADDIE Model, with five stages including needs analysis, design, development, evaluation, and reporting. The Research Roadmap of Tsunami Early Warning (RRTEW) is an operational form of the Research Roadmap of Excellent Field of Science Unesa: Tsunami Science which is included in the Research Master Plan (RMP) and the Strategic Plan (RP) for Unesa Research in 2020-2030. RRTEW was given to 15 experts through a validation process using the Expert Validation Sheet. Research data in the form of scores from expert assessments were analyzed using a single measure interrater coefficient correlation (r_s) to determine validity and using Cronbach's alpha (α) to determine RRTEW reliability. In addition, the results of the validation and input from experts will be used as a reference for revising RRTEW. The evaluation of all components of RRTEW by three experts was declared valid and reliable. The implications of this research are expected to: (1) provide an example of a Research Roadmap of Excellent Field of Science Unesa: Tsunami Science in tertiary institutions; (2) contributing thoughts to policymakers regarding the development of a Research Roadmap of Excellent Field of Science Unesa: Tsunami Science; (3) contributing thoughts to the academic community in increasing research in the form of developing a Research Roadmap of Excellent Field of Science Unesa: Tsunami Science.

Keywords: *Research Roadmap, Science Tsunami, Educational Design Research (EDR)*

1. INTRODUCTION

The industrial revolution 4.0 and Society 5.0 is a fundamental change in the industrial sector which has entered a new era. The Industrial Revolution 4.0 and Society 5.0 have also forced universities to produce graduates who have superior competence in global competition. Competencies that must be owned by graduates include Critical Thinking (Atabaki et al., 2015; Birgili, 2015; Temel, 2014), Collaboration (Griffin & Care, 2015), Creativity (Dwikoranto et al., 2019; Wicaksono et al., 2019; Zulkarnaen et al., 2017), Problem Solving (Jatmiko et al., 2016; Pandiangan et al. 2017). In addition, the main pillar of the 4.0 Industrial Revolution and Society 5.0 are of course digital-based technology that college graduates must master, including Internet of Things, Big Data, Augmented Reality, Cyber Security, Artificial Intelligence, Robotic Automation, Simulation, Integrated Systems, Additive Manufacturing, and Cloud Computing. This is a challenge in itself that must be resolved by universities in Indonesia. Besides, in 2020 there are only eleven state universities in Indonesia that have the status of legal entities. There are only eleven state universities that have legal entity status, of the total state universities in Indonesia there are 122 universities. The latest news from the Ministry of Education and Culture of the Republic of Indonesia encourages state universities to become a legal entity.

This opportunity from the Ministry of Education and Culture of the Republic of Indonesia, as well as the challenges of industrial revolution 4.0 and Society 5.0, has been responded positively by Unesa as one of the State Universities with the status of a Public Service Agency to become Legal Entity University. The development of the achievement of Unesa's vision in 2020-2030 Recognize Regional Teaching University is also one of the references for preparing Unesa to change its status from Public Service Agency to become Legal Entity University. Strengthened as a campus institution, Unesa has received accreditation with a rating based on decree number 5245/SK/BAN-PT/Akred/PT/XII/2017. Besides, there is also an urgent need related to Study Program Accreditation and Accreditation of 9 criteria for Higher Education. One of the preparations that need to be carried out is that Unesa must have a Research Roadmap of Excellent Field of Science Unesa: Tsunami Science in 2020-2030.

Research Roadmap of the Excellent Field of Science Unesa which are included in the Research Master Plan (RMP) and the Unesa Research Strategic Plan in 2020-2030. The fact that until 2020 Unesa does not have this official document. One of Unesa's excellence in science is research related to tsunami science. Tsunami is one of the most unpredictable hazards (Madlazim & Supriyono, 2014; Madlazim et al., 2020; Madlazim & Hariyono, 2020). In Indonesia, it has also been proven that areas that are often affected by the Tsunami disaster (Madlazim et al., 2020; Madlazim & Hariyono, 2020). To cultivate this, it is necessary to have a Research Roadmap of the Excellent Field of Science Unesa: Tsunami Science. One form of operation is the Research Roadmap of Tsunami Early Warning (RRTEW).

Research Urgency - Until 2020 there is no Research Roadmap of the Excellent Field of Science Unesa document that is included in the Research Master Plan and the Unesa Research Strategic Plan in 2020-2030. Therefore, it is very important to carry out specific research to produce a Research Roadmap of the Excellent Field of Science Unesa: Tsunami Science. One form of operation is the Research Roadmap of Tsunami Early Warning (RRTEW).

Research Objective - This research aims to produce a Research Roadmap of the Excellent Field of Science Unesa: Tsunami Science. One form of operation is the Research Roadmap of Tsunami Early Warning (RRTEW).

2. METHODS

The design of this research was Educational Design Research (EDR) (Plomp, 2013). It aims to produce a Research Roadmap of the Excellent Field of Science Unesa: Tsunami Science. This research will be conducted for 8 months to be exact May - December 2020. The research place is chosen at the Surabaya State University (Unesa). The Research Roadmap of Tsunami Early Warning (RRTEW) is an operational form of the Research Roadmap of the Excellent Field of Science Unesa: Tsunami Science which is included in the Research Master Plan and the Strategic Plan for Unesa Research 2020-2030. The results of this development are expected to answer the need that until 2020 Unesa does not have the official document. Including Unesa does not yet have a Research Roadmap of the Excellent Field of Science Unesa: Tsunami Science in 2020-2030. This research was conducted using the modified ADDIE Model, with five stages including needs analysis, design, development, evaluation, and reporting. The research flow diagram is shown as shown in Figure 1.

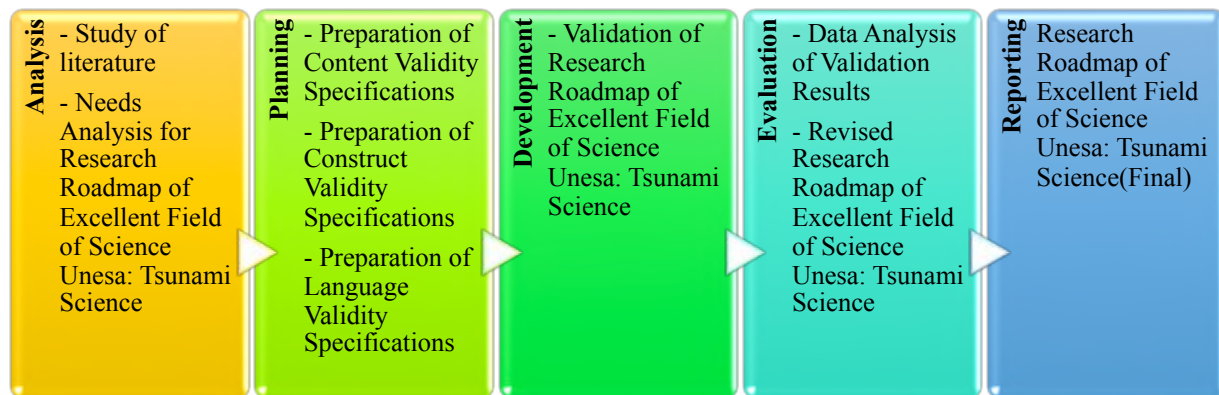


Figure 1. Development of Research Roadmap of Excellent Field of Science Unesa: Tsunami Science

RRTEW was given to 15 experts through a validation process to get suggestions and improve quality. The revision results according to input 3 validators will be used as a reference for revising RRTEW. Research data in the form of scores from expert assessments were analyzed using a single measure interrater coefficient correlation (r_c) to determine validity and using Cronbach's alpha (α) (Malhotra, 2011; Jatmiko et al., 2018) to determine the reliability of RRTEW. Looking for validity: If Single measure interrater coefficient correlation (r_c) or r count (r_c) $>$ r table, then it is declared valid. Looking for Reliability: (a) If the value of Cronbach Alpha (α) $>$ 0.60, it is declared reliable. (b) If the value of Cronbach Alpha (α) $<$ 0.60, it is declared unreliable.

3. RESULTS AND DISCUSSION

The Research Roadmap of Tsunami Early Warning (RRTEW) which had been developed was then validated by 15 experts. The results of the Roadmap Content, Construction, and Language Validation are presented in Table 1.

Table 1. Validation of Research Roadmap of Tsunami Early Warning (RRTEW)

| Aspects of RRTEW Assessment | Validity and Reliability | | | |
|---|--------------------------|----------|------|----------|
| | Score | Validity | r. | α |
| Content Validity | | | | |
| 1. RRTEW has a novelty according to the R&D aspect | 3.80 | VV | 0.45 | 0.88 |
| 2. RRTEW has a novelty according to the Technology Aspect | 3.70 | VV | | |
| 3. RRTEW has a novelty according to Product aspects | 3.70 | VV | | |
| 4. RRTEW has a novelty according to the stages of Product Design, Product Prototype, and Product Commercialization | 3.80 | VV | | |
| 5. RRTEW meets the demands of the times according to the R&D aspect | 3.85 | VV | | |
| 6. RRTEW meets the demands of the times according to the Technology Aspect | 3.70 | VV | | |
| 7. RRTEW meets the demands of the times according | 3.70 | VV | | |
| 8. RRTEW meets the demands of the times according to the stages of Product Design, Product Prototype, and Product Commercialization | 3.80 | VV | | |
| Conclusion: The results of the RRTEW content validity can be used. | | | | |
| Construct Validity | | | | |
| 1. RRTEW is developed logically according to the R&D Aspect | 3.70 | VV | 0.40 | 0.87 |
| 2. RRTEW is developed logically according to the Technology Aspect | 3.80 | VV | | |
| 3. RRTEW is developed logically according to the Product Aspect | 3.70 | VV | | |
| 4. RRTEW is developed logically according to the stages of Product Design, Product Prototype, and Product Commercialization | 3.80 | VV | | |
| 5. RRTEW has a logical and reasonable physical size | 3.60 | VV | | |
| 6. RRTEW has interesting and easy to read fonts | 3.80 | VV | | |
| 7. Consistency of RRTEW layout | 3.80 | VV | | |
| 8. RRTEW has elements of a harmonious layout | 3.75 | VV | | |
| 9. RRTEW has a complete layout element | 3.80 | VV | | |
| 10. RRTEW has a layout that can speed up understanding | 3.80 | VV | | |
| 11. Typography of RRTEW content is relatively simple | 3.80 | VV | | |
| 12. Typography of RRTEW Unesa is easy to read | 3.80 | VV | | |
| 13. Typography of RRTEW content makes it easy to understand | 3.80 | VV | | |
| 14. The illustration of RRTEW content is considered appropriate | 3.70 | VV | | |
| Conclusion: The results of the RRTEW construct validity can be used. | | | | |
| Language Validity | | | | |
| 1. RRTEW has precise sentence structure | 3.90 | VV | 0.38 | 0.89 |
| 2. RRTEW has sentence effectiveness | 3.50 | VV | | |
| 3. RRTEW has a standardized term | 3.80 | VV | | |
| 4. RRTEW makes it easier to understand messages or information | 3.80 | VV | | |
| 5. RRTEW has a precise language | 3.75 | VV | | |
| 6. RRTEW can correct spelling | 3.90 | VV | | |
| 7. RRTEW has a consistent use of terms | 3.80 | VV | | |
| 8. RRTEW has consistent use of symbols or icons | 3.80 | VV | | |
| Conclusion: The results of the RRTEW language validity can be used. | | | | |

Keterangan: r. = Single measure interrater coefficient correlation; α = Cronbach's alpha ; VV = Very Valid

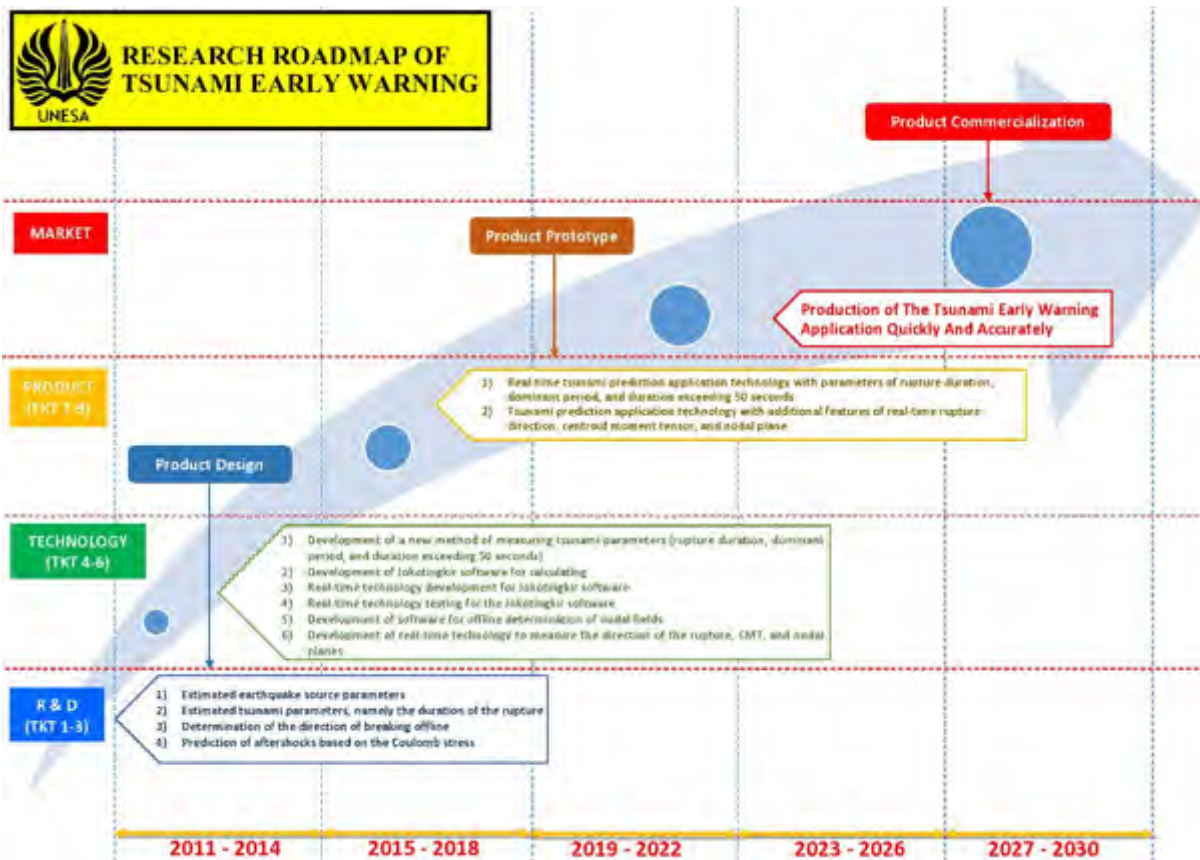


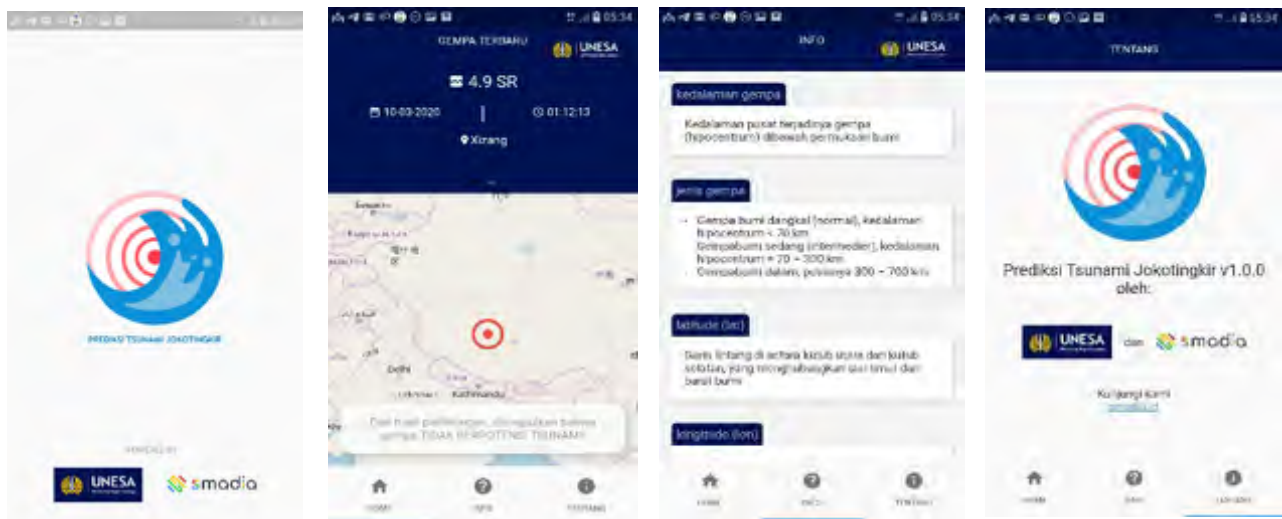
Figure 2. *Research Roadmap of Tsunami Early Warning (RRTEW)*

The evaluation of all RRTEW components by 15 experts was declared valid and reliable. The implications of RRTEW can then be used as a reference in the development of Unesa 2020-2030. The results of this validity are supported by the opinion of Plomp (2013) which states that a good product must meet the validity requirements. The product validity can be tested by testing the content validity and construct validity. The content validity is there is a need for the intervention and its design is based on state-of-the-art (scientific) knowledge. (Nieveen et al., 2007). Construct validity is the intervention is “logically” designed (Nieveen et al., 2007). One of the operational forms of Unesa's flagship is Tsunami Early Warning.

Figure 2 shows the 2020-2030 Research Roadmap of Tsunami Early Warning at the R&D stage consisting of: (1) Estimated earthquake source parameters; (2) Estimated tsunami parameters, namely the duration of rupture; (3) Determination of the direction of breaking offline; (4) prediction of aftershocks based on the Coulomb stress. The technology stage consists of: (1) Development of new method of measuring tsunami parameters (rupture duration, dominant period, and duration exceeding 50 seconds); (2) Development Jokotingkir software for calculating; (3) Real-time technology development for Jokotingkir software; (4) Real-time testing technology for Jokotingkir software; (5) Development of software for offline determination of nodal fields; (6) Development of real-time technology to measure the direction of the rupture, CMT, and nodal planes.

The Product Stage consists of: (1) Real-time tsunami prediction application technology with parameters of rupture duration, dominant period, and duration exceeding 50 seconds; (2) Tsunami prediction application technology with additional features of real-time rupture direction, centroid moment tensor, and nodal plane. The Market section consists of: Production of the Tsunami Early Warning Application Quickly and Accurately. The results of this development answer the need that until 2020 Unesa does not have this official document. Including Unesa does not yet have a Research Roadmap of Excellent Field of Science Unesa: Tsunami Science in a concrete operational form as presented in Figure 2. Figure 2 is supported by the results of research on the theme of Tsunami which is still a favorite in the last 10 years (Gusman et al., 2017; Heidarzadeh et al., 2019; Jayaratne et al., 2016; Kuswandi & Triatmadja, 2019; Lomax & Michelini, 2013; Lomax & Michelini, 2011; Lomax & Michelini, 2012 Madlazim et al., 2020; Mikami et al., 2012; Newman et al., 2011; Ozaki, 2011; Power et al., 2017; Socquet et al., 2019; Suppasri et al., 2013; Takabatake et al., 2019; Triatmadja & Benazier, 2014; Triatmadja & Nurhasanah, 2012; Tsushima et al., 2011; Ulrich et al., 2019; Watkinson & Hall, 2017; Yeh et al., 2013).

Several international-level studies and publications examining tsunamis in Indonesia (Bisri & Sakurai, 2017; Esteban et al., 2013; Giachetti et al., 2012; Hamzah et al., 2000; Seng, 2013; Taubenböck et al., 2009; Watkinson & Hall, 2017; Widiastuti et al., 2019; Omira et al., 2019; Sassa & Takagawa, 2019; Suppasri et al., 2015; Kongko and Hidayat, 2014), this shows that the trend of Tsunami research in Indonesia has still become a topic of interest to the international community. One of the trends generated by researchers based on the Research Roadmap of Tsunami Early Warning (RRTEW) is Joko Tingkir's Tsunami Prediction. Tsunami Prediction Joko Tingkir will provide a warning through notification if there is a potential earthquake (Madlazim et al., 2020) in Figure 3.



(Source: Playstore/PrediksiTsunamiJokotingkir)

Figure 3. Tsunami Prediction Joko Tingkir

The implications of this research are expected to: (1) provide an example of a Research Roadmap for Excellent Field of Science: Tsunami Science in tertiary institutions; (2) contributing thoughts to policymakers regarding the development of a Research Roadmap of Excellent Field of Science Unesa: Tsunami Science; (3) contributing thoughts to the academic community in increasing research in the form of developing a Research Roadmap of Excellent Field of Science Unesa: Tsunami Science.

4. CONCLUSIONS

One of the operational forms of the Unesa Research Roadmap for Excellent Science: Tsunami Science is the Research Roadmap of Tsunami Early Warning (RRTEW) has been declared valid and reliable. The Unesa Research Roadmap for Excellent Science: Tsunami Science can be used in the development of Unesa in 2020-2030. This research implies that it is necessary to socialize the Unesa Research Roadmap for Excellent Science: Tsunami Science to the entire Unesa academic community. In addition, each lecturer is also conditioned to have a Research Roadmap individually or in clumps so that research in the Unesa environment can progress rapidly. The benefit for other researchers is that it can be used as a comparison in developing a research roadmap related to tsunami science in their country.

ACKNOWLEDGMENTS

The authors sincerely thank the Surabaya State University PBNP for supporting this research. This work is funded by PNPB, Surabaya State University, Indonesia under grant number B/22653/UN38.9/LK.04.00/2020. This article has also benefited from constructive reviews from two anonymous reviewers in Science of Tsunami Hazards.

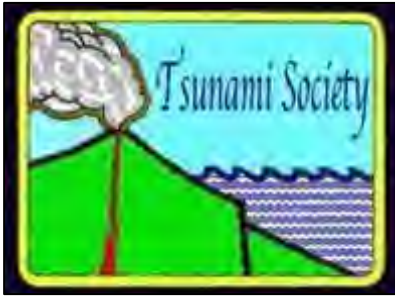
REFERENCES

- Atabaki, M., S. Keshtiaray, N. and Yarmohammadian, M. H. (2015). Scrutiny of critical thinking concept. *International Education Studies*, 8(3), 93-102.
- Birgili, B. (2015). Creative and critical thinking skills in problem-based learning environments. *Journal of Gifted Education and Creativity*, 71-73.
- Bisri, M. B. F., & Sakurai, A. (2017). Disaster education and school safety governance after the 2004 Indian Ocean Tsunami in Indonesia: from national policy to local implementation. In *Disaster Risk Reduction in Indonesia* (pp. 189-212). Springer, Cham.
- Dwikoranto, Madlazim, and Erman. (2019). Project based laboratory learning as an alternative learning model to improve sciences process skills and creativity of physic teacher candidate. *Journal of Physics: Conference Series*, 1387(012074): 2-7.
- Widiastuti 1,a, Siswo Poerwanto,2,b, Hernawan3,c , B.Firdiansyah4,d, Sugiharto. 2019. Effectiveness of game model on tsunami disaster anticipation in two provinces of Indonesia, year 2019. *Science of Tsunami Hazards*. Vol. 38, No. 4, page 179
- Esteban, M., Tsimopoulou, V., Mikami, T., Yun, N. Y., Suppasri, A., & Shibayama, T. (2013). Recent tsunamis events and preparedness: Development of tsunami awareness in Indonesia, Chile and Japan. *International Journal of Disaster Risk Reduction*, 5, 84-97.

- Giachetti, T., Paris, R., Kelfoun, K., and Ontowirjo B. 2012. "Tsunami Hazard Related to a Flank Collapse of Anak Krakatau Volcano, Sunda Strait, Indonesia." *Geological Society, London, Special Publications 2012* 361:79–90.
- Griffin, P., & Care, E. (2015). *Assesment and Teaching of 21st Century Skills: Methods and Approach*. New York: Springer.
- Gusman, A.R., Satake, K. & Harada, T., 2017. Rupture process of the 2016 Wharton Basin strike-slip faulting earthquake estimated from joint inversion of teleseismic and tsunami waveforms, *Geophys. Res. Lett.*, 44, 4082–4089.
- Hamzah, L., N. T. Puspito and F. Imamura (2000), Tsunami catalog and zones in Indonesia, *J. Nat. Disast. Sci.*, 22(1), 25-43.
- Heidarzadeh, M., Muhari, A. & Wijanarto, A.B., 2019. Insights on the source of the 28 September 2018 Sulawesi Tsunami, Indonesia based on spectral analyses and numerical simulations, *Pure Appl. Geophys.*, 176, 25–43.
- Jatmiko, B., Prahani, B. K., Munasir, Supardi, Z. A. I., Wicaksono, I., Erlina, N., Pandiangan, P., Althaf, R., & Zainuddin (2018). The comparison of OR-IPA teaching model and problem-based learning model effectiveness to improve critical thinking skills of pre-service physics teachers. *Journal of Baltic Science Education*, 17 (2), 1-22.
- Jatmiko, B., Widodo, W., Martini, Budiyo, M., Wicaksono, I., & Pandiangan, P. (2016). Effectiveness of the INQF-based learning on a general physics for improving student's learning outcomes. *Journal of Baltic Science Education*, 15(4), 441-451.
- Jayaratne, M. P. R., Premaratne, B., and Adewale, A. 2016. "Failure Mechanisms and Local Scour at Coastal Structures Induced by Tsunami." *Coastal Engineering Journal* 58(4).
- Kongko, W., and Hidayat, R. (2014). Earthquake - Tsunami in South Jogjakarta Indonesia: Potential, Simulation Models, and Related Mitigation Efforts, 2(3), 18–22.
- Kuswandi and Triatmadja, R. 2019. "The Use of Dam Break Model to Simulate Tsunami Run-up and Scouring Around a Vertical Cylinder." *Journal of Applied Fluid Mechanics* 12(5):1395–1406.
- Lomax, A. & Michelini, A., 2013. Tsunami early warning within five minutes, *Pure Appl. Geophys.*, 170, 1385–1395.
- Lomax, A. and Michelini, A. (2011), Tsunami early warning using earthquake rupture duration and *P*-wave dominant period: the importance of length and depth of faulting, *Geophys. J. Int.*, 185, 283–291, DOI: 10.1111/j.1365-246X.2010.04916.x
- Lomax, A. and Michelini, A. (2012), Tsunami Early Warning Within Five Minutes. *Pure and Applied Geophysics*, Volume 170, Issue 9–10, pp 1385–1395.
- Madlazim and Hariyono, E. (2020). Mechanism of increasing preparedness tsunami: OMBAK - learning model development. *Science of Tsunami Hazards*, 39 (3), 156.
- Madlazim and Supriyono (2014). Improving experiment design skills: Using the Joko Tingkir program as a learning tool of Tsunami topic. *Science of Tsunami Hazards*, 33 (2), 133.
- Madlazim, Rohadi, S., Koesuma, S., Meilianda, E. (2020). Development of earthquake and tsunami early warning application based on android. *Science of Tsunami Hazards*, 39(2), 183.
- Madlazim,, Rahmadiarti, F., Masriyah,, Indana, S., Sunarti, T., & Prahani, B.K. (2020). An OrSAEv learning model to improve the disaster preparedness of STEM teacher candidates. *World Transactions on Engineering and Technology Education*, 18(2), 231-236.

- Malhotra, N.K. (2011). *Review of marketing research: Special issue—marketing legends*. New York: Emerald Group Publishing Limited.
- Mikami, T., Shibayama, T. and Esteban, M. 2012. “Filed Survey of The 2011 Tohoku Earthquake and Tsunami in Miyagi and Fukushima Prefectures.” *Coastal Engineering Journal* 54(1).
- Newman, A.V., Hayes, G., Wei, Y., and Convers, J. (2011), The October 25 2010 Mentawai tsunami earthquake, from real-time discriminants, finite-fault rupture, and tsunami excitation, *Geophys. Res. Lett.*, 38, L05302, doi:10.1029/2010GL046498.
- Nieveen, N., McKenney, S., and van. Akker. (2007). *Educational Design Research*. New York: Routledge.
- Omira, R., Dogan, G.G., Hidayat, R., Husrin, S., Prasetya, G., Annunziato, A., Proietti, C., Probst, P., Paparo, M.A., Wronna, M., Zaytsev, A., Pronin, P., Giniyatullin, A., Putra, P.S., Hartanto, D., Ginanjar, G., Kongko, W., Pelinovsky, E., and Yalciner, A.C. The September 28th, 2018, tsunami in Palu-Sulawesi, Indonesia: A post-event field survey. *Pure and Applied Geophysics*, 2019, vol. 176, 1379-1395.
- Ozaki, T. (2011), Outline of the 2011 off the Pacific coast of Tohoku Earthquake (Mw 9.0) - Tsunami warnings/advisories and observations, *Earth Planets Space*, 63, 827–830, doi:10.5047/eps.2011.06.029
- Pandiangan, P., Sanjaya, M., Gusti, I., & Jatmiko, B. (2017). The validity and effectiveness of physics independent learning model to improve physics problem solving and self-directed learning skills of students in open and distance education systems. *Journal of Baltic Science Education*, 16(5), 651-665.
- Plomp, T. (2013). Preparing education for the information society: The need for new knowledge and skills. *International Journal of Social Media and Interactive Learning Environments*, 1(1), 3-18.
- Power, W., Clark, K., King, D.N., Borrero, J., Howarth, J., Lane, E.M., Goring, D., Goff, J., Chagué-Goff, C., Williams, J., Reid, C., Whittaker, C., Mueller, C., Williams, S., Hughes, M.W., Hoyle, J., Bind, J., Strong, D., Litchfield, N. & Benson, A., 2017. Tsunami runup and tide-gauge observations from the 14 November 2016 M7.8 Kaikōura earthquake, New Zealand, *Pure Appl. Geophys.*, 174, 2457–2473.
- Sassa, Sh., and Takagawa, T. Liquefied gravity flow-induced tsunami: first evidence and comparison from the 2018 Indonesia Sulawesi earthquake and tsunami disasters. *Landslides*, 2019, vol. 16, 195-200.
- Seng, D. S. C. (2013). Tsunami resilience: Multi-level institutional arrangements, architectures, and system of governance for disaster risk preparedness in Indonesia. *Environmental science & policy*, 29, 57-70.
- Socquet, A., Hollingsworth, J., Pathier, E. & Bouchon, M., 2019. Evidence of supershear during the 2018 magnitude 7.5 Palu earthquake from space geodesy, *Nat. Geosci.*, 12, 192–199.
- Suppasri, A. Shuto, N., Imamura, F., Koshimura, S., Mas, E., Yalciner, A. C .2013. “Lessons Learned from the 2011 Great East Japan Tsunami: Performance of Tsunami Countermeasures, Coastal Buildings, and Tsunami Evacuation in Japan.” *Pure and Applied Geophysics* 170(6–8):993–1018.

- Suppasri, A., K. Goto, A. Muhari, P. Ranasinghe, M. Riyaz, M. Affan, E. Mas, M. Yasuda and F. Imamura (2015), A decade after the 2004 Indian Ocean tsunami: the progress in disaster preparedness and future challenges in Indonesia, Sri Lanka, Thailand, the Maldives, *Pure Appl. Geophys.*, 172, 3313-3341, doi:10.1007/s00024-015-1134-6.
- Takabatake, T et al. 2019. "Field Survey and Evacuation Behaviour during the 2018 Sunda Strait Tsunami." *Coastal Engineering Journal* 61(4):423–43.
- Taubenböck, H., Goseberg, N., Setiadi, N., Lämmel, G., Moder, F., Oczipka, M., ... & Birkmann, J. (2009). " Last-Mile" preparation for a potential disaster-Interdisciplinary approach towards tsunami early warning and an evacuation information system for the coastal city of Padang, Indonesia. *Natural Hazards and Earth System Science* 9 (2009), Nr. 4, 9(4), 1509-1528.
- Temel, S. (2014). The effects of problems based learning on pre service teachers's critical thinking dispositions and perceptions of problems solving ability. *South African Journal of Education*, 34(1), 1-20.
- Triatmadja, R. and Benazier., 2014. "Simulation of Tsunami Force on Tows of Buildings In Aceh Region After Tsunami Disaster In 2004", *Journal of Science of Tsunami Hazard*, Volume 33, Number 3, Page 156-169.
- Triatmadja, R. and Nurhasanah, A. 2012. "Tsunami Force On Buildings With Openings And Protection." 6(4):1–17.
- Tsushima, H., Hirata, K., Hayashi, Y., Tanioka, Y., Kimura, K., Sakai, S., Shinohara, M., Kanazawa, T., Hino, R., and Maeda, K. (2011), Near-field tsunami forecasting using offshore tsunami data from the 2011 off the Pacific coast of Tohoku Earthquake, *Earth Planets Space*, 63, 821–826.
- Ulrich, T., Vater, S., Madden, E.H., Behrens, J., van Dinther, Y., van Zelst, I., Fielding, E.J., Liang, C. & Gabriel, A.A., 2019b. Coupled, physics-based modeling reveals earthquake displacements are critical to the 2018 Palu, Sulawesi tsunami, *Pure Appl. Geophys.*, 176, 4069–4109.
- Watkinson, I.M. & Hall, R., 2017. Fault systems of the Eastern Indonesian triple junction: evaluation of quaternary activity and implications for seismic hazards, *Geol. Soc. Lond. Spec. Publ.*, 441, 71.
- Wicaksono, I., Wasis, and Madlazim. (2017). The effectiveness of virtual science teaching model (VS-TM) to improve student’s scientific creativity and concept mastery on senior high school physics subjects. *Journal of Baltic Science Education*, 16(4): 549-561.
- Yeh, H., Sato, S., and Tajima, Y. 2013. "The 11 March 2011 East Japan Earthquake and Tsunami: Tsunami Effects on Coastal Infrastructure and Buildings." *Pure and Applied Geophysics* 170(6–8):1019–31.
- Zulkarnaen, Supardi, Z.A.I., & Jatmiko, B. (2017). Feasibility of Creative Exploration, Creative Elaboration, Creative Modeling, Practice Scientific Creativity, Discussion, Reflection (C3PDR) Teaching Model to Improve Students’ Scientific Creativity of Junior High School. *Journal of Baltic Science Education*, 16(6), 1020-1034.

**SCIENCE OF TSUNAMI HAZARDS****Journal of Tsunami Society International****Volume 40****Number 1****2021****SIMULATION OF TSUNAMI ALONG NORTH SUMATRA AND PENINSULAR MALAYSIA
ALLIED WITH THE INDONESIAN TSUNAMI OF 2004 USING A SHALLOW WATER
MODEL****Md. Fazlul Karim***Department of Mathematical and Physical Sciences, East West University, Dhaka-1212, Bangladesh**Email: fkarim@ewubd.edu***ABSTRACT**

The linear polar coordinate shallow water model of Ismail et al. (2006) is used to simulate Tsunami effect along North Sumatra and Penang Islands allied with Indonesian tsunami of 2004. The study of Ismail et al (2006) was based on the assumption that the primary displacement of the water surface at the source zone in the form of sea level rise and fall is equal to the stationary move of the sea floor deformation in the rupture region, which is not completely precise. The dynamics of seafloor displacement over a short period of time was ignored in that study. The major factor, which determines the initial amount of a tsunami, is the amount of vertical sea floor deformation (Iguchi, 2011). The properties of Indonesian tsunami 2004 are related to the scale of the bottom displacement (Kowalik et al. 2005). In this paper, a reassessment of the initial tsunami source of 2004 Indonesian tsunami taking the amount of vertical sea floor deformation and the dynamics of seafloor displacement over a short period is considered as the initial condition of tsunami generation. The computed maximum water levels along the coastal belts of Sumatra and Penang in Peninsular Malaysia compare well with the observed water level data obtained through post tsunami surveys. The results of this study suggest that a linear cylindrical polar coordinate shallow water model can be applied to simulate different aspects of tsunami.

Keywords: *Indonesian Tsunami 2004, Shallow Water Equation, North Sumatra, Peninsular Malaysia*

1. INTRODUCTION

On December 26, 2004 a shocking mega thrust earthquake happened along 1200 km of the subduction zone west of Sumatra and Thailand in the Indian Ocean with an intensity of $M_w = 9.0$ having Epicenter at 3.32° N, 95.85° E (Yalciner et al. 2005). The earthquake also activated a massive tsunami that propagated throughout the Indian Ocean and caused extreme inundation and extensive damage along the coasts of 12 rim countries of the Indian Ocean.

With the present level of knowledge it is feasible to simulate tsunami propagation by (Imamura et al. 1996, Titov and Gonzalez 1997, Imteaz and Imamura 2001, Kowalik et al. 2005, Roy and Izani 2005). The numerical approaches allow complete flexibility in specifying tsunami source regions and generation mechanisms.

A cylindrical polar coordinate model ensures very well resolution near the coast and coarse resolution away from the coast by suitably locating the Pole near the coast (Roy et al 1999). Haque et al.(2003) improved the model of Roy et al. (1999) for achieving finer resolution along the coastal belt of Bangladesh. Using the concepts of these two studies Ismail et al (2006) developed a shallow water model in Cylindrical Polar coordinates to simulate the tsunami along the coastal belts of North Sumatra and Penang Islands allied with 2004 Indonesian tsunami.

Karim et al (2016) simulated propagation of 2004 global tsunami generated by the sea bed deformation using a non-linear polar coordinate shallow water model. Roy et al (2007) developed a non-linear polar coordinate shallow water model for tsunami computation along North Sumatra and Penang Island in peninsular Malaysia. Karim et al. (2007) developed a shallow water model for computing Tsunami along the west coast of Peninsular Malaysia and Thailand using boundary-fitted curvilinear grids.

In this study, the linear polar coordinate shallow water model of Ismail et al. (2006) has been used to simulate the effect of 2004 Sumatra tsunami taking into account the initial sea floor deformation as an initial condition of tsunami source generation. This model is extending from Penang in Peninsular Malaysia to the west of Sumatra Island in Indonesia and the source of the Indonesian tsunami is within the model domain. The model has also been applied to simulate other related features of tsunami surrounding these Islands.

2. MATHEMATICAL FORMULATION

2.1. Governing Equations

A Cylindrical Polar coordinate system is defined where the Pole, O , is at the undisturbed level of the sea surface ($r\theta$ -plane) and Oz is directed vertically upwards. The displaced position of the free surface is $z = \zeta(r, \theta, t)$ and the position of the sea floor is $z = -h(r, \theta)$, so that the total depth of the fluid layer is $\zeta + h$. Following Roy et al. (1999), the depth-averaged linear shallow water equations are:

$$\frac{\partial \zeta}{\partial t} - \frac{\partial \kappa}{\partial t} + \frac{1}{r} \frac{\partial}{\partial r} [r(\zeta + h - \kappa)v_r] + \frac{1}{r} \frac{\partial}{\partial \theta} [(\zeta + h - \kappa)v_\theta] = 0 \quad (1)$$

$$\frac{\partial v_r}{\partial t} - f v_\theta = -g \frac{\partial \zeta}{\partial r} - \frac{F_r}{\rho(\zeta + h - \kappa)} \quad (2)$$

$$\frac{\partial v_\theta}{\partial t} + f v_r = -\frac{g}{r} \frac{\partial \zeta}{\partial \theta} - \frac{F_\theta}{\rho(\zeta + h - \kappa)} \quad (3)$$

where

v_r = radial component of velocity of the sea water

v_θ = tangential component of velocity of the sea water

F_r = radial component of frictional resistance at the sea bed

F_θ = tangential component of frictional resistance at the sea bed

f = Coriolis parameter = $2 \Omega \sin \varphi$

Ω = angular speed of the earth

φ = latitude of the location

g = acceleration due to gravity

κ = sea floor deformation

The parameterizations of F_r and F_θ are done by conventional quadratic law:

$$F_r = \rho C_f v_r \sqrt{v_r^2 + v_\theta^2} \quad \text{and} \quad F_\theta = \rho C_f v_\theta \sqrt{v_r^2 + v_\theta^2} \quad (4)$$

where ρ is the sea water density and C_f is the friction coefficient.

2.2. Boundary Conditions

For a closed boundary the normal component of velocity is considered as zero. Radiation type of boundary conditions are used for open boundaries which allow the disturbance created within the analysis area to go out of the area. The model area is bounded by the straight lines $\theta = 0$ and $\theta = \Theta$

through the pole O and the circular arc $r = R$ with center at O . Following Roy et al. (1999) northern, southern and western open sea boundary conditions are respectively

$$v_\theta + \sqrt{(g/h)} \zeta = 0 \quad \text{along } \theta = 0 \quad (5)$$

$$v_\theta - \sqrt{(g/h)} \zeta = 0 \quad \text{along } \theta = \Theta \quad (6)$$

$$v_r - \sqrt{(g/h)} \zeta = 0 \quad \text{along } r = R \quad (7)$$

2.3. Transformation in the radial direction

For uniform grid of size $\Delta\theta$ in the tangential direction, the arc distance between two consecutive radial grid lines decreases towards the pole and increases away from the pole. Thus the arc distance increases as we move away from the coast although the grid size $\Delta\theta$ is constant. To obtain uneven resolution in the radial direction (fine to coarse), according to Haque et al. (2003), the following transformation is used:

$$\eta = c \ln \left(1 + \frac{r}{r_0} \right) \quad (8)$$

where, r_0 is of the order of total radial distance of the analysis area and c is a scale factor.

From this transformation we obtain a relationship between Δr and $\Delta\eta$ which is as follows:

$$\Delta r = \frac{r + r_0}{c} \Delta\eta \quad (9)$$

This relation shows that keeping a constant value of $\Delta\eta$, we can generate variable Δr , which increases with increase of r . So, we obtain uneven resolution (fine to coarser) in the radial direction in the physical domain while in the computational domain ($\eta\theta$ -plane) the resolution remains uniform.

Using the above transformation, equations (1) – (3) transform to:

$$\frac{\partial \zeta}{\partial t} - \frac{\partial \kappa}{\partial t} + \frac{ce^{-\eta/c}}{r_0(e^{\eta/c} - 1)} \frac{\partial}{\partial \eta} \left\{ (\zeta + h - \kappa) (e^{\eta/c} - 1) v_r \right\} + \frac{1}{r_0(e^{\eta/c} - 1)} \frac{\partial}{\partial \theta} \left\{ (\zeta + h - \kappa) v_\theta \right\} = 0 \quad (10)$$

$$\frac{\partial v_r}{\partial t} - f v_\theta = - \frac{gce^{-\eta/c}}{r_0} \frac{\partial \zeta}{\partial \eta} - \frac{C_f v_r \sqrt{v_r^2 + v_\theta^2}}{(\zeta + h - \kappa)} \quad (11)$$

$$\frac{\partial v_\theta}{\partial t} + f v_r = - \frac{g}{r_0(e^{\eta/c} - 1)} \frac{\partial \zeta}{\partial \theta} - \frac{C_f v_\theta \sqrt{v_r^2 + v_\theta^2}}{(\zeta + h - \kappa)} \quad (12)$$

The boundary conditions (5)-(7) remain unchanged due to this transformation.

3. GRID GENERATION AND NUMERICAL SCHEME

Pole of the coordinate system is located in the mainland of Penang at O ($5^{\circ} 22.5'N$, $100^{\circ} 30' E$) and the model area extends from Penang in Peninsular Malaysia to the west of Sumatra (Fig.1).

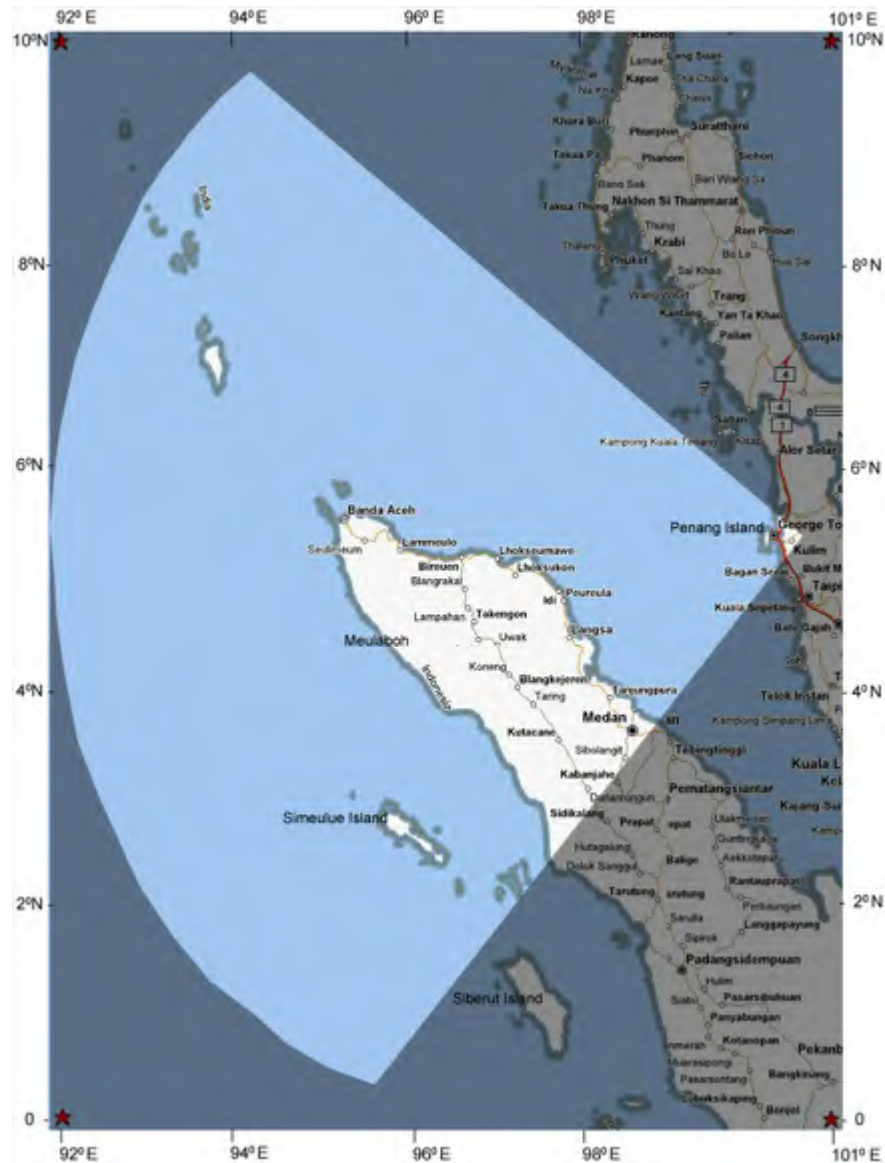


Figure 1: Map of the model domain including North Sumatra and Penang Island

The orthogonal grid system is generated through the intersection of a set of straight lines through O given by $\theta = \text{constant}$ and a set of concentric circles, with centre as O , given by $r =$

constant. The angle between any two consecutive radial lines is $\Delta\theta = 0.3333^\circ$, whereas the distance between two successive circular grid lines, Δr , increases as we proceed towards the open sea. After the transformation (8), both $\Delta\theta$ and $\Delta\eta$ become uniform. In the transformed domain the discrete grid points (η_i, θ_j) are defined by:

$$\eta_i = (i - 1) \Delta\eta; \quad i = 1, 2, 3, \dots, M$$

$$\theta_j = (j - 1) \Delta\theta; \quad j = 1, 2, 3, \dots, N$$

where, $M = 778$ and $N = 277$ also $\Delta\theta = 0.3333^\circ$ and $\Delta\eta = 1/1077$, so that in the computational domain η ranges from 0 to $777/1077$. Although $\Delta\eta$ is taken as a constant, Δr increases with r according to the Eq. (9) and varies from 0.5 km to 1.0 km. Thus we obtain a finer mesh near the coast and gradually coarser mesh in the deep sea.

The sequence of time is given by:

$$t_k = k\Delta t, \quad k = 1, 2, 3, \dots \quad (13)$$

Although, in the physical domain N grid lines meet at the Pole, in the computational domain this point is considered as N distinct grid points which are generated automatically. Since the pole is considered at the land, where no computation is done, there is no problem of instability during numerical computation. In the computational domain a staggered grid system is used, which is similar to Arakwa C system.

The governing equations (10) – (12) and the boundary conditions (5) – (7) are discretised by finite-differences (forward in time and central in space) and are solved by a conditionally stable semi-implicit method. Moreover, the CFL criterion has been followed in order to ensure the stability of the numerical scheme. Along the closed boundary, the normal component of the velocity is considered as zero, and this is easily achieved through appropriate stair step representation as mentioned earlier. The time step is taken as 5 seconds that ensures stability of the numerical scheme. In the solution process, the value of the friction coefficient C_f is taken as 0.0033 throughout the physical domain. The depth data used in this study are collected from the Admiralty bathymetric charts.

4. INITIAL CONDITION

The generation mechanism of the 26 December Indonesian tsunami is mainly due to the static sea floor uplift caused by abrupt slip at the India/Burma plate interface. A detailed description of the estimation, based on Okada (1985), of the extent of earthquake rupture (92°E to 97°E and 3°N to 10°N) along with the maximum uplift (507 cm) and subsidence (474 cm) of the seabed has been reported in Kowalik et al. (2005). According to this estimation, the source is elongated along the fault zone from south-east to north-west with uplift to subsidence from west to east. Following Kowalik et

al. (2005), a source, of the same extent with maximum rise of 5 m and maximum fall of 4.75 m of the sea surface, is assigned as the initial condition. The vertical cross section of the source along 121st grid line is shown in Fig. 2. Other than source region, the initial sea surface elevations are taken as zero everywhere. Also the initial radial and tangential components of velocity are taken as zero throughout the domain.

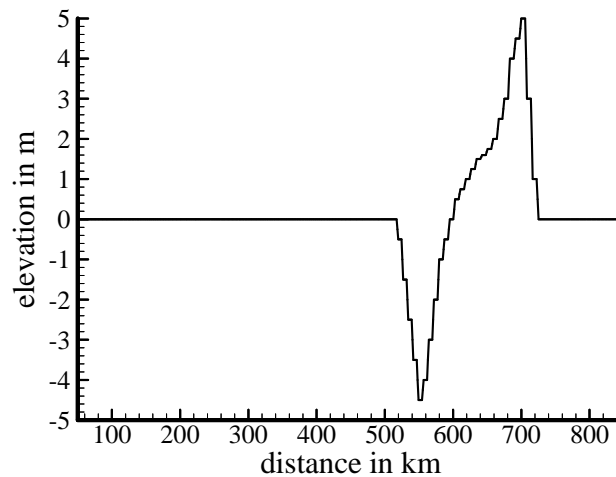


Figure 2: Vertical cross-section of the source along 121st grid line

5. RESULTS AND DISCUSSIONS

The effects of the Indonesian tsunami of December 2004 along the coasts of North Sumatra and Penang Islands are investigated. Numerical simulation of this potential tsunami is performed in the framework of linear shallow-water equations in cylindrical polar coordinate system.

5.1. Simulated water levels along North Sumatra

Figure 3 describes the computed time series of water levels at two locations of North Sumatra along east and west coasts. The maximum elevation of the water level near the coastline of Banda Aceh (north-west of Sumatra) is approximately 9.2 m (Fig. 6a). At approximately 20 min after the generation, the water level starts decreasing and reaches the level of -4.4 m. Then the water level increases continuously to reach a level of 9.2 m before going down again and the oscillation continues for several hours. The computed result also shows the withdrawal of water from the coastal region before arrival of high surge. The computed time series of water level at Medan coast (north-east of Sumatra) indicates that the maximum elevation along this coast is 3 m and that the arrival of tsunami surge is preceded by the withdrawal of water (Fig.3b). The oscillations continue for several hours in both the locations and the damping is rather slow.

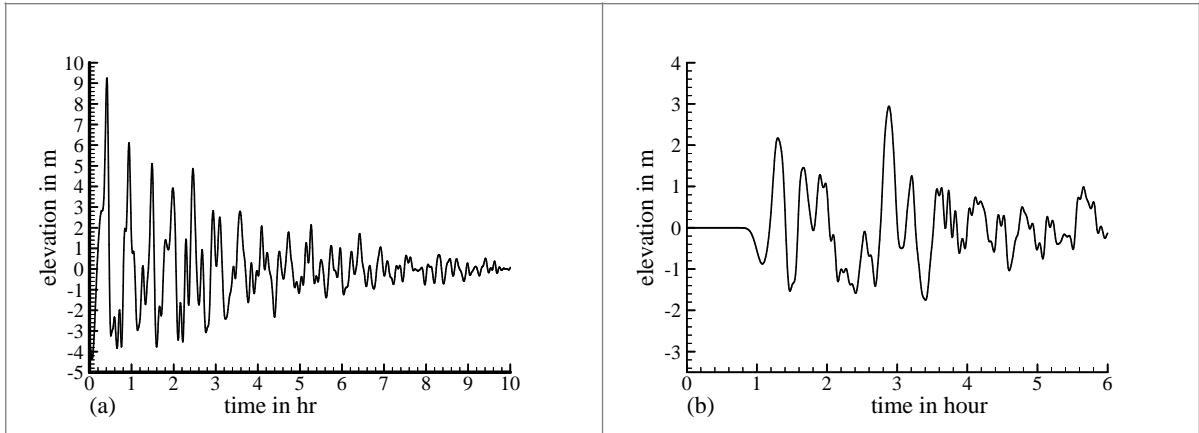


Figure 3: Time series of computed elevation at coastal locations of Sumatra Island associated with the tsunami source at Sumatra 26 December, 2004: (a) Banda Aceh, (b) Medan coast The computed results indicate that the North Sumatra is vulnerable for very strong tsunami surges due to the permanent source near Sumatra along the Burma/India interface.

This can be seen from Fig. 4, where the curves of maximum elevations have been drawn along the west and east coasts of North Sumatra. The maximum elevation along the east coast has exceeded 15 m at Medan (Fig. 4a).

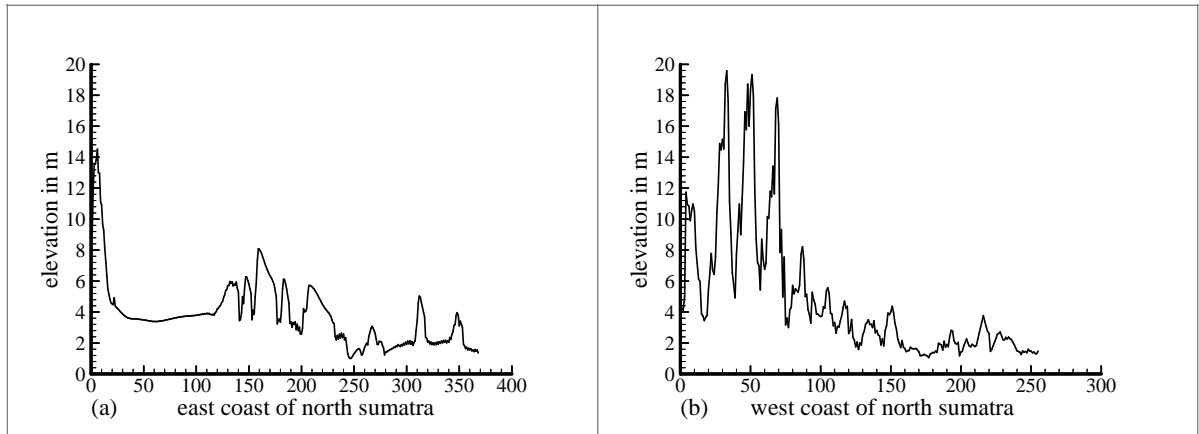


Figure 4: Maximum elevation associated with source 26 December 2004 at Sumatra along the north coasts of Sumatra Island: (a) east coast, (b) west coast On the other hand, the surge intensity is found to be highest at the west coast; the highest elevation in excess of 17 m is attained at the north of Meulaboh (Fig. 4b).

The same intensity of surge is attained along the Simeulue Island, which is located at the west of North Sumatra. The computed peak elevation surrounding the North Sumatra can be seen from the contour plot of maximum elevation in Fig. 5. From the contour plot it is evident that that the surge amplitude is increasing very fast near the north-west part of Sumatra.

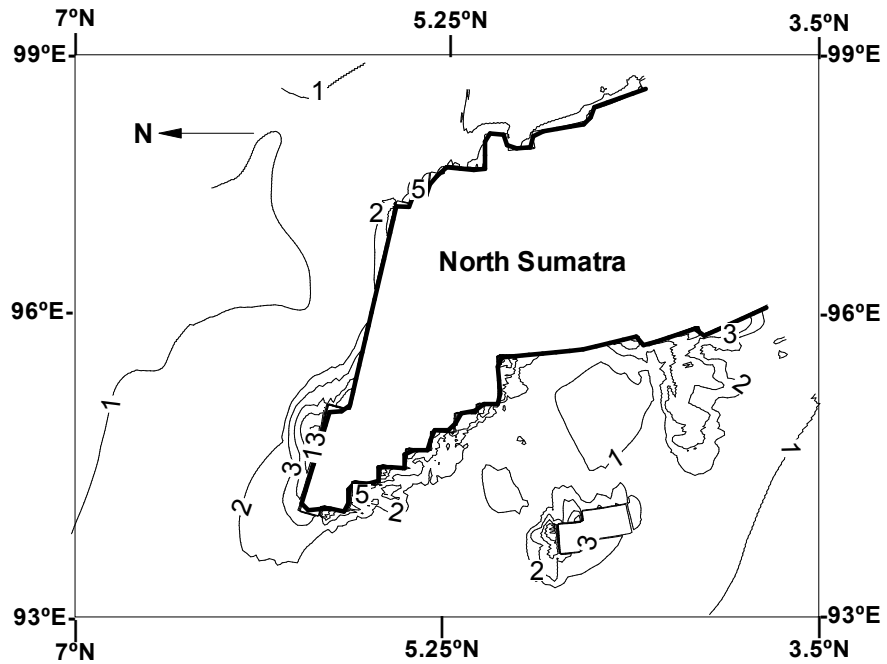


Figure 5: Contour of maximum water levels around the two coasts of North Sumatra.

Table 1. Observed and computed water levels above the mean sea level at different locations of Penang Island. (Source: The authors conducted this survey)

| Location name | Observed water level (m) | Computed water level (m) |
|-------------------------------|--------------------------|--------------------------|
| Batu Ferringhi (north penang) | 3.3 | 3.2 |
| Taluk Bahang | > 2.0 | 2.62 |
| Tanjung Tokong | 2.80 | 1.0 |
| Tanjong Bunga | 3.0 | 2.5 |
| Pasir Panjang | >2.0 | 3.2 |
| Kuala Pulau Betung | 2.0 | 2.24 |

5.2. Simulated water levels along Penang Island

The water levels at different locations of the coastal belt of Penang Island are also stored at an interval of 30 seconds. Fig. 6 depicts the computed time series of water levels at two locations on the north and west coasts of Penang Island. The maximum amplitude at Batu Ferringhi (north coast) is approximately 2.6 m (Fig. 6a).

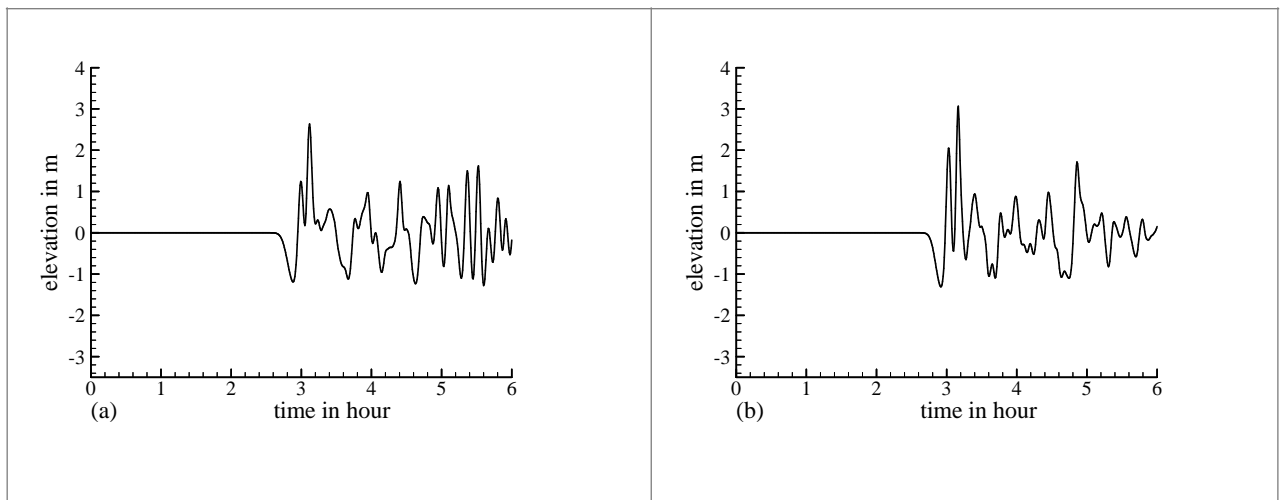


Figure 6: Time series of computed elevation at two coastal locations (a) Batu Ferringhi, (b) Pasir Panjang of Penang Island associated with the tsunami source at Sumatra 26 December, 2004.

It is seen that at approximately 2.80 hrs after the generation of tsunami at the source, the water level starts decreasing (withdrawal of water) and reaches level of -1.2 m. Then the water level increases continuously to reach a level of 2.7 m at 2 hrs 40 min before going down again. The computed water level at Pasir Panjang (west coast) shows the same pattern as that of Batu Ferringhi with the maximum water level of approximately 3.2 m (Fig. 6b). The computed results indicate that the west coast of Penang Island is vulnerable for very strong tsunami surges due to the permanent source near Sumatra.

This can be seen from Fig. 7, where the curves of maximum elevations have been drawn along two coastal belts of Penang Island. The maximum elevation along the west coast (north to south) has exceeded 3.6 m at Tanjung Bunga (Fig. 7a). On the other hand, the surge intensity is found to be highest at the north coast; the highest elevation in excess of 2.7 m is attained at Teluk Bahang (Fig. 7b).

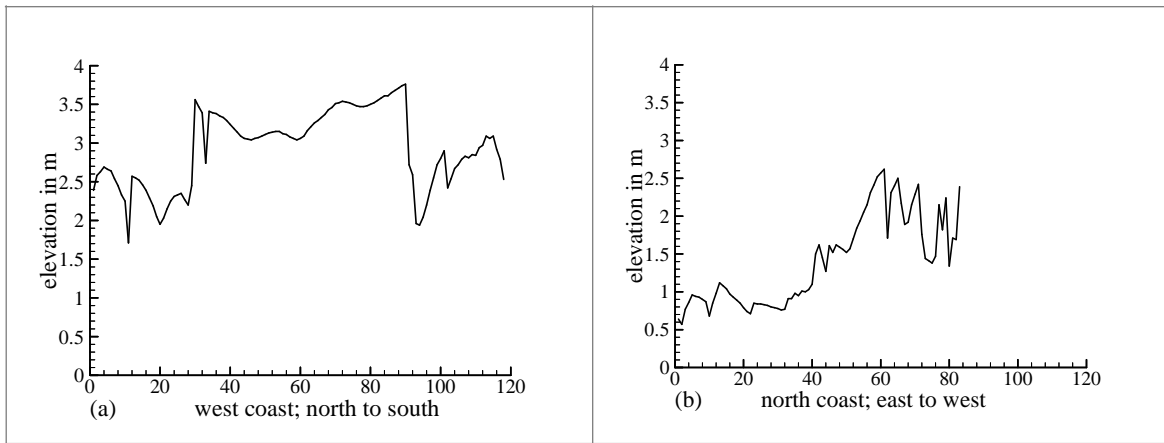


Figure 7: Maximum elevation associated with source 26 December 2004 at Sumatra along two coasts of Penang Island: (a) west coast, (b) north coast

The computed peak elevation surrounding the Penang Island is also presented in the contour plot (Fig. 8). From the figure it is clear that the surge amplitude is increasing very fast near the shore of the Penang Island. The computed results show that the west coast of Penang Island is vulnerable to a stronger tsunami surge.

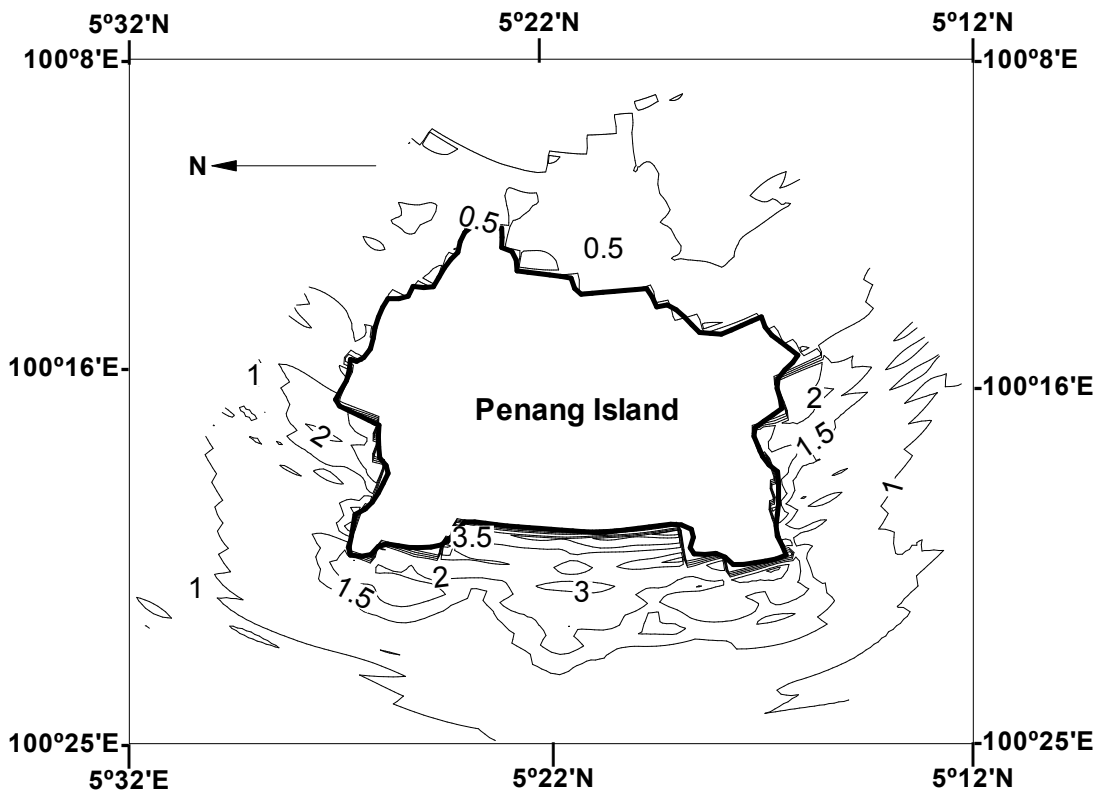


Figure 8: Contour of maximum water levels around the four coasts of Penang. Lastly, a post tsunami survey report on water levels at different locations of Penang Island, along with the computed water

levels, is shown in Table 2. It is found that agreement between the simulated and observed values is satisfactory.

Table 2. Observed and computed water levels above the mean sea level at different locations of North Sumatra

| Location name | Observed maximum tsunami amplitude near the shore | Computed water level |
|-------------------|---|----------------------|
| Simeulue Island | > 3 m | 3.4 m |
| Meulaboh | 1.5 m | 1.8 m |
| Medan | >2.5 m | 2.9 m |
| Banda Aceh | - | 9.2 m |
| Meulaboh Aronghan | 15 m | > 14 m |
| St 176, WPT 17 | > 15 m | 18 m |

Source: measured by the Turkish-Indonesian-USA team during the field survey on Sumatra on January 21-29, 2005

6. CONCLUSIONS

In this paper, the model of Ismail et al. (2006) has been used to simulate the water levels along North Sumatra and Penang Island in Peninsular Malaysia. The simulated results are found to be in good agreement with the observed data collected through post tsunami surveys. The computed results indicate that the linear polar coordinate shallow water model is able to estimate the effects of tsunami along Sumatra and Penang islands in Peninsular Malaysia with realistic accuracy.

REFERENCES

Haque, M.N.; Miah, S., Roy, G.D.:(2003): A Cylindrical Polar Coordinate Model with Radial Stretching for the coast of Bangladesh, Proc. Int. Conf. App. Math. & Math. Phy. (ICAMMP), Shahjalal Univ. of Sc. & Tech. Sylhet, Bangladesh, pp 77-87.

Ismail, A. I. M., Karim, M. F., Roy, G. D. (2006): "Simulation of Tsunami along Sumatra and Penang Islands Associated with the Indonesian Tsunami of 26 December 2004 using a Linear Polar Coordinate Shallow Water Model". International Conference. on Mathematical Modelling and Computation, University Brunei Darussalam, Brunei. 5 - 8 June 2006.

- Imamura. F.; Gic,E.C.:(1996): Numerical Model for Tsunami Generation due to Subaqueous Landslide Along a coast- A case study of the 1992 Flores tsunami, Indonesia; Sc. Tsunami Hazards, 14 (1): 13-28.
- Imteaz. A. M.; Imamura. F.:(2001): A Non-Linear Numerical Model for Stratified Tsunami Waves and its Application, Sc. of Tsunami Hazards, Vol.19, pp.150-159.
- Iguchi, T. (2011): “A mathematical analysis of tsunami generation in shallow water due to sea bed deformation,” Proceedings of the Royal Society of Edinburgh, 141A, 551-608.
- Karim, M. F.; Sankar, D. S.; Yunus, E. (2016): “On the open sea propagation of 2004 global tsunami generated by the sea bed deformation, “International Journal of Applied Engineering Research, 11 (4) 2686-2692.
- Karim, M. F., Roy, G. D., Ismail, A. M., Meah, M. A. (2007): “A shallow water model for computing Tsunami along the west coast of Peninsular Malaysia and Thailand using boundary-fitted curvilinear grids,” Journal of Science of Tsunami Hazards, Volume 26, No. 1, 21 - 41.
- Kowalik. Z.; Knight. W.; Logan. T.; (2005) Whitmore. P.:Numerical Modeling of The Global Tsunami, Sc. of Tsunami Hazards, Vol.2, No.1, pp.40.
- Okeda, Y. (1985): Surface Deformation due to Shear and Tensile Faults in a Half Space; Bull. Seism. Soc. Am., 75: 1135-1154.
- Roy, G. D., Karim, M. F., Ismail, A. I. M. (2007): A Non-Linear Polar Coordinate Shallow Water Model for Tsunami Computation along North Sumatra and Penang Island. Journal of Continental Shelf Research, 27, 245–257.
- Roy, G. D., (1995): Estimation of expected maximum possible water level along the Meghna estuary using a tide and surge interaction model. Environment International. 21(5), 671-677.
- Roy, G.D.; Humayun Kabir, A.B.;Mandal, M.M.; Haque, M.Z.(1999): Polar Coordinate Shallow Water storm surge model for the coast of Bangladesh, Dyn. Atms. Ocean, 29, 397-413.
- Roy, G. D., Izani, A. M. I. (2005): An investigation on the propagation of 26 December 2004 tsunami waves towards the west coast of Malaysia and Thailand using a Cartesian coordinates shallow water model, Proceedings of the International Conference in Mathematics and Applications, Mahidol University, Thailand, 389-410.
- Titov,V.V., Gonzalez, F.I. (1997): Implementation and Testing of the Method of Splitting Tsunami (MOST) Model; NOAA Technical Memorandum ERL, PMEL -112, Contribution No. 1927 from NOAA/Pacific Marine Environmental Laboratory: pp 11.

Yalciner, A. C., Karakus, H., Ozer, C and Ozyurt, G. (2005): Understanding the generation, propagation, near and far field impacts of tsunamis, Lectures Notes, Middle East Tech. Univ., Ankara, Turkey



SCIENCE OF TSUNAMI HAZARDS

Journal of Tsunami Society International

Volume 40

Number 1

2021

THE GREAT LISBON EARTHQUAKE AND TSUNAMI OF 1 NOVEMBER 1755 Evaluation of the Compression Convergence Mechanism

George Pararas-Carayannis

ABSTRACT

The Great Lisbon earthquake of 1 November 1755 was an unprecedented, extremely destructive seismic event with a moment magnitude (M_w) estimated to range from 8.5 to 9.0. Its epicenter was off the southwest coast of Portugal in the abyssal plain close to the Gorringe Bank along the Azores-Gibraltar fracture zone (AGFZ), which has been created by complex tectonic interactions between the Eurasian, African and Iberian plates. Shortly after the earthquake, huge tsunami waves engulfed and caused extreme destruction and loss of life in the lower part of Lisbon, in many smaller towns along the Tagus river estuary, as well as along Portugal's southern region of Algrave, in Morocco, in Gibraltar, and elsewhere. The far-field tsunami impact affected both North and South America, the Caribbean region and Northern Africa. The present study examines the source parameters of the earthquake and its unusual mechanism of tsunami generation, based on bathymetry, gravity anomalies and overall geomorphological features of the eastern segment of the AGFZ which indicate the existence of a large area of subsidence, characterized by a grabben with an approximate orientation of N45E, adjacent to a thrust fault, apparently both caused by continent to continent convergence/collision. Additionally, the present study evaluates: a) the dimensions and orientation of the 1755 tsunami generating area; b) the net ocean floor crustal displacements; c) the total energy release; e) the extensional, transcurrent and compressional forces of this tectonic regime; and f) the statistical approximation of earthquake and tsunami recurrence frequencies in the region. Additional objectives are the documentation of the historic aspects of this disaster, and of the complex interactions of on-going active continent to continent convergence near the AGFZ fault zone which, in addition to this great 1755 earthquake, has resulted in numerous lesser magnitude historical tsunamigenic events in the region. The present study speculates that the 1755 earthquake resulted, not from the rupture and subsidence of one short segment, but from a combination of at least two successive ruptures along the eastern segments of AGFZ, closer to the Iberian plate where a seismic gap existed and excessive stress had accumulated.

Keywords: *Lisbon earthquake, Gorringe Bank, Azores-Gibraltar fracture zone AGFZ, continent/ continent compression convergence/collision, folding reverse faulting.*

Vol 40 No. 1, page 62 (2021)

1. INTRODUCTION

In 1755, Lisbon was one of the most beautiful and largest cities in Europe, with an estimated population of 275,000. This great city of Portugal was legendary for its wealth, prosperity and sophistication. Its architecture was complemented by that of the suburbs, including a majestic aqueduct constructed by King D. Joao V. in 1731, the Jeronimus Church, and the Tower of Belem (Fig. 1).

Conquered by the Moors in 1147, it was kept under Moorish influence during the Middle Ages and Renaissance. This may be seen in the design of the streets in the quarters surrounding St. George Castle and extending as far as Rossio, the central part of the city. The Rosario, or main square, was the commercial center of Lisbon. The Estatus Palace, situated to the north, was where illustrious visitors to the Kingdom were lodged. On the east side, Saint Dominic Church and the All Saint's Royal Hospital, with its magnificent façade, were erected. On top of the hill, an ancient royal residence was situated. To the west, the church and its Convent were among the most magnificent buildings. Other famous buildings near the city center include the Cathedral, St. Paul's Church, St. Nicholas' Church, and St. Roch's Church.



Fig. 1. The Great Palace Square of Lisbon

In the morning of 1 November 1755, a great earthquake and tsunami generated on the eastern section of the Azores-Gibraltar fracture zone (AGFZ) with epicenter about 200 km WSW of Cape St. Vincent, struck Lisbon. It was Sunday and the religious holiday of All Saints. Most of Lisbon's population were praying in six magnificent cathedrals, including the great Basilica de Sao Vincente de Fora. Within minutes, this great thriving city-port of Lisbon, capital of the country, of the vast Portuguese empire, and a seat of learning in Europe, was

reduced to rubble by the two major shocks of this great earthquake, and by the waves of a subsequent catastrophic tsunami. Most of these wonderful architectural structures were either destroyed or sustained considerable damage. A huge fire completed the destruction of this great city.

This great earthquake was an unprecedented event which occurred along the eastern segment of the Azores-Gibraltar fracture zone (AGFZ), which is the boundary of active tectonic interaction between the African and the Eurasian plates. This eastern section includes both strike-slip and thrust faults which are capable of producing major earthquakes, with variable tsunamigenic efficiencies.

This destructive natural disaster of 1 November 1755 which has been historically misnamed as “The Great Lisbon Earthquake”, did not affect only the capital of Portugal, but many of its other cities, as well. As indicated in the scientific literature, the tsunami that was generated by this event struck and caused extensive destruction in other coastal areas of countries in Europe Northern Africa, as well as the Caribbean Sea and in North and South America (Lander and Lockridge, 1989; Mader, 2001; Heinrich et al., 1994).

The following sections provide documentation of this great disaster, an evaluation of other historical events that may help understand the complex interactions of on-going active continent-to-continent convergence near the AGFZ fault zone, where numerous lesser magnitude historical tsunamigenic events have occurred.

2. THE GREAT LISBON EARTHQUAKE OF 1 NOVEMBER 1755

2.A Earthquake Epicenter Magnitude, and Tsunami Source Parameters

The main shock of the great earthquake struck Portugal at 9:40 in the morning of 1 November 1775 (see Fig. 2 map of Portugal). At that time, there were no instruments to record or measure earthquakes but experts have estimated that the magnitude of the great Lisbon earthquake must have been 8.6 or even greater. The observations of the effects and the ground motions suggest a moment magnitude (M_w) estimate ranging from 8.5 to 9.0.

The epicenter of the earthquake was initially reported in the literature to be 38.0°N , 9.0°W . in the Atlantic Ocean, about 200 km (120 miles) WSW of Cape St. Vincent. However, this estimate appeared to be incorrect. It is believed that the epicenter was further south and west than what had been postulated since the first of the tsunami waves reached Lisbon about 40 minutes after the quake struck. A subsequent estimate gave the epicenter coordinates as 36°N , 11°W .

Based on the tsunami travel time of 40 minutes to Lisbon, an amplitude of the wave being up to 20 meters in height with a period of one hour (Mader, 2001), and on estimates of reverse wave refraction from Lisbon and other locations, the most probable location of the epicentral area must have been close to the eastern segment of the AGFZ and southwest of Cape St. Vincent, where there is a large area of subsidence characterized by a grabben as well as an adjacent thrust fault. Such a thrust fault of about 50 km in length (31 mi) and dip slip of more than 1 km (0.62 mi), was identified by a 1992 seismic reflection survey along the AGFZ (Gràcia, 2003).

This estimate appears to be more accurate, as it is supported by the near field tsunami travel times of an earlier unpublished study by the present author, regarding the source parameters and the orientation of the tsunami generating area. These initial source parameters of the tsunami generating area were subsequently used for the numerically calculated far field refraction and tsunami travel times reported in the literature (Mader, 2001).



Fig. 2. Map of Portugal, showing the Tagus river estuary.

2B. Aftershocks

Two major aftershocks which occurred on December 11 and December 23, 1755 caused added agony and despair to survivors. Strong aftershocks continued for many weeks but there was no way to measure their magnitudes.

2C. Tectonic Setting

It is believed that the great 1755 Lisbon earthquake occurred along the Azores-Gibraltar fracture zone (AGFZ) which marks the poorly-defined boundary of active tectonic interaction between the African and the Eurasian plates which converge at a rate of about 3.8 mm/year. Major fault zones along this boundary include both strike-slip and thrust faults. These include the Horseshoe Fault, the Marques Pombal Fault, the Gorringe Bank Fault and the Cadiz Subduction Zone (Batista, 2020). This is an active seismic region where large earthquakes occur with frequency along the boundary separating the Eurasian and African tectonic plates (Grimison & Chen, 1986)

The tectonic interaction on the eastern segment of AGFZ involves a thrusting component in NW direction along a NE-trending strike plane, as well as folding and reverse faulting (Grácia et al, 2003). Gravimetry measurements support this conclusion. Some of the larger earthquakes, particularly those occurring closer to the eastern section of the AGFZ, are capable of generating tsunamis. It is postulated that the 1755 earthquake probably occurred along such a thrust fault near the Gorringe Bank.

2D. Duration of Felt Ground Motions

Review of eyewitness accounts indicates that there were three distinct quake shocks over a ten-minute period. The first shock was followed by an even more powerful second shock, and this was the one that sent buildings toppling down in Lisbon and elsewhere in Portugal. According to reports, the tremors and the ground motions from this second shock lasted for three-and-one-half minutes, which was extremely long even for an earthquake of such great magnitude. Its intensity was XI (extreme). Gigantic fissures of up to 5 meters (16 feet) wide, tore through the center of Lisbon. The following third shock was less powerful.

2E. Lisbon Destruction by the Earthquake

It was Sunday, a beautiful day and a great religious holiday in Portugal when the great earthquake struck. It was a little after 9:30 in the morning and most of the people of Lisbon were either already in the churches or on their way to them. According to an eye-witness, "*a strange, frightful noise underground, which resembled the hollow, distant rumbling of thunder,*" was first heard. He reported that his own house swung from side to side "*with a motion like that of a wagon driven violently over wrought stones.*"

Soon as the quake started, the churches began to rock and sway. The heavy chandeliers began to swing above the heads of the terrified parishioners. Most of the people ran to the streets. The first shock was succeeded by a more violent and longer lasting shock.

The quake's rocking ground motions weakened and cracked many Lisbon's buildings which collapsed into the city's narrow streets, crashing the panicked survivors seeking escape. People ran to the edge of the city and into the fields. Others sought refuge on the banks of the Tagus river, only to perish shortly thereafter by the waves of a huge tsunami. The destruction caused by the earthquake was beyond description. Lisbon's great cathedrals, Basilica de Santa Maria,

Sao Vicente de Fora, Sao Paulo, Santa Catarina, the Misericordia - all full of worshipers - collapsed, killing thousands. Lisbon's whole quay and the marble-built Cais De Pedra along the Tagus disappeared into the river, burying with it hundreds of people who had sought refuge (see Fig. 3 map of Lisbon and of the Tagus river estuary).



Fig. 3. Map of Lisbon and locations near the Tagus river estuary).

Lisbon was not the only [Portuguese](#) city affected by the catastrophe. Throughout the south of the country, in particular the [Algarve](#), destruction was rampant. The tsunami destroyed some coastal fortresses in the Algarve and, at lower levels, it razed several houses. Almost all the coastal towns and villages of the Algarve were heavily damaged, except [Faro](#), which was protected by the sandy banks of [Ria Formosa](#). In [Lagos](#), the waves reached the top of the city walls. Other towns in different Portuguese regions, such as [Peniche](#), [Cascais](#), and even [Covilhã](#) (which is located near the [Serra da Estrela](#) mountain range in central inland Portugal) were affected. The shock waves of the earthquake destroyed part of Covilhã's castle walls and its large towers.



Fig. 4. Depiction of Tsunami and Earthquake damage of Lisbon

2F. Earthquake Effects Widely Felt

The Lisbon earthquake caused considerable damage not only in Portugal but also in Spain - particularly in Madrid and Seville (see Fig. 4 artistic depiction of tsunami and earthquake damage). The shock waves were felt throughout Europe and North Africa, over an area of about 1,300,000 square miles. In Europe, ground motions were felt in Spain, France, Italy, Switzerland, Germany, and as far to the north as the Duchy of Luxembourg, Sweden Finland and Greenland. Unusual phenomena were observed at great distances. For example, seiches were observed in Finland. In Italy, an ongoing volcanic eruption of Vesuvius stopped abruptly.

Precursory phenomena also had been widely observed prior to the great earthquake. For example in Spain, there had been reports of falling water levels. Turbid waters and a decrease in water flow in springs and fountains had been reported in both Portugal and Spain.

In North Africa the quake caused heavy loss of life in towns of Algeria and Morocco - more than 400 miles south of Lisbon. The town of Algiers was completely destroyed. Tangiers suffered great loss of lives and extensive damage. The earthquake was particularly destructive in Morocco, where approximately 10,000 people lost their lives. Archival records document that the coastal towns of Rabat, Larache, Asilah, and Agadir (named Santa Cruz while under Portuguese rule) suffered much damage. Even the interior cities of Fez, Meknes and Marrakesh were similarly damaged. In Meknes, numerous casualties occurred. Churches, mosques and many other buildings collapsed.

On the island of [Madeira](#), [Funchal](#) and many smaller settlements suffered significant damage. Almost all of the ports in the [Azores](#) archipelago suffered most of their destruction from the tsunami, with the sea penetrating about 150 meters (490 ft) inland. Portuguese towns in northern Africa were also affected by the earthquake, such as [Ceuta](#) and [Mazagon](#), where the tsunami hit hard the coastal fortifications of both towns, in some cases going over it, and flooding the harbor area. In Spain, the tsunamis swept the [Andalusian](#) Atlantic Coast, nearly destroying the city of [Cadiz](#), killing at least 1/3 of its population.

2G. The Great Lisbon Fire

Whatever the earthquake shocks and the tsunami waves spared from destruction, a great fire - which started soon thereafter – finished (see Fig. 5. Artistic depiction of The Great Lisbon Fire). Within minutes the fire spread and turned Lisbon into a raging inferno. Unable to run, hundreds of patients in the Hospital Real burned to death. Remaining survivors ran to the hills and the fields outside the city. Fanned by steady northeast winds, the great fire burned out of control through the ruins of the city for more than 3 days. The fire swept everything in its path and destroyed houses, churches and palaces. Lisbon's magnificent museums, and its magnificent libraries - housing priceless documents and papers dealing with the great history of Portugal's great past - burned to the ground. Archives and other precious documents were completely destroyed. Works of art, tapestries, books, manuscripts, including the invaluable records of the India Company were destroyed. Also burned were the king's palace and its 70,000-volume library. Over two hundred fine, priceless paintings, including paintings by Titan, Reubens, and Coreggio, were burned in the palace of the Marques de Lourcal.



Fig. 5. Artistic depiction of The Great Lisbon Fire

2H. Death Toll and Destruction from the Earthquake, the Tsunami and the Fire

The earthquake destroyed Lisbon and other major cities in Portugal. More than 18,000 buildings, representing about 85% of the total were completely demolished, included famous palaces and libraries and those that had sustained limited earthquake damage were destroyed by the subsequent great fire. In the first two minutes of the earthquake, about 30,000 people lost their lives. The total death toll in Lisbon, a city of 230,000, was estimated to be about 90,000. Another 10,000 people were killed in Morocco. The total death toll in Portugal, Spain and Morocco was estimated to range from 40,000 to 50,000.

2.I. Recurrence Frequency of Earthquakes and Tsunamis Along the Azores-Gibraltar fracture zone (AGFZ).

Although the Lisbon earthquake of 1755 was a rare and unusual combination of seismic and tsunami events, a recurrence in the future is a certainty given the continuous collision of the continents of Africa with the continent of Eurasia. However in the absence of adequate historical earthquake data, it is not possible to provide a statistical probability of recurrence frequency for a large event similar to the Great Lisbon Earthquake and Tsunami of 1755 magnitude earthquakes in this region, although lesser magnitude events can occur with relatively higher frequency.

3. THE TSUNAMI OF 1 NOVEMBER 1755 IN LISBON

Shortly after the earthquake struck, a tsunami wave of 20 meters crashed over the harbor quays, engulfed the lower part of Lisbon on the shore of the Tagus river and submerged much of the lower part of the city - including its newly built, marble quay of Cais De Pedra which disappeared into the river. About 20,000 of terrified survivors who had rushed to the open space of the docks and the waterfront quay for safety after the first earthquake shock, lost their lives to the tsunami waves that followed. All boats moored in Lisbon's harbor were also destroyed. The following is an eyewitness account of the tsunami.

3A. Eyewitness Account of the Tsunami

Rev. Charles Davy was a survivor of this great Lisbon disaster. The following is an excerpt from his account describing (*in Archaic English*) his observations of the tsunami on Lisbon's waterfront (*Source of historical depiction: Eva March Tappan, ed., The World's Story: A History of the World in Story, Song and Art, 14 Vols., (Boston: Houghton Mifflin, 1914), Vol. V: Italy, France, Spain, and Portugal, pp. 618-628*). (see: Fig. 6. Another artistic rendition of the 1755 tsunami disaster along the waterfront of Lisbon).



Fig. 6. Artistic rendition of the 1755 tsunami disaster along the waterfront of Lisbon.

"You may judge of the force of this shock, when I inform you it was so violent that I could scarce keep on my knees; but it was attended with some circumstances still more dreadful than the former. On a sudden I heard a general outcry, "The sea is coming in, we shall be all lost." Upon this, turning my eyes towards the river, which in that place is nearly four miles broad, I could perceive it heaving and swelling in the most unaccountable manner, as no wind was stirring. In an instant there appeared, at some small distance, a large body of water, rising as it were like a mountain. It came on foaming and roaring, and rushed towards the shore with such impetuosity, that we all immediately ran for our lives as fast as possible; many were actually swept away, and the rest above their waist in water at a good distance from the banks.

For my own part I had the narrowest escape, and should certainly have been lost, had I not grasped a large beam that lay on the ground, till the water returned to its channel, which it did almost at the same instant, with equal rapidity. As there now appeared at least as much danger from the sea as the land, and I scarce knew whither to retire for shelter, I took a sudden resolution of returning back, with my clothes all dripping, to the area of St. Paul's. Here I stood some time, and observed the ships tumbling and tossing about as in a violent storm; some had broken their cables, and were carried to the other side of the Tagus; others were whirled around with incredible swiftness; several large boats were turned keel upwards; and all this without any wind, which seemed the more astonishing.

It was at the time of which I am now speaking, that the fine new quay, built entirely of rough marble, at an immense expense, was entirely swallowed up, with all the people on it, who had fled thither for safety, and had reason to think themselves out of danger in such a place: at the same time, a great number of boats and small vessels, anchored near it (all likewise full of people, who had retired thither for the same purpose), were all swallowed up, as in a whirlpool, and nevermore appeared.

This last dreadful incident I did not see with my own eyes, as it passed three or four stones' throws from the spot where I then was; but I had the account as here given from several masters of ships, who were anchored within two or three hundred yards of the quay, and saw the whole catastrophe. One of them in particular informed me that when the second shock came on, he could perceive the whole city waving backwards and forwards, like the sea when the wind first begins to rise; that the agitation of the earth was so great even under the river, that it threw up his large anchor from the mooring, which swam, as he termed it, on the surface of the water: that immediately upon this extraordinary concussion, the river rose at once near twenty feet, and in a moment subsided; at which instant he saw the quay, with the whole concourse of people upon it, sink down, and at the same time every one of the boats and vessels that were near it was drawn into the cavity, which he supposed instantly closed upon them, inasmuch as not the least sign of a wreck was ever seen afterwards.

This account you may give full credit to, for as to the loss of the vessels, it is confirmed by everybody; and with regard to the quay, I went myself a few days after to convince myself of the truth, and could not find even the ruins of a place where I had taken so many agreeable walks, as this was the common rendezvous of the factory in the cool of the evening. I found it all deep water, and in some parts scarcely to be fathomed.”

3B. Tsunami Effects in the Tagus River Estuary in Lisbon and along the west, north, and south coasts of Portugal

For most coastal regions of Portugal, the destructive effects of the resulting tsunami were more disastrous than those of the earthquake. The first three of the tsunami waves were particularly destructive along the west and south coasts of Portugal.

At the mouth of the Tagus river estuary and upstream, there was an initial recession of the water which left exposed large stretches of the river bottom. Shortly afterwards, the first of the tsunami waves arrived. It swamped Bugie Tower and caused extensive damage to the western part of Lisbon, the area between Junqueria and Alcantara. The same wave continued upstream spreading destruction and demolishing the Cais de Pedra at Terreiro do Paco and part of the nearby customhouse. The maximum wave height at this location was estimated to be about 6 meters. Boats which were overcrowded with quake survivors seeking refuge, capsized and sank. There were two more large waves. It is estimated that the largest tsunami run-up in the Tagus estuary was about 20 meters.

At the coastal town of Cascais, about 30 km west of Lisbon, large stretches of the sea floor were initially exposed, then the arriving tsunami waves demolished several boats. Field investigations of the Cascais – Cabo da Roca west of Lisbon indicate that the tsunami's impact on the Atlantic coast of Portugal was great and that even huge boulders were moved. At Cabo Raso for example, a 20 ton boulder was found turned upside down at an elevation of 10 meters. Another large boulder of 25 tons near Forte de San José, moved inland for at least 30 m. (Scheffers & Kelletat, 2005) (see Fig. 7 & 8). Further north of the mouth of Tagus river west of Lisbon the same field investigations indicated tsunami run-up ranging in certain areas from 20 to 25 meters.



Fig. 7. Tsunami boulder of about 20 tons, turned upside down at +10 m east of Cabo Raso.
(Photograph source: Scheffers & Kelletat, 2005)



Fig. 8. Tsunami boulder of 25 tons near Forte de San José, moved inland for at least 30 m.
(Photograph source: Scheffers & Kelletat, 2005)

At Peniche, a coastal town about 80 km north of Lisbon, many people were killed by the tsunami. In Setubal, another coastal town 30 km south of Lisbon, the water reached the first floor of buildings.

The tsunami destruction was particularly severe in the province of Algarve (Figs. 9 & 10), in southern Portugal, where almost all the coastal towns and villages were severely damaged, except Faro, which was protected by sandy banks. In some coastal regions of Algarve, the maximum tsunami wave run-up was 30 meters. According to reports, the waves demolished coastal fortresses and razed houses to the ground. In Lagos, the waves reached the top of the city walls.



Fig. 9. The State of Algarve in Portugal where there was substantial tsunami damage



Fig. 10. Peninsula of Faro, Province of Algarve, Southern Portugal.

3C. Far Field Effects and Travel Times of the 1755 Tsunami

The 1 November 1755 Lisbon earthquake generated a destructive tsunami with far-field effects which have been well documented in the Literature. According to official reports, large waves caused damage and destruction on coastal areas in Brazil.

4. THE 1755 TSUNAMI GENERATING SOURCE

4A. The Azores-Gibraltar Fracture Zone (AGFZ) - Tsunami Generating Area

The 1755 tsunami was generated on the Azores-Gibraltar Fracture Zone (AGFZ), which is the major seismic zone in the Eastern Atlantic Ocean between the Azores and the Strait of Gibraltar (Fig. 11). This zone is the product of complex interactions between the African, Eurasian, and Iberian plates. The Eurasia–Nubia plate boundary segment between the Azores and the Strait of Gibraltar, has been the place of tsunamigenic earthquakes in the past. The tectonic regime is extensional in the Azores, transcurrent along the Gloria Fault, and compressional in the Strait of Gibraltar, although not clearly defined.

A recent study (Batista, 2010) presented an overview of six major historical earthquakes that have occurred in the region and provided relevant data which indicates certain constraints on tsunami generating mechanisms. According to this study, six historical events occurred in the eighteenth-century between 1722 and 1761, while the twentieth-century events occurred much later between 1941 and 1975, and speculates that major tsunamigenic earthquakes occur in the Iberia-Maghreb areas along the boundaries of the block where these past historical earthquakes occurred, which is a region with relatively unknown tectonic dynamics. This conclusion is valid, and indeed the crustal displacements in the region where the 1755 earthquake are not fully understood.

However, it is the assessment of the present study that the source of the great tsunami that was generated by the 1755 earthquake resulted, not from the rupture and subsidence of one short segment, but from a combination of at least two successive ruptures along the eastern segments of AGFZ, closer to the Iberian plate where a seismic gap existed and excessive stress had accumulated and involved both folding and reverse faulting (Gràcia et al, 2003). The presence of two epicenter foci in the region is indicative of seismic stress transference along a convergence tectonic boundary of sequential ruptures, and of crustal displacements that contributed to the generation of the great tsunami.

In 1755, there were no instruments in existence to record the Lisbon earthquake and thus determine its epicenter. As reported in recent times, the epicenter was assumed to be at 38.0°N, 9.0°W., about 200 km WSW of Cape St. Vincent. However the tsunami travel time to Lisbon was approximately 40 minutes, which suggests that the epicenter and the tsunami generating area must have been further south and west of the reported location. Based on the tsunami source characteristics and the tsunami wave travel times the present study estimated the source dimensions and orientation of the tsunami generating area as shown in Fig..

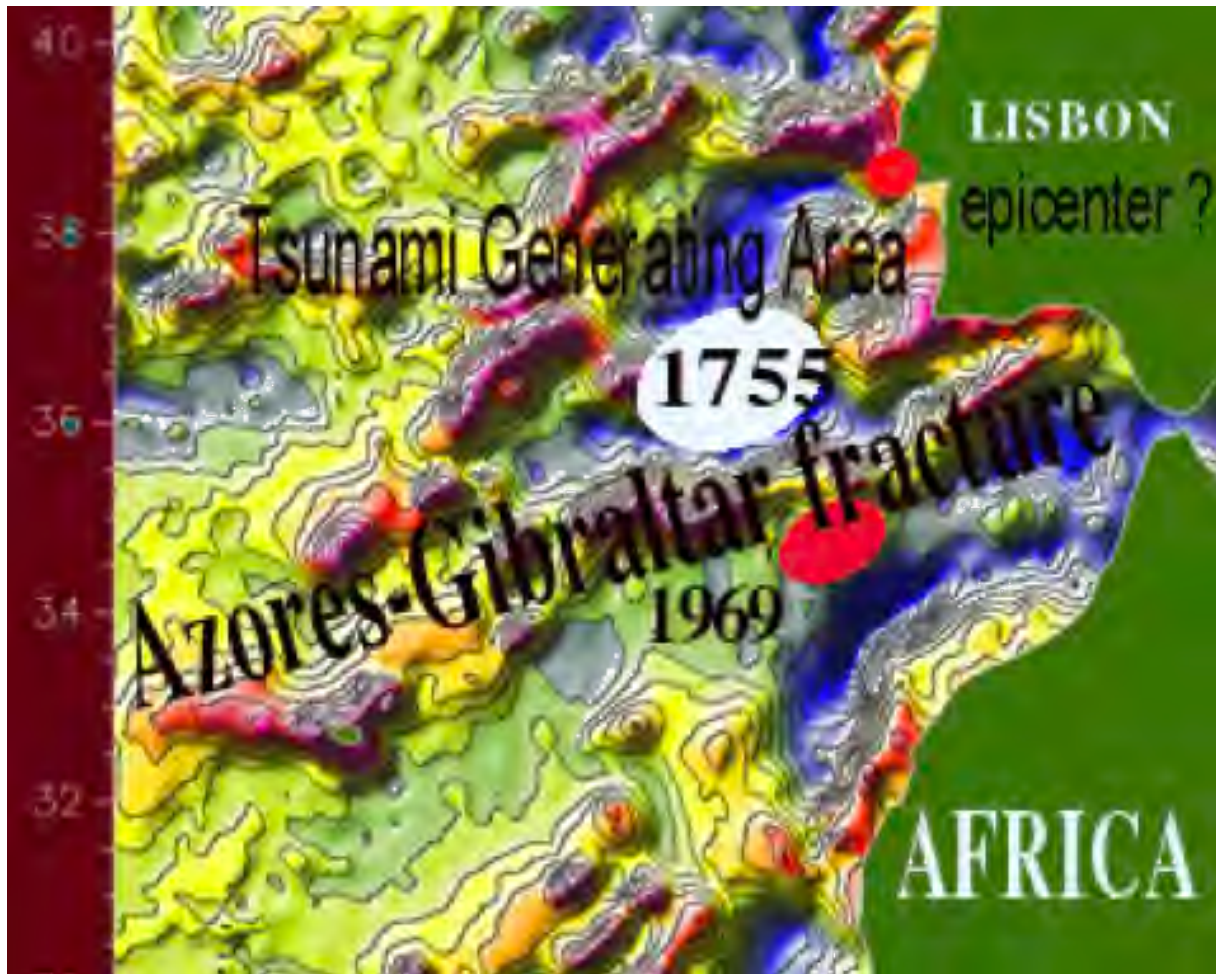


Fig. 11. Generating Areas of the 1755 and 1969 tsunamis along the Azores-Gibraltar Fracture Zone (AGFZ) superimposed on bathymetry and gravity anomaly map (Source: Pararas-Carayannis, 2001)

Numerical modeling studies of the small tsunami generated by the February 28, 1969 quake in the same general area of the Atlantic (Heinrich, Batista, and Miranda, 1994), have suggested that the epicenter of the Lisbon earthquake was close to that of the 1969 event which produced only a small tsunami. The epicenter of the 1969 quake was centered south of Gorringe bank near the Azores-Gibraltar fracture zone in the Atlantic Ocean (see map). However, the travel time to Lisbon for the first wave of the 1755 tsunami indicates that its generating area was somewhat north of the 1969 event. It took about 40 minutes for the first wave to reach Lisbon in 1755. The travel time to Lisbon from the 1969 quake was closer to 50 minutes.

In the absence of seismological source parameters for the 1755 Lisbon quake, Dr. Charles Mader used the reported Lisbon tsunami wave characteristics to estimate source dimensions and tsunami travel times (personal communication March 2001, see also reference below (Mader, 2001).

Since the initial tsunami wave was a drop of about 20 meters in Lisbon and the observed period was about 1 hour, it was postulated that the tsunami generating area was fairly wide, involving considerable ocean floor subsidence. He estimated that a tsunami source region of about 300 kilometers in radius (282,000 square kilometers), dropping about 30 meters, located in the region of the 1969 earthquake near the Gorringe bank could generate the type of wave which occurred in Lisbon.

As presented earlier, the epicenter of the 1755 Lisbon earthquake could not have been at 38 N, 9 W, as postulated because there is no significant tectonic interaction at this location. More likely the quake's epicenter and the tsunami generating area were further south and west. A more probable tsunami generating area - where subsidence is possible - would have been north of the Gorringe Bank along the Azores-Gibraltar fracture zone (AGFZ), rather than south where the 1969 tsunami was generated (and as postulated by Heinrich, Batista, and Miranda (1994)).

The AGFZ zone marks the boundary of active continent-to-continent convergence between the African and the Eurasian plates. Compression along this boundary appears to result in an echelon overlapping and staggering arrangement of a series of faults, some being thrust or reverse types with the net result being a wide distribution of grabbens and horsts. These oceanic features have resulted from subsidence or upward displacements of crustal blocks. Each of these features is relatively short, but collectively they form the wide linear zone, known as the AGFZ, in which the strike of the individual features is oblique to that of the zone as a whole.

The AGFZ is an active seismic region where large earthquakes can occur with frequency. Some of the larger earthquakes, particularly those occurring closer to the eastern section of AGFZ are capable of generating tsunamis. The tectonic interaction on the eastern segment involves a thrusting component in NW direction. However, because of differences in source parameters and mechanisms of continent-to-continent compression (and possibly triple junction interaction with the Atlantic oceanic plate), each earthquake in this region, regardless of magnitude, will not have the same efficiency for tsunami generation. This is the reason why the 1969 quake generated a small tsunami, even though it had a rather large magnitude $M_s=7.9$ and involved thrust faulting. It is believed that the tsunamigenic efficiency of the 1755 Lisbon earthquake was greater because of large-scale subsidence and thrust faulting caused by continent-to-continent convergence and compression. The generating area was in the abyssal plain, north of the Gorringe Bank along the Azores- Gibraltar fracture zone (AGFZ), a region characterized also by negative gravity anomalies as shown in Fig. 11.

About 30 minutes after the earthquake struck Lisbon, the sea level near the Bugie Tower at the mouth of the Tagus river, begun to recede. About 10 minutes later the first large wave arrived, so the tsunami travel time from the source region to Lisbon was approximately 40 minutes. It took less than an hour for this first tsunami to reach Morocco and Algiers, and about 7 hours to reach the Caribbean and the U. S. East coast.

5. TSUNAMI FAR FIELD IMPACT

Remarkable tsunami waves and effects were recorded and reported everywhere, on both sides of the Atlantic. Waves up to 18 meters (60 feet) in height hit a vast area stretching from Finland to North Africa and across the Atlantic to Martinique and Barbados causing much destruction and loss of life. Lakes as far north as Sweden were affected as well as the river Dal in Norway, 1800 miles (about 2,890 kilometers) away, which overflowed its banks. The following are some additional observations in Spain, Gibraltar, the Mediterranean Sea, Morocco, France Great Britain, Ireland, Belgium and Holland, Madeira and the Azores islands, and Antilles, Antigua, Martinique, and the Barbados

Spain: In southwestern Spain, the tsunami caused damage to Cadiz and Huelva, and the waves penetrated the Guadalquivir River, reaching Seville.

Gibraltar: In Gibraltar, the sea rose suddenly by about two meters. In Ceuta the tsunami was strong.

Mediterranean Sea: in the Mediterranean Sea, it decreased rapidly.

Morocco: Caused great damage and casualties to the western coast of Morocco, from Tangier, where the waves reached the walled fortifications of the town, to Agadir, where the waters passed over the walls, killing many. Tsunami waves with heights up to as 20 metres (66 ft) swept along the coast of North Africa.

France Great Britain, Ireland, Belgium and Holland: The tsunami reached, with less intensity, the coast of France, Great Britain, Ireland, Belgium and Holland. A three-metre (ten-foot) tsunami hit Cornwall on the southern British coast. Galway, on the west coast of Ireland, was also hit, resulting in partial destruction of the "Spanish Arch" section of the city wall.

Madeira and the Azores islands: Madeira and in the Azores islands damage was extensive and many ships were in danger of being wrecked.

Antilles, Antigua, Martinique, and Barbados: The tsunami crossed the Atlantic Ocean, reaching the Antilles in the afternoon. Reports from Antigua, Martinique, and Barbados note that the sea first rose more than a meter, followed by large waves.

6. NUMERICAL MODELING STUDIES OF TSUNAMI TRAVEL TIMES AND HEIGHTS

Numerical modeling studies of tsunami propagation generated for the 1755 Lisbon earthquake in the Atlantic were performed initially by Charles Mader (Mader, 2001), based on earlier estimates of source parameters of dimensions and crustal displacements provided by the present author. The postulated source parameters were based on the orientation of the AGFZ seismic zone which – as mentioned - marks the boundary of active continent to continent convergence between the African and the Eurasian plates, as well as on the tsunami's initial impact times (40 minutes after the quake) on Lisbon and on other near-field points of observations and calculation of first tsunami wave arrival. Using these times of the tsunami's initial impacts and by means of reverse tsunami refraction back towards the postulated source, an envelop of the tsunami's generation area was estimated, which was used subsequently for the far-field modeling studies of the tsunami propagation across the

Atlantic (Mader, 2001). Based on this preliminary analysis, the postulated tsunami source parameters of the tsunami generating area were estimated to be about 300-kilometer radius and to have involved approximately 282,000 square kilometers. The postulated source had the same approximate West Northwest orientation of the AGFZ and had involved about 30 meters of subsidence near the Gorringer bank, in the same region as the earthquake in 1969.

Using these postulated tsunami source parameters and computer modeling simulation was performed using the SWAN code which solves the nonlinear long wave equations and included Coriolis and frictional effects (Mader, 2001). The height of the tsunami at Saba Island in outer Caribbean was estimated at 7 meters after 7 hours of travel. The offshore deep-water tsunami amplitudes along the east coast of USA, along the Caribbean and in the Gulf of Mexico, were estimated to have been about 2 meters in height and having periods ranging from 1.25 to 1.5 hours. However, the run-up amplification is probably two to three times the estimated deep-water wave amplitude.

It took nearly 7 hours for the tsunami waves to reach the east coast of North America and South America, and about 8-hours to reach the Gulf of Mexico (Fig.) The maximum tsunami runup on the shores was estimated to be about 3 meters. However, in the Gulf of Mexico, the offshore tsunami deep-water amplitudes were estimated to have been less than a meter (Mader, 2001).

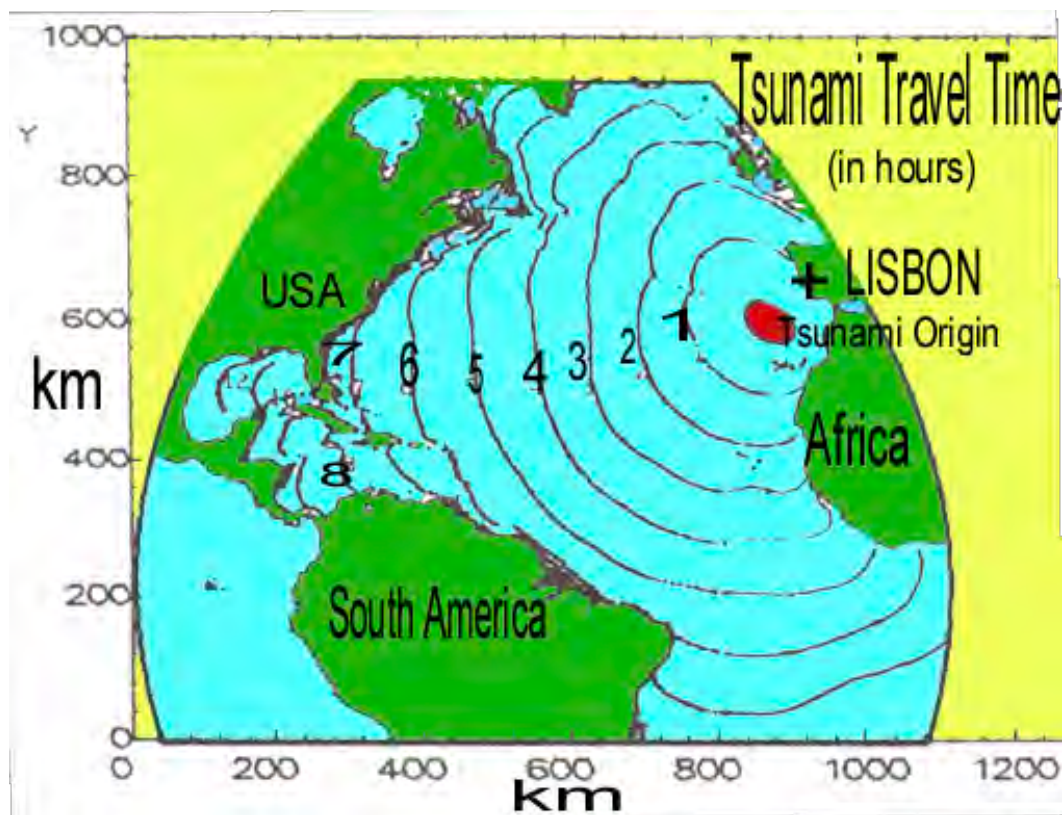


Fig. 12. Travel Time Chart of the Great Lisbon Tsunami (Source: Mader, 2001)

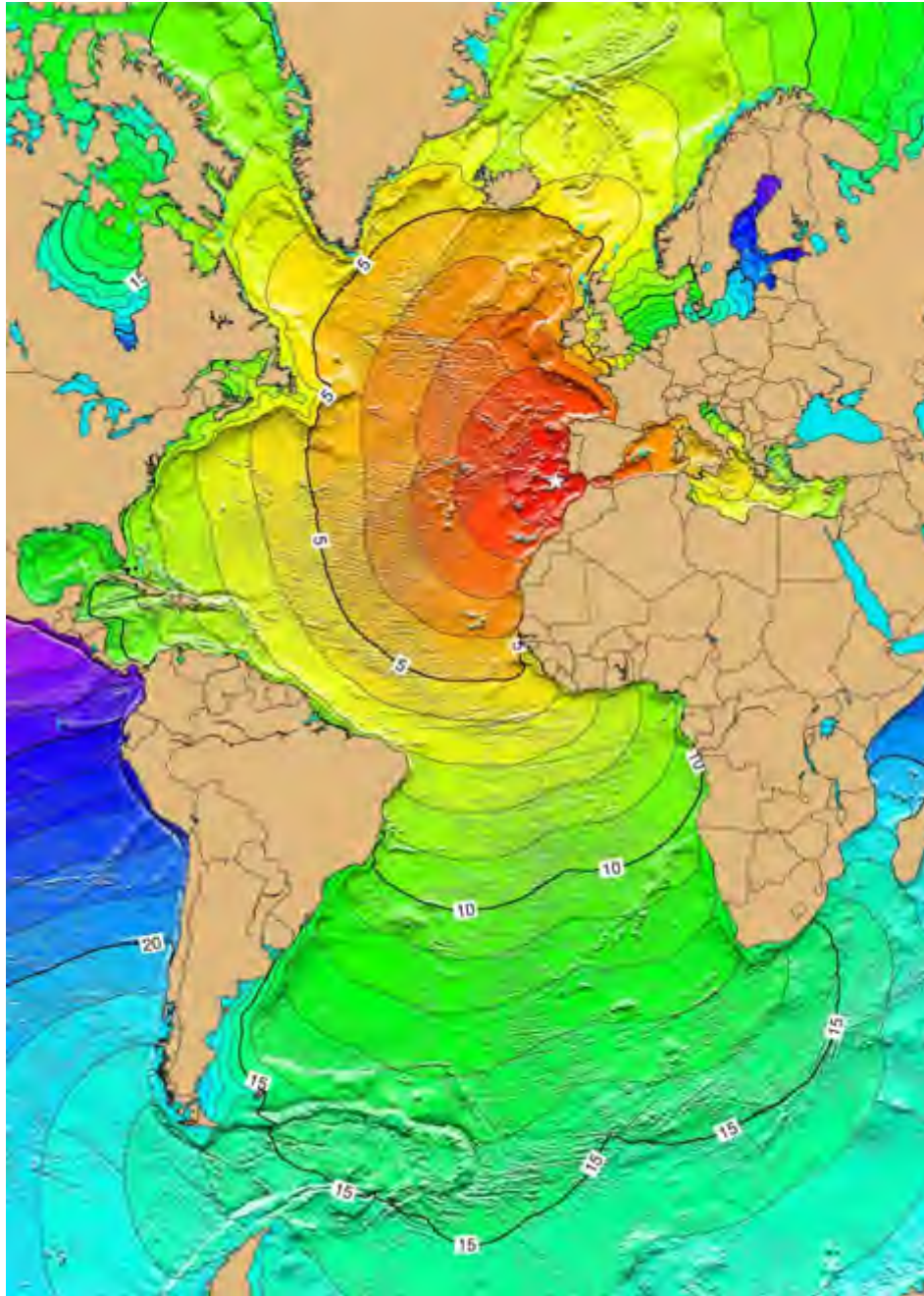


Fig. 13. More Extensive refraction diagram and Tsunami Travel Times based on the generating source parameters of the 1755 Lisbon tsunami determined by an earlier investigation (Mader, 2001 & Pararas-Carayannis) Source: NOAA- National Center for Environmental Information - Global Historical Tsunami Database.

All other subsequent modeling studies, as the one above provided by NOAA-National Center for Environmental Information - Global Historical Tsunami Database used the same source parameters, although tsunami travel times were extended beyond the Atlantic Ocean (Fig. 13).

CONCLUSIONS

The Great Lisbon tsunami of 1755 was most probably generated in the abyssal plain north of the Gorringe Bank along the Azores- Gibraltar fracture zone (AGFZ). The bathymetry, gravity anomalies and overall geomorphologic features of the eastern segment of the AGFZ indicate the existence of a large area of subsidence, characterized by a grabben with an approximate orientation of N45E caused by continent to continent collision, as well as folding and reverse faulting.

The eastern section of AGFZ is an area of active tectonic interaction, capable of producing large earthquakes with variable tsunamigenic efficiencies. Although the Lisbon earthquake of 1755 was a rare and unusual combination of seismic and tsunami events, a recurrence in the future is a certainty. However, in the absence of adequate historical earthquake data, it is not possible to provide a statistical probability as to when an event similar to the Great Lisbon Earthquake and Tsunami of 1755 may recur.

REFERENCES

Batista, A.M., 2020. Tsunamis Along the Azores Gibraltar Plate Boundary. Pure and Applied Geophysics 177(B4) April 2020 DOI: [10.1007/s00=024-019-02344-8](https://doi.org/10.1007/s00=024-019-02344-8)

Gràcia Eulàlia, Dañobeitia, Juanjo; Vergés, Jaume; & Parsifal Team, 2003. Mapping active faults offshore Portugal (36°N 38°N): Implications for seismic hazard assessment along the southwest Iberian margin. *Geology*, vol. 31, Issue 1, p.83, Jan 2003.

Grimison N.L. and Chen Wang-Pin, 1986. The Azores-Gibraltar Plate Boundary: Focal mechanisms, depths of earthquakes, and their tectonic implications, *Journal of Geophysical Research Atmospheres* 91(B2):2029-2048, February 1986. DOI: [10.1029/JB091iB02p02029](https://doi.org/10.1029/JB091iB02p02029)

Heck, N.H., 1947, List of seismic sea waves, *Bull. Seismol. Soc. Am.*, v. 37, no. 4, p. 269-284.

Heinrich Ph., Baptista M. A. & Miranda P., 1994. Numerical Simulation of 1969 Tsunami Along the Portuguese Coasts, Preliminary Results, *Science of Tsunami Hazards*, 12, 3-24 (1994).

Kozak, Jan T., and Charles James D. , Paper abridged and edited from drafts of a longer work in progress by V. S. Moreira, C. Nunes and J. Kozak on the Lisbon Earthquake of 1755. Institute of Rock Mechanics, Czech Academy of Science, National Information Service for Earthquake Engineering (NISEE) of the University of California, Berkeley.

Lander James F. and Lockridge Patricia A., 1989, United States Tsunamis 1690-1988 National Geophysical Data Center Publication 41-2 (1989).

Mader, C., 2001. Modeling the 1755 Lisbon Tsunami. *Science of Tsunami Hazards* 19(2) January 2991.

Milne, J. 1912, Catalog of destructive earthquakes, Brit. Assn. Adv. Sci. Rept. 81st Mtg., 1911, p. 649-740.

Pararas-Carayannis, George, 2001, The Potential for Tsunami Generation along the Azores-Gibraltar Fracture Zone, (unpublished paper).

Scheffers Anja and Kelletat Dieter, 2005. TSUNAMI RELICS ON THE COASTAL LANDSCAPE WEST OF LISBON, PORTUGAL. Science of Tsunami Hazards, Vol 23, No.1, pp. 3-16, 2005.

Svyatlowski, A.E., 1957. Tsunamis--destructive waves originating with underwater earthquakes in seas and oceans [Russian], Izdatel'stvo Akad. Nauk SSSR, p. 1-69, Eng. transl. by V. Stevenson, Hawaii Inst. Geophys., Transl. Ser. 8, 1961.

Tappan March Eva, ed., 1914. The World's Story: A History of the World in Story, Song and Art, 14 Vols., (Boston: Houghton Mifflin, 1914), Vol. V: Italy, France, Spain, and Portugal, Source: Modern History Sourcebook: Historical Depictions of the 1755 Lisbon Earthquake Rev. Charles Davy: The Earthquake at Lisbon, 1755, pp. 618-628.

NOTE: Some of the images presented have been modified from the Kozak Collection of Images of Historical Earthquakes, National Information Service for Earthquake Engineering (NISEE) of the University of California, Berkeley, from the Lisbon Museum and from unpublished work of Dr. Charles Mader (permission granted).

ISSN 8755-6839



SCIENCE OF TSUNAMI HAZARDS

Journal of Tsunami Society International

Volume 40

Number 1

2021

Copyright © 2021 - TSUNAMI SOCIETY INTERNATIONAL

WWW.TSUNAMISOCIETY.ORG

TSUNAMI SOCIETY INTERNATIONAL, 1741 Ala Moana Blvd. #70, Honolulu, HI 96815, USA.

WWW.TSUNAMISOCIETY.ORG